

Analysis of enforced RANK signaling in B cells in vivo

Yasemin Begüm Alankus

Dissertation zur Erlangung des akademischen Grades Doktor
der Naturwissenschaften (Dr. rer. nat) der Fakultät für
Biologie der Ludwig-Maximilians-Universität München

München, 2016

Erstgutachter: Prof. Dr. Heinrich Leonhardt

Zweitgutachter: Prof. Dr. Jürgen Ruland

Promotionsgesuch eingereicht: 08.11.2016

Tag der mündlichen Prüfung: 28.06.2017

Eidesstattliche Erklärung

Ich versichere hiermit an Eides statt, dass die vorliegende Dissertation selbständig und ohne unerlaubte Hilfe angefertigt ist.

Weiterhin erkläre ich, dass die Dissertation nicht ganz oder in wesentlichen Teilen einer anderen Prüfungskommission vorgelegt worden ist und dass ich mich nicht anderweitig einer Doktorprüfung ohne Erfolg unterzogen habe.

München, den 28.6.2017

Yasemin Begüm Alankus

Acknowledgements

First and foremost, I would like to thank my supervisor Prof. Dr. med. Jürgen Ruland, for accepting me into his lab, and providing me with all the expertise and resources I needed for my research. I would also like to thank Prof. Dr. Heinrich Leonhardt for his endorsement and for presenting this thesis at the Department of Biology of the Ludwig-Maximilians Universität München. Furthermore, I would like to thank my thesis committee advisors, Prof. Dr. Mathias Heikenwälder and Prof. Dr. rer. nat. Marc Schmidt-Supprian, for their insightful comments and support. Additionally, I would like to thank Prof. Dr. med Wilko Weichert, Dr. med. Mindaugas Andrulis and Univ.-Prof. Dr. med. Stephan Macher-Göppinger for their collaboration on this research project. I would also like to thank the IMPRS PhD Program at the Max Planck Institute, and the coordinators Dr. Hans-Jörg Schäffer, Dr. Ingrid Wolf and Maxi Reif, for enabling me to start and complete my PhD, and their support during the process.

I would also like to thank all my current and former colleagues for the support and stimulating discussions they have provided. First of all, I would like to thank Dr. Nathalie Knies, both for her supervision and her friendship. I would also like to thank Kerstin Burmeister for her never-ending support in the mouse facility, and Tanja Ruff, for her excellent technical support, as well as her happy and energetic spirit. Another thank you goes out to Torben Gehring, for his valuable contributions to the project during his Master thesis. A big thank you is in order to everyone else in AG Ruland, especially Nicole Hanneschläger, Dr. Maike Buchner, Veronika Ecker, Dr. Oliver Gorka, Dr. Urszula Domanska and Dr. Konstanze Pechloff. Additionally, I would like to thank Prof. Dr. Florian Greten and Dr. Özge Canli for their continuous support. I would also like to thank Fuat Sakirler, the best partner in crime anyone

can ask for, for cheering me on and pushing me forward.

Last but not least, I would like to thank my parents, for teaching me the value of higher education, intellectuality and independence. I would like to dedicate this thesis to them, as a token of my endless appreciation and love.

Zusammenfassung

Die Fehlregulation zentraler Signalwege, die zu einem gesteigerten Überleben, gesteigerter Proliferation oder reduzierter Apoptose der Zelle führen, wurde für fast alle malignen hämatologischen Erkrankungen beschrieben. Einer der bekanntesten Signalwege, der das Überleben und die Proliferation in hämatopoetischen Zelle reguliert, ist der NF- κ B-Signalweg. Insbesondere wurden Mutationen und Deletionen in den Schlüsselkomponenten dieses Signalweges in diffus großzelligen B-Zell Lymphomen vom aktivierten Typ gefunden (ABC-DLBCL). Das Molekül Receptor Activator of NF- κ B (RANK), welches in ca. 8% der Tumoren von ABC-DLBCL Patienten mutiert ist, führt im physiologischen Kontext nach Bindung seines Liganden RANKL zu einer Aktivierung der NF- κ B, MAPK und PI3K Signalwege. Eine umfangreiche Literaturrecherche die ergab, dass eine RANK Fehlregulation auch in malignen B-Zell Erkrankungen, wie der chronisch lymphatischen Leukämie (CLL), dem multiplen Myelom und dem Hodgkin Lymphom beschrieben ist. Dennoch sind die *in vivo* Konsequenzen fehlgesteuerter RANK Signalleitungen in B-Zellen weitgehend unklar. Deshalb ist die hier durchgeführte Studie darauf ausgerichtet durch konditionale Mutagenese ein neues Mausmodell zu entwickeln, bei welchem die Expression der lymphomassoziierten RANK(A756G) selectiv *in vivo* induziert werden kann, um die Effekte von mutierter RANK(A756G) Expression auf B-Zellen zu analysieren.

Die Analyse dieser Tiere ergab, dass die RANK(A756G) Expression ab dem pre-B-Zell Stadium in Mäusen eine lymphoproliferative Autoimmunerkrankung mit Systemic Lupus Erythematosus (SLE)-ähnlichen Eigenschaften verursacht. Hierzu gehören eine spontane Produktion von antinukleären Antikörpern (ANA), eine massive B1-B-Zell Expansion und eine Immunkomplex-Akkumulation mit Nephritis bishin zum Nierenversagen. Eine detaillierte Analyse der RANK(A756G)- exprim-

ierenden B-Zellen ergab, dass diese im Vergleich zu wildtyp B-Zellen besser überlebten und durch die Aktivierung der ERK, JNK und PI3K Signalwege verstärkt proliferierten. Durch diese induzierte RANK Aktivierung werden Gene wie zum Beispiel Bcl-2 und Cyclin D1 induziert, die für das Überleben und die Zellteilung wichtig sind, und apoptotische Gene, wie zum Beispiel APC und PTEN herabreguliert. Dies wurde jedoch ausschließlich nach RANKL Bindung beobachtet. Stromazellen aus dem Knochenmark und aktivierte CD4+ T Zellen exprimieren RANKL und verursachen somit eine starke Aktivierung und Proliferation der RANK(A756G)-transgenen B-Zellen. Im Einklang mit dieser Erkenntnis wurde beobachtet, dass es im Knochenmark von RANK(A756G)CD19-Cre Mäusen eine substantielle Expansion stark aktivierter unreifer B- Zellen gab. Als Zusammenfassung wird folgendes Modell vorgeschlagen: Die RANK(A756G)-RANKL Interaktion treibt eine vorzeitige Aktivierung von B-Zellen im Knochenmark die dazu führt, dass sich ein autoreaktives B-Zell-Repertoire anreichert. Durch den Überlebens- und Proliferationsvorteil der Zellen, akkumulieren diese und werden zusätzlich durch CD4+ T Zellen aktiviert, was letztendlich zu einer Autoimmunerkrankung bei Mäusen führt. Die vorliegende Studie zeigt, dass eine deregulierte und aberrant aktivierte RANK Signalwirkung ausreichend ist, um die B-Zell-Homeostase in vivo zu durchbrechen und Autoimmunität zu induzieren. Basierend auf dem bekannten pathophysiologischen Zusammenhang zwischen Autoimmunität und Lymphomentstehung, liefern diese Daten und das neuartige Mausmodell auch eine Grundlage für das Verständnis der RANK(A756G)-Mutation bei humanen Lymphomen.

Abstract

Dysregulation of several cellular signaling pathways that lead to enhanced cell survival, proliferation, and reduced apoptosis has been described for all hematopoietic malignancies. One of the most prominent pathways that regulates cell survival and proliferation is NF- κ B. Recently, a set of mutations leading to deregulation and overactivation of the NF- κ B pathway have been detected in human Activated B cell-like Diffuse Large B cell lymphoma (ABC DLBCL). Among these mutations, a mutation in the Receptor Activator of NF- κ B (RANK) gene, the K240E mutation, which leads to an amino acid change from Lysine to Glutamic acid at position 240, was found in 8% of ABC-DLBCL tumors. RANK is a transmembrane receptor that exerts after physiological binding to its ligand RANKL prosurvival, proliferative and anti-apoptotic effects on target cells through the activation of NF- κ B, MAP kinase and PI3K pathways. Deregulation of RANK-RANKL signaling, disruption of the balance between RANK/RANKL concentrations and overexpression of RANK have also previously been described for cases of Hodgkin's lymphoma, Multiple myeloma and B cell chronic lymphocytic leukemia (B-CLL). However, the *in vivo* consequences of the deregulation in RANK signaling are not well understood. Therefore, the study at hand generated and analyzed a novel mouse model to determine the effects of B cell restricted enforced RANK(A756G) expression in B cells, through conditional mutagenesis.

We observed that the enforced RANK(A756G) expression starting as early as in the pre-B cell stage drives an autoimmune disease with Systemic Lupus Erythematosus (SLE)-like symptoms, such as presence of anti-nuclear antibodies, B1-B cell expansion and deteriorating renal function with immunoglobulin complex accumulation in kidneys and kidney failure. The RANK(A756G) expressing B cells showed

enhanced survival and proliferation through the activation of ERK, JNK and PI3K pathways. Activation of these pathways led to increased expression of genes important for survival and proliferation, such as Bcl-2 and Cyclin D1, as well as decreased expression of pro-apoptotic genes such as APC and PTEN. The pro-survival and proliferative effect of RANK(A756G) expression was shown to be ligand dependent. Stromal cells in the bone marrow and activated CD4+ T cells express RANKL and this led to a strong activation of transgenic B cells *ex vivo*. In line with this finding, we observed in the bone marrow of RANK(A756G)CD19-Cre mice a massive accumulation with immature B cells that were highly activated. Together, based on these findings, we propose the following model: Enforced RANK-RANKL binding drives premature activation of B cells in the bone marrow, leading to an autoreactive B cell repertoire with enhanced survival and proliferative advantage, that over time accumulate and drive an autoimmune disease in mice. Thus, the study at hand shows that selectively deregulated and aberrantly activated RANK signaling is sufficient to disrupt B cell homeostasis and trigger spontaneous autoimmunity. Based on the known pathophysiological link between autoimmunity and lymphomagenesis, these results and our new genetic mouse model provide the basis for the understanding of RANK(A756G) function during human lymphomagenesis.

Contents

Declaration	I
Acknowledgements	II
Zusammenfassung	IV
Abstract	VI
Table of Contents	VIII
1 Introduction	1
1.1 The Immune System and Adaptive Immunity	1
1.1.1 General Features of the Immune System	1
1.1.2 B2 B Lymphocyte Development	2
1.1.3 B1 B Lymphocyte Development	5
1.1.4 B Cell Receptor Signaling and Antibody Secretion	8
1.2 B Cell Checkpoints and Pathology	10
1.2.1 Checkpoints in B Lymphocyte Development	10
1.2.2 Autoreactive B Lymphocytes and Autoimmune Disorders . . .	11
1.2.3 B Lymphocyte Development and Lymphoid Malignancies . . .	13
1.3 Receptor Activator of NF- κ B: Function and Pathology	15

1.3.1	Characteristics and Function of Receptor Activator of NF- κ B Signaling	15
1.3.2	Receptor Activator of NF- κ B and Pathology	18
2	Research Objective	20
3	Materials	22
3.1	Chemicals and Reagents	22
3.2	Antibodies	22
3.2.1	Western Blot Antibodies	22
3.2.2	Cell Stimulation	23
3.2.3	Flow Cytometry Antibodies	23
3.2.4	Direct Immunofluorescence Antibodies	24
3.3	Primers	24
3.3.1	RANK(K240E) cDNA Generation and Site-directed Mutagenesis	24
3.3.2	Southern blot Amplification Probe	25
3.3.3	Genotyping	25
3.3.4	Real-Time PCR	26
3.3.5	Ig Clonality and Somatic Hypermutation PCRs	26
4	Methods	27
4.1	Polymerase Chain Reaction (PCR)	27
4.2	Genotyping PCR	28
4.3	Real-Time PCR	29
4.4	Ig Clonality PCR	29
4.5	Detecting Somatic Hypermutation Frequency	30
4.6	Molecular Cloning and Retroviral Transduction	31

4.7	Southern Blot	33
4.8	Cell Culture	34
4.9	Cell Purification	34
4.10	Cell Stimulation	35
4.11	Preparing Cell Lysates and Western Blot Analysis	36
4.12	Enzyme-Linked Immunosorbent Assay (ELISA)	37
4.13	Flow Cytometry and Fluorescence-activated Cell Sorting (FACS)	38
4.14	Histology	39
4.15	Immunofluorescence	40
4.16	Statistical Analysis	40
5	Results	41
5.1	RANK(A756G) Mutation <i>in vitro</i>	41
5.2	Mouse Model of Conditional RANK(A756G) Expression	42
5.2.1	Targeting of the ROSA26 Locus	42
5.2.2	B cell-specific expression of RANK(A756G)	45
5.2.3	RANK(A756G) ^{CD19-Cre} mice have splenomegaly, lymphadenopathy and show reduced survival	47
5.2.4	RANK(A756G) ^{CD19-Cre} mice have immune deposits in kidneys and accompanying proteinuria	49
5.2.5	RANK(A756G) expression in B cells leads to B cell activation, proliferation and B1 B cell expansion	49
5.2.6	RANK(A756G) expressing B cells upregulate MHCII and CD86 in the bone marrow	54
5.2.7	RANK(A756G) ^{CD19-Cre} mice have significantly increased anti- nuclear antibodies and immunoglobulins in serum	54

5.2.8	RANK(A756G) ^{CD19-Cre} mice have a polyclonal B cell repertoire and show increased somatic hypermutation	58
5.3	Cellular implications of RANK(A756G) expression in B cells	59
5.3.1	RANK(A756G) expressing B cells are dependent on RANKL for survival and proliferation <i>in vitro</i>	59
5.3.2	Murine RANKL activates RANK(A756G) expressing B cells <i>in vitro</i>	60
5.3.3	<i>In vitro</i> and <i>in vivo</i> activated T cells express RANKL	62
5.3.4	<i>In vitro</i> activated T cells induce a more activated phenotype in RANK(A756G) expressing B cells than in wildtype B cells .	64
5.3.5	ST2, a bone marrow stromal cell line, induces a more activated phenotype and an increased proliferative capacity in RANK(A756G) expressing B cells	65
5.3.6	RANK(A756G) expressing B cells show activation of PI3K and MAPK pathways upon RANKL stimulation	66
5.3.7	RANK(A756G) expressing B cells differentially express genes related to survival, proliferation and signaling	68
6	Discussion	70
	Nomenclature	75
	List of Figures	79
	Bibliography	86

Chapter 1

Introduction

1.1 The Immune System and Adaptive Immunity

1.1.1 General Features of the Immune System

The immune system has evolved to protect the host from invading pathogens. It is equipped with various tools that serve this purpose and can be roughly divided into two branches, based on their mechanisms of action. The first branch, the innate immune system provides a rapid response to an invading organism. This response usually lacks specificity and memory, is mainly driven by different cells of the myeloid lineage, such as the macrophages, neutrophils and dendritic cells, and is orchestrated through an array of cytokines and chemokines [1]. Danger signals are detected via pattern recognition receptors (PRRs) that recognize certain common motifs on the surface of pathogens, namely, pathogen-associated-molecular-patterns (PAMPs) [1, 2]. Detected pathogens are phagocytosed and thus eliminated. Innate immunity initiates inflammatory response and orchestrates an adaptive immune response through the presentation of the processed antigens to the cells of the adaptive immune system [3]. Adaptive immunity, on the other hand, takes longer time to respond, is strictly antigen specific, is capable of developing memory for a previously encountered antigen and is driven by the cells of the lymphoid lineage, namely the B cells and T cells. It is the precise crosstalk between these two branches of the immune system that makes it so efficient in detecting and eliminating the diverse

repertoire of pathogens the host encounters during the course of its lifetime [1, 4].

The major players in adaptive immunity are the B and T cells. One trait the two cell types have in common is the presence of an antigen receptor on the cell surface [5]. The antigen receptor is highly specific to a certain antigen and is generated by somatic gene rearrangements during the early development of a B or T cell. B and T cells arise from common lymphoid progenitors in the bone marrow. T cell precursors then migrate to the thymus where they continue their development, whereas B cells remain in the bone marrow. Once lymphocytes acquire a correctly rearranged antigen receptor in the primary lymphoid tissues they are developing in, they migrate into secondary lymphoid tissues, namely the spleen and lymph nodes, where they encounter their respective antigen, carried in via blood or the lymphatic system. B cells recognize intact antigens, whereas T cells can only recognize antigens that have been phagocytosed, processed as peptides and docked on major histocompatibility complex molecules on the surface of antigen presenting cells (APCs). Once the antigen is recognized, T cells provide cell-mediated immunity, through which the infected cell can be eliminated by cytotoxic T cells that are positive for the surface marker cluster of differentiation 8 (CD8). Alternatively, CD4 positive T cells can induce cytokine secretion and help orchestrate a cellular response for the antigen to be eliminated. B cells on the other hand, provide humoral response against the antigen. Upon recognition of the antigen and depending on the cytokine help from the environment, B cells secrete a variety of antibodies that aid the elimination of antigen [1, 6, 7, 8].

B cells play a primary role in humoral immunity, can present extracellular pathogens and toxins to T cells and are therefore indispensable for a fully functioning adaptive immune system. So far, two main subtypes of B cells have been discovered, namely, the B1 B cells and the B2 B cells, with distinct developmental stages and functions [9]. The next section will focus on the development of B2, or “conventional” B lymphocytes.

1.1.2 B2 B Lymphocyte Development

B2 B cells develop in the fetal liver and adult bone marrow in humans, as in

all mammals, from multipotent, self-renewing hematopoietic stem cells (HSCs), throughout the host's life [10]. Early development of B2 B cells depends on the interaction of B cell precursors with the bone marrow stroma and is strictly coordinated through temporal regulation of cytokine and chemokine secretion, as well as transcription factor expression. The HSCs in the bone marrow initially differentiate into multipotent progenitor cells (MPPs). MPPs are capable of differentiating into either myeloid or lymphoid cells, but are no longer capable of self-renewal. MPPs express the FLT3 receptor on their surface, and through their interaction with the FLT3 ligand on the bone marrow stromal cells, can further differentiate into common lymphoid progenitors (CLP). From then on, the CLPs commit to a B cell lineage through the interaction of the interleukin-7 (IL-7) receptors on their surface with the IL-7 secreted from the bone marrow stromal cells, becoming pro-B cells. B cell specific transcription factors such as E2A and early B-cell factor (EBF) are also expressed during this developmental stage. Murine pro-B cells depend on IL-7 for survival, whereas the human pro B cells do not. The stages of differentiation from a pro-B cell to a pre-B cell and then an immature B cell is marked by the production and surface expression of an antigen receptor, or the B cell receptor (BCR) [1, 11].

The BCR consists of two chains, namely, the heavy chain (H-chain) and the light chain (L-chain), which are produced by gene rearrangement through somatic recombination. In humans, as well as in mice, there are several variable (V), diversity (D), joining (J) and constant (C) gene segments in the genome, for the formation of a heavy chain. The gene rearrangement process is initiated by the upregulation of recombination-activating genes RAG-1 and RAG-2 and the activation of the VDJ recombinase complex. The VDJ recombinase complex brings about the cutting and joining of the D-J region first, and then that of the V region, to form a correctly rearranged VDJ region. Once the H-chain is rearranged, a surrogate light chain is expressed to form the pre-B cell receptor during the pre-B cell stage. Successful signaling from the pre-B cell receptor halts any further recombination events in the heavy chain locus (allelic exclusion), and leads to cell survival and proliferation. Light chain rearrangement from V and J regions in the genome and the binding to the constant region, which mediates the effector functions of an antibody, leads to the production of a successfully rearranged antigen receptor, surface immunoglobulin

M (IgM), and the progress into the immature B cell stage. The maturation of a B cell is marked by the double expression of IgM and IgD on its surface [1, 12].

The random joining of V, D and J segments from a selection of available gene segment sequences provides combinatorial diversity for the antigen receptor. The inaccurate splicing of the segments can result in frameshifts, and hence in the production of a different protein, providing junctional diversity to the receptor repertoire. During the ligation of the spliced segments, the enzyme deoxyribonucleotidyltransferase (TdT), which is a part of the VDJ recombinase complex, can add random untemplated nucleotides, contributing further to diversity. All these mechanisms of diversification ensure that the host is supplied with a large enough antigen receptor repertoire that will suffice for the entirety of the host's life, with the limited available space in the genome [13, 14].

Once the B2 B cells reach the immature stage, they egress from the bone marrow and move to peripheral lymphoid tissues via the circulation. Upon reaching the spleen, they acquire different functions, depending on their location. B cells that reside in the marginal zone of the splenic pulp (MZ B cells) serve as a first line of defense against blood-borne pathogens and show primarily T cell independent humoral responses. MZ B cells do not recirculate and remain in the spleen. Once the MZ B cells encounter their respective antigens, they develop into plasma cells without the need of T cell help, and secrete mainly IgM antibodies that have low antigen affinity [15, 16].

Most mature naive B2 B cells migrate to the B cell follicles in the spleen and lymph nodes and are called follicular B cells (FO B cells). Once they are activated by their respective antigen, they phagocytose, process and start presenting its epitopes on their surface on MHC II molecules, they move to the boundary between the follicle and T cell area, where they can get T cell help from CD4+ T cells that can detect the same antigen. This interaction is mainly mediated by MHCII presentation of the antigen by B cells, costimulation of the B cell through CD40 receptor (on B cells)- CD40 ligand (on T cells) binding and secretion of cytokines such as IL-21. Once all these signals are received by the B cell, it undergoes germinal center (GC) reaction, driven mainly by the transcription factor Bcl-6 and starts prolifer-

ating (clonal expansion) [17, 18]. One of the most important genes upregulated for a GC reaction is activation-induced deaminase (AID). AID is expressed specifically in activated B cells and deaminates cytidine residues in immunoglobulin V regions, leaving uridine residues, whose presence in DNA triggers DNA repair response. During DNA repair new mutations are introduced to the V region, which leads to the expression of altered antigen receptors. B cells which have a receptor with stronger affinity towards the antigen bind the available antigen, get further T cell help and survive in the GC, whereas the B cells with lower affinity receptors undergo apoptosis. This process through which a BCR repertoire with a higher affinity towards a specific antigen is generated, is called affinity maturation through somatic hypermutation (SHM) [1, 19, 20]. A second process that occurs through the activity of AID is class-switch recombination (CSR). When AID deaminates cytidine residues in the “switch regions”, the induced double stranded breaks are repaired and the C region of the μ chain is replaced by other Ig classes. Affinity maturation and CSR results in further diversification of the B cell repertoire [1].

Proliferating B2 B cells with a high affinity BCR become plasma cells and start producing somatically hypermutated and class switched antibodies, a developmental stage initiated by the expression of the transcription factor B-lymphocyte induced maturation protein-1 (Blimp-1) [21]. Short lived plasma cells can survive around 2-3 weeks after antigen encounter, whereas long lived plasma cells migrate to the bone marrow where they can reside for the life of the host [22]. Alternatively, B2 B cells can become memory cells after the GC reaction and contribute to immunological memory [21, 22].

1.1.3 B1 B Lymphocyte Development

Murine B1 B cells are derived from the fetal liver and are sustained in the periphery by self-renewal, rather than being continuously produced *de novo* in the bone marrow, in contrast to B2 B cells. They are the main cell population in the peritoneal and pleural cavities, and are found rarely in the spleen or lymph nodes [23]. There is ongoing debate about whether B1 and B2 B cells are derived from a common progenitor and the divergence is driven by antigen-dependent selection (the

selection model), or instead arise from different precursors of separate lineages (the lineage hypothesis) [24]. Considerable evidence has gathered in favor of the lineage hypothesis. B1 B cells are further divided as B1a (CD5+) and B1b (CD5-) cells [25].

B1 B cells are generated mainly before birth, starting as early as day 8.5 of mouse embryonic development, continuing into the first weeks after birth, and are sustained through self-renewal from then on, with a slow turn-over rate [26]. B1 cell development strongly depends on BCR ligation and nuclear factor-kappa B (NF- κ B) signaling. Studies have shown that the H-chain V segments used by B1 B cells are more restricted than that of B2 B cells, meaning that the B1 B cell repertoire is less diverse [27]. B1 B cells secrete polyreactive low-affinity antibodies against self-antigens, antigens expressed by apoptotic cells and several PAMPs [28]. The general polreactivity of B1 B cells ensures sustained BCR signaling and allows them to escape negative selection during development [29]. Self-reactivity of B1 B cells makes them the major supplier of “natural antibodies” of IgM class, which are present even in the absence of microorganisms, as was shown for germ-free mice [30]. B1 B cells are capable of class switching into any antibody *in vitro*, whereas *in vivo*, they preferentially switch to IgA [31].

B1 B cells can produce high levels of polyreactive IgM antibody at infection sites, or can migrate from the peritoneal cavity to the spleen or mucosal tissue in response to intraperitoneal or blood-borne pathogens and secrete IgM or IgA, respectively. There is also evidence that B1b cells contribute to immunological memory formation after an infection and a memory B cell population that resemble B1 B cells have been detected in the peritoneal cavity of mice [31, 32].

A population of CD5+ B cells has also been shown to exist in adult humans, although they do not reside in the peritoneal cavity as a distinct cell population. Although B1 B cells have various roles in tissue maintenance and pathogen elimination, their self-reactivity makes them prone to becoming pathological and B1 B cells have been implicated in autoimmune diseases [33]. Surface marker proteins of different subtypes of conventional B cells in mice throughout their developmental stages are shown below in Table 1.1 [34].

B cell subpopulation	Positive Surface Markers	Negative Surface Markers
pre-pro-B	CD43, CD93, CXCR4, B220, Flt3, IL7R	CD19, ckit ^{low} , CD24 ^{low} , IgM
pro-B	CD19, CD43, CD24, B220, IL7R	BP1, Flt3, ckit ^{low} , IgM
pre-B	CD19, CD25 ^{var} , CD24, B220, BP1, Siglec-G, IL7R	CD43 ^{low} , ckit, IgM
Immature B	CD19, CD24, CD93, B220, IgM	CD43, CD23, IgD
Transitional B	CD19, CD24, CD93, CD21 ^{var} , CD23 ^{var} , B220, IgM ^{high}	IgD ^{low}
Marginal zone	CD1d, CD9, CD21 ^{high} , CD22 ^{high} , CD35 ^{high} , B220, IgM	CD93, CD23, IgD ^{low}
Regulatory	CD1d ^{high} , IgM ^{high} , CD5, CD19, CD24, TIM	CD62L, CD93 ^{var} , IgD ^{var}
Follicular	CD19, CD22, CD23, CD38, B220, IgD	CD1d ^{low} , CD21/35 ^{low} , CD93, IgM ^{low}
Activated B	CD27, CD69, CD80, B220, Flt3, MHCII ^{high} , IgM, IgD	CD138, CXCR4
Germinal Center B	CD19, CD37, CD20, GL7, Siglec2, IgM/G/A/E	CD93, CD38 ^{low} , IgD ^{var}
Plasmablast	CD19, CD138, CXCR4, MHCII, IgM/G/A/E+	B220 ^{low} , Flt3
Plasma cell (long lived)	CD138, CXCR4 ^{high}	CD19, CD38 ^{low} , B220 ^{low} , MHCII, Ig
Plasma cell (short lived)	CD138, CD93, CXCR4 ^{high}	CD19, CD38 ^{low} , B220 ^{low} , MHCII ^{low} , Ig
Memory B	IgM/G/A/E+, B220	CD38 ^{var} , CD62L ^{var} , CD80 ^{var} , CD95 ^{low} , IgD ⁻

Table 1.1: Expression of surface markers on conventional mouse B cells during their development and differentiation.

1.1.4 B Cell Receptor Signaling and Antibody Secretion

The B cell receptor essentially consists of a surface immunoglobulin accompanied by signaling proteins $Ig\alpha$ and $Ig\beta$ that contain cytosolic immunoreceptor tyrosine-based activation motifs (ITAMs) [1]. BCR crosslinking activates the receptor associated Src-family protein tyrosine kinases (Blk, Fyn or Lyn) which in turn phosphorylate the ITAMs of $Ig\alpha$ and $Ig\beta$. Phosphorylated ITAMs bind and activate the spleen tyrosine kinase (Syk), which initiates a signaling cascade through Bruton's tyrosine kinase (BTK) that results in the activation of phospholipase C- γ 2 (PLC- γ), cleavage of membrane bound phospholipid PIP_2 , initiation of Ca^{2+} influx, activation of mitogen-activated protein kinases (MAPKs) and the activation of transcription factor NF- κ B via the Carma1/Malt1/Bcl-10 (CBM) complex, along with several other transcription factors such as AP-1 and NFAT. These transcription factors induce transcription of specific genes, leading to cell proliferation, differentiation and cytokine signaling. While receptors with an ITAM motif positively regulate signaling cascades, receptors with an immunoreceptor tyrosine-based inhibitory motifs (ITIMs) inhibit signaling pathways. Receptors with an ITIM motif recruit inhibitory phosphatases SHP and SHIP that remove the phosphate groups added by the tyrosine kinases. One example of an ITIM-containing inhibitory receptor is programmed death 1 (PD-1), which is induced transiently on activated B, T and myeloid cells to keep the signaling pathways in check. A detailed scheme of the BCR signaling cascade can be seen in Figure 1.1 [1, 35, 36].

Antigen dependent signaling from the BCR is enhanced when the BCR co-receptor is also bound by its respective ligand. The BCR co-receptor consists of CD19, CD21 and CD81, from which CD21 binds fragments of complement on the pathogen. This induces phosphorylation of the cytosolic tail of CD19, enhancing the signal coming from the BCR [37]. Upon antigen stimulation, B cells also up-regulate surface molecules CD80 and CD86, along with MHCII, which provide a costimulatory signal for T cells during B-T cell interaction [1, 38].

As mentioned above, antigen recognition by the BCR along with T cell help leads to antibody class switching. Different cytokines induce switching to different classes of antibodies, namely, IgG, IgE and IgA. IL-4 induces IgG1 and IgE switch,

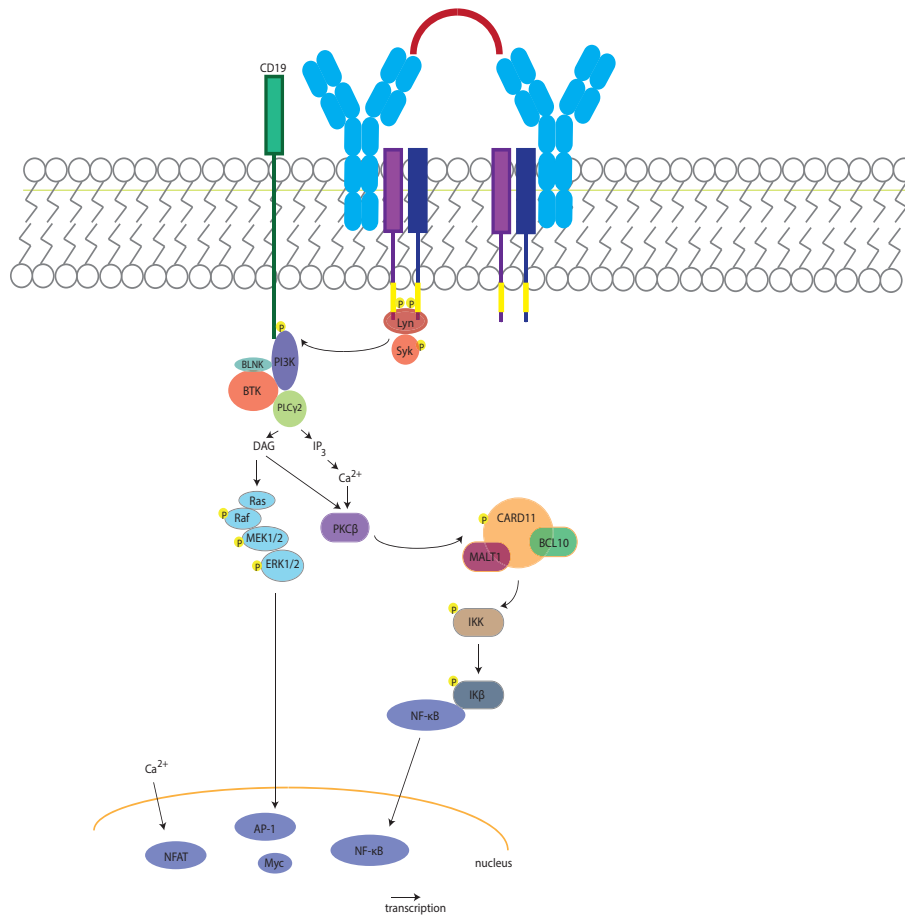


Figure 1.1: B cell receptor signaling cascade. Crosslinking of the BCR following receptor-specific antigen binding activates a signaling cascade through which receptor associated Src-family protein kinases phosphorylate the ITAMs of Ig α and Ig β , which phosphorylate and activate Syk and BTK, leading to the activation of PLC- γ 2. PLC- γ 2 then cleaves the membrane bound PIP_2 into IP₃ and DAG. IP₃ and DAG conduct the Ca^{2+} influx regulated activation of PKC β , which leads to the activation of the NF- κ B pathway through the assembly of the CBM complex. DAG also mediates the activation of MAPKs and the transcription factor AP-1 through small G proteins Ras and Raf. IP₃ regulated Ca^{2+} influx also leads to the activation of the transcription factor NFAT. NFAT, AP-1 and NF- κ B transcription factors in turn, induce expression of genes related to cell survival, proliferation and differentiation.

whereas interferon gamma (IFN- γ) induces IgG3 switch [39, 40]. Antibody classes are determined by the C region of IgH locus and they operate in distinct locations with distinct effector functions. IgA acts in the gut lumen as dimers, IgG and IgM are

prevalent in the blood, and IgE is mostly associated with mast cells below epithelial surfaces. IgG and IgA are effective in neutralization and opsonization of the antigen, while IgM is essential in activating the complement system and IgE is important for the sensitization of mast cells [1].

B cells are an essential part of the adaptive immune system, both due to their antigen presenting role and to their primary role in humoral immunity. B cell development and differentiation is intricate, temporally and spatially strict and involves many genetic recombination and mutation events. It is therefore necessary that developmental stages are strictly regulated with several checkpoints. Failure of these checkpoints results in severe pathology, in the form of lymphoid malignancies or autoimmunity. The next section focuses on B cell checkpoints and their breakdown during pathology.

1.2 B Cell Checkpoints and Pathology

1.2.1 Checkpoints in B Lymphocyte Development

One of the vital features of B cell effector mechanisms is the ability to discriminate self from non-self. During several stages of B cell development, the newly generated antigen receptors are checked for autoreactivity. The initial checkpoint is in the bone marrow, after the immature B cell stage, and is known as the central tolerance [41]. Immature B cells, which have no strong reactivity to self antigens and express surface IgM are allowed to mature and leave the bone marrow. The cells that bind self antigens that are ubiquitously expressed surface molecules undergo apoptosis (clonal deletion) or receptor editing, a process through which the receptor can be modified to become non-autoreactive [1, 42]. Cells that recognize soluble self molecules that are more weakly cross-linked, become anergic, a state of permanent unresponsiveness, and move to the periphery, where their clones are quickly outgrown by potent, non-self reactive B cells via their survival and proliferative advantage [42]. Some self-reactive B cells might escape this checkpoint, if their antigen is not available to them or they have a low affinity for self antigens, and

move to the periphery along with the non-autoreactive immature B cells, and are allowed to mature [1].

In case autoreactive B cells escape the central tolerance checkpoint, they may be inactivated in the periphery. Here the innate immune system comes into play. In the presence of an external antigen, the innate immune system provides signals that activate adaptive immunity to respond to the infection. If an antigen is recognized by B cells in the absence of infection, and hence in the absence of pro-inflammatory cytokines and co-stimulatory surface molecules, this leads to an inactivating negative signal and to the elimination of the autoreactive B cell. This second checkpoint mechanism is known as peripheral tolerance [43].

1.2.2 Autoreactive B Lymphocytes and Autoimmune Disorders

Some B cells which have low affinity for self antigens manage to escape the checkpoints, simply due to the fact that their respective antigen was not presented, or due to a breakdown in the tolerance mechanisms and an alteration in BCR signaling thresholds [44]. Another mechanism through which B cells can become autoreactive is somatic hypermutation in the germinal centers. Some B cells might acquire mutations that increase their affinity for self-antigens and fail to be eliminated [45]. These autoreactive B cells might occasionally detect their antigens in the presence of costimulation, for instance during an infection.

One such example is the activation of B cells specific for chromatin components in systemic lupus erythematosus (SLE). SLE is a systemic autoimmune disease, characterized by extensive secretion of anti-nuclear antibodies (ANAs), such as autoantibodies against DNA, chromatin proteins or ribonucleoproteins, and aggregation of immune deposits in organs, mostly kidneys, leading to lupus nephritis and kidney failure [46]. In an event of extensive apoptosis and reduced clearance of apoptotic cells, possibly as a result of an infection, B cells that recognize nuclear proteins might get the opportunity to bind to and internalize their antigens. DNA from apoptotic cells are enriched in unmethylated CpG residues, which are rare in humans compared

to microbes and thus serve as PAMPs for Toll-like receptor (TLR)9, an intracellular innate immunity receptor. TLR9 might bind its PAMP in endosomes and send a co-stimulatory signal, leading to the activation and expansion of an autoreactive B cell clone. These B cells can, in addition to secreting auto-reactive antibodies, present the antigen to auto-reactive T cells and activate them [1].

Another instance where autoreactive B cells can be activated is when their previously nonimmunogenic self antigen adopts an immunogenic form. For example, some autoreactive B cells that are specific for IgG are not activated under steady state conditions, despite the abundance of IgG in blood, because IgG is monomeric and does not cross-link the BCR. However, during a severe infection, IgG molecules dimerize and can be detected by autoreactive B cells, leading to the production of anti-IgG antibodies. If the immune complexes are cleared rapidly after an infection, this does not constitute a problem for the host. However, long-lasting exposure of the autoreactive B cells to their antigen leads to sustained production of these anti-IgG antibodies, also known as rheumatoid factor, since it is commonly seen in rheumatoid arthritis [1]. Rheumatoid arthritis is an autoimmune disease characterized by inflammation of joints. It is mediated by both CD4+ T cells and B cells, which upon T cell help generate arthritogenic antibodies in a pro-inflammatory environment, leading to tissue destruction.

Autoimmune disorders are defined by Davidson and Diamond as “clinical syndromes mediated by the abnormal activation of B cells or T cells, or both, in the absence of ongoing infection or other discernible cause” [47]. They can present either as a systemic disease or an organ-specific disease [48]. Autoimmune disorders can arise from a general defect in the selection or death of B or T cells, or due to abnormal response to one particular self-antigen. Genetic factors are crucial in determining the susceptibility to autoimmune diseases. Defects in the Fas ligand or its receptor, which mediate apoptosis in activated immune cells, mutations in the MHC alleles, or genetic alterations in genes encoding cytokines or antigen coreceptors are implicated in the development of autoimmune disorders, mostly working in concert with each other [49]. Vulnerability of the target organ to autoimmune-induced damage is also shown to be determined genetically. An autoimmune disorder can be initiated by environmental factors, infection, as mentioned above, non-infectious

agents such as drugs that alter the immune phenotype, or loss of regulatory cells that moderate immune response. As the disease progresses, it is possible that the autoantigens targeted by T and B cells increase due to the pro-inflammatory environment and constant antigen presentation, which makes it clinically difficult to determine the initiating antigen [50].

The common objective of therapeutic approaches to autoimmune diseases is to down-modulate the immune system activity. One strategy to achieve this is to block molecules such as TNF- α , interleukin receptors or CD4 [51]. In SLE, CD40 ligand blockade was shown to be highly effective in murine mouse models, but not in humans due to side effects [52, 53]. The first biological drug approved by the FDA for treatment of SLE is belimumab, which is a monoclonal antibody that blocks B-cell activating factor (BAFF), a cytokine that regulates B cell survival and differentiation [54]. Further knowledge on the involvement of B and T cells in the progression of autoimmune disorders, along with genetic factors and initiating antigens is necessary to develop effective courses of treatment.

1.2.3 B Lymphocyte Development and Lymphoid Malignancies

B cell development and differentiation contains several steps where the genomic integrity is compromised or cells expand rapidly. When these processes, inherently risky and error prone, go awry, the consequences for the organism can be severe, and lead to malignancies, namely, leukemias and lymphomas [55]. One such process is the V(D)J recombination. During the recombination events that lead to the generation of Ig heavy and light chains, double stranded breaks that are induced by RAG enzymes can be repaired in an aberrant fashion, leading to chromosomal translocation. Chromosomal translocations typically lead to the replacement of the regulatory elements of a gene by a part of another gene, resulting in dysregulated gene expression. Later in the life of a B cell, i.e. during GC reaction, SHM and CSR, which also require induction of DNA breaks, chromosomal translocations may arise. Dysregulated expression of several genes such as Bcl-2, cyclin D1, Bcl-6, that are important for cell proliferation and apoptosis leads to malignancies like follicular

lymphoma, mantle-cell lymphoma or Burkitt lymphoma, respectively [56, 57, 58].

Lymphomas are generally named after the normal B cell counterpart of malignant B cells. In mature B cell lymphomas, the malignant cells are usually arrested at a certain B cell developmental stage [55]. In Hodgkin's lymphoma for instance, the malignant Hodgkin and Reed-Sternberg (HRS) cells originate from GC B cells [59]. Diffuse large B-cell lymphoma (DLBCL), which is the most common non-Hodgkin's lymphoma in adulthood (30-40% of the cases) have two subtypes based on their gene expression profiling [60]. GC B-cell-like DLBCLs (GCB DLBCLs) have a gene-expression profile that resembles a B cell undergoing GC reaction (such as high expression of GC B cell signature gene *Bcl-6*), and thus are thought to originate from GC B cells, whereas activated B-cell-like DLBCLs (ABC DLBCLs) have a gene expression profile that resembles activated B cells, with a pronounced expression of $\text{NF-}\kappa\text{B}$ target genes such as cyclin D2 and *Bcl-2*. ABC DLBCLs are therefore postulated to arise from pre-plasma cells, and are arrested at this developmental stage [61]. Mutations of several genes that lead to dysregulation of the $\text{NF-}\kappa\text{B}$ pathway is a hallmark of ABC DLBCLs. In 30% of ABC DLBCL cases, the activity of A20, which is a negative regulator of the $\text{NF-}\kappa\text{B}$ pathway is impaired by inactivating mutations or deletions. Positive regulators such as *CARD11*, *TRAF2*, *TRAF5* and receptor activator of $\text{NF-}\kappa\text{B}$ (*RANK*) are also affected by activating somatic mutations that enhance their ability to activate the $\text{NF-}\kappa\text{B}$ pathway. The collective inhibition of $\text{NF-}\kappa\text{B}$ inactivating genes with the activation of $\text{NF-}\kappa\text{B}$ activating genes lead to constitutive activation of the $\text{NF-}\kappa\text{B}$ pathway and thus to uncontrolled cell proliferation and reduced cell death, promoting lymphomagenesis [62].

Since different subtypes of lymphoma originate from B cells at different developmental stages, with distinct gene expression profiles, the strategies for treating each subtype along with the response to treatment from each subtype are also different. ABC DLBCLs for instance, have a worse prognosis compared to GCB DLBCLs [61]. The elucidation of gene expression profiles may help develop differential treatments for these two subtypes of DLBCLs. ABC DLBCL cases that do not respond to conventional therapies can additionally be treated with selective $\text{NF-}\kappa\text{B}$ inhibitors, such as, bortezomib, which is a proteasome inhibitor that prevents degradation of

inhibitors of the NF- κ B pathway [63]. However, 17% of ABC DLBCL patients are refractory to bortezomib and further understanding of the NF- κ B mechanism may unravel further treatment options [64].

As mentioned above, one of the genes that carry somatic mutations in ABC DLBCL patients is RANK. The next section focuses on the function of RANK and its putative role in development of pathology.

1.3 Receptor Activator of NF- κ B: Function and Pathology

1.3.1 Characteristics and Function of Receptor Activator of NF- κ B Signaling

RANK (also designated TNFRSF11A), is a homo-trimerizing transmembrane receptor that belongs to the tumor necrosis factor (TNF) superfamily. RANK trimerizes after binding its ligand, the RANK ligand (RANKL, also designated TNFSF11) which can be found both in membrane-bound and soluble form. The cleavage of soluble RANKL from the membrane bound form is mediated by a metalloprotease, TNF- α convertase (TACE). Murine RANKL shares 83% homology with human RANKL. RANK is not the only receptor for RANKL that is so far discovered. Osteoprotegerin (OPG, also designated as TNFRSF11B), a soluble protein distinct from RANK, binds and neutralizes RANKL and balances RANK signaling by acting as a decoy receptor. Upon binding its ligand and trimerizing, RANK, which lacks kinase activity itself, recruits TRAFs 2,3,5 and 6 to its cytoplasmic domain to distinct binding motifs, which in turn activate MAPKs and the canonical and non-canonical NF- κ B pathways. RANK signaling is also essential in the induction of transcription factors c-fos and NFATc1/NFAT2. A detailed scheme of the RANK signaling pathway is shown in Figure 1.2 [65, 66, 67].

NF- κ B is a transcription factor complex that comprises different dimeric subunits which slightly differ in function. The first family of NF- κ B proteins is the REL family,

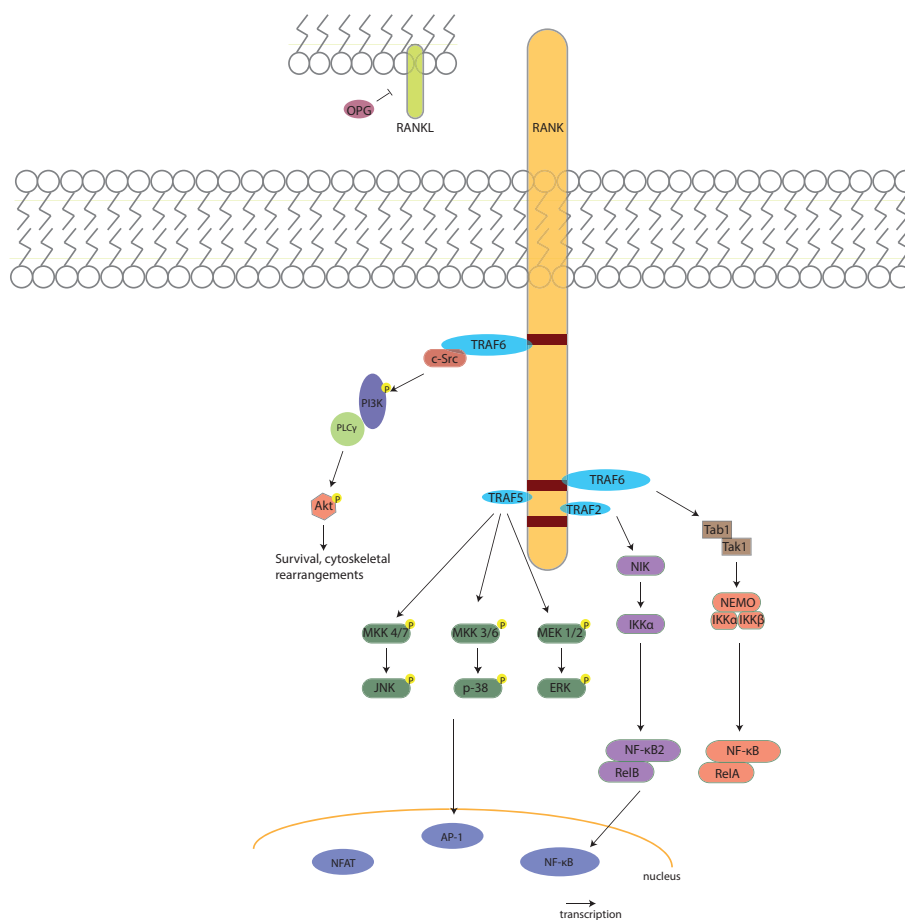


Figure 1.2: Receptor Activator of NF- κ B signaling cascade. Upon binding its ligand, RANKL, RANK recruits TRAFs which relay the signal downstream, and induce the activation of JNK, ERK and p38 MAPKs, the PI3K pathway and the alternative and canonical NF- κ B pathways, leading to cell survival, proliferation and osteoclastogenesis. RANKL can be found in membrane-bound or soluble form, cleaved by metalloproteases. OPG, a soluble decoy receptor for RANKL distinct from RANK is essential in balancing the RANK-RANKL signaling axis and abrogating signaling by binding excess RANKL.

with members RELA (also known as p65), RELB and c-REL. The second family comprises the proteins NF- κ B1 (also known as p105) and NF- κ B2 (also known as p100), which are precursors that are processed to form the mature proteins p50 and p52, respectively. Combination of these proteins in dimers gives rise to two slightly different pathways, namely the canonical and non-canonical pathway. The canonical pathway utilizes RELA, c-REL and p50 dimers, which are normally sequestered in the cytoplasm by inhibitor of κ B proteins (I κ B) in the steady state. Once a

signaling pathway is activated, i.e. after by the binding of RANKL to RANK, the TRAFs that are recruited to the cytoplasmic domain, bind and activate the $I\kappa B$ kinase complex (IKK), which then phosphorylates $I\kappa B$ by its β subunit, and marks it for ubiquitinylation. The non-canonical pathway on the other hand, utilizes the RELB-p52 dimers and is regulated by the α subunit of the IKK complex, and the NF- κB inducing kinase (NIK). After the degradation of $I\kappa B$, released transcription factor dimers can translocate to the nucleus and induce the expression of many downstream genes which are involved in cell survival, proliferation, motility and cytokine secretion [68, 69, 70].

MAPKs, the second major pathway activated by RANK-RANKL signaling, also activate a variety of cellular responses involved in cell growth, proliferation, apoptosis and inflammation. There are three main families of MAPKs discovered so far; extra-cellular signal regulated kinases (ERKs), Jun amino-terminal kinases (JNKs) and p38/stress-activated protein kinases (SAPKs). MAPKs are activated by a sequential phosphorylation process involving upstream protein kinases (MAPK kinases, e.g. TAK1) which are activated by adaptor proteins recruited to the cytoplasmic domain of RANK (TRAFs 2/5 and 6). The activated MAPKs lead to the translocation of several transcription factors to the nucleus for upregulation of genes of interest [71, 72, 73]. RANK-RANKL signaling also leads to the activation of PI3K and Akt signaling, whose downstream target genes include many that are important for survival, proliferation and growth, metabolism and angiogenesis, through adaptor proteins Gab2 and Cbl [74, 75]. Taken together, the RANK-RANKL signaling activates several downstream pathways through an intricate network of adaptor proteins, which are all important in cell proliferation, apoptosis, differentiation and metabolism.

RANK is a master regulator in osteoclast differentiation and thus is vital in bone homeostasis [76]. Bone is crucial for the sustenance of skeletal strength, maintenance of calcium reservoirs and the development of immune cells. Bone homeostasis is maintained by the constant breakdown (resorption) and synthesis of the bone, by the two main cell types osteoclasts and osteoblasts, respectively [77]. RANK is expressed on osteoclast precursors, and when it binds the RANKL expressed by the stromal cells in the bone, osteoclast maturation is triggered through the transcription factors

c-fos, *NFatc1/NFAT2* and $\text{NF-}\kappa\text{B}$ [78]. Studies in RANK and RANKL knockout mice showed that they develop osteopetrosis, a condition marked by abnormally hardened bones, due to the lack of mature osteoclasts breaking the bone down [79]. In contrast, an overactivation of this pathway, for instance due to loss of OPG, leads to osteoporosis, as a result of enhanced bone resorption [80].

Further studies in genetically manipulated mice have shown that RANK-RANKL signaling is also important in organogenesis and immune reactions. RANK signaling was shown to be involved in the development of secondary lymphoid tissues, through its role on lymphoid tissue inducer cells during embryogenesis [81]. RANK and RANKL knockout mice show a lack of peripheral lymph nodes and Peyer's patches, along with developmental abnormalities in the spleen [82]. RANK signaling is also important for thymus development, especially for the development of medullary thymic epithelial cells that are essential for the negative selection of autoreactive T cells [83]. RANK and RANKL knockout mice also show defects in mammary gland development [84]. In the immune system, RANK is expressed mainly on dendritic cells (DCs) and RANKL on activated T cells. Macrophages and monocytes also express RANK to some extent, and B cells can upregulate surface RANK expression in response to CD40 ligation. RANK-RANKL ligation is important for DC survival and cytokine production, indicating a possible role of RANK in antigen presentation [85]. Absence of RANK signaling *in vivo* however can fully be compensated by the closely related CD40 signaling, since these mice show no abnormalities in DC development [86]. RANK and RANKL knockout mice show abnormalities in B and T cell development, respectively, although it was later shown that the effect of RANK signaling on B cell development is not cell intrinsic, and rather stems from a disturbed microenvironment in the bone marrow, where B cells develop [82, 87]. Overall, RANK-RANKL signaling was shown to be important in organogenesis, bone homeostasis, immune system development and reaction to antigen, and plays a central role in the osteo-immunological network.

1.3.2 Receptor Activator of $\text{NF-}\kappa\text{B}$ and Pathology

Given its role in the activation of a variety of pathways, dysregulation of RANK

signaling has been implicated in the development of several diseases. Mutations in RANK have been linked to the development of bone diseases such as Paget's disease or autosomal-recessive osteopetrosis [88, 89]. Disruption of the balance between RANK/RANKL concentrations in the bone environment in favor of RANKL was shown to cause osteoporosis in post-menopausal women [90]. Similarly, high RANKL expression in the synovium is the cause of bone destruction in rheumatoid arthritis [91].

Dysregulation of RANK-RANKL signaling has also been implicated in many types of cancer. RANK expression on primary tumors is a poor prognostic marker in breast cancer, and has been associated with bone metastasis [92]. Expression of RANK on prostate cancer cells is also shown to aid in the metastasis to bone [93]. Giant cell tumors of bone are shown to overexpress RANK and RANKL [94]. Among lymphoid malignancies, cultured Hodgkin's lymphoma disease cells (Hodgkin and Reed Sternberg cells) co-express RANK and RANKL on their surface, leading to an autocrine positive feedback loop that enhances survival [95]. Multiple myeloma cells are also shown to disrupt the RANKL/OPG balance in favor of RANKL, either by expressing RANKL themselves or inducing the bone marrow stromal cells to overexpress RANKL, leading to bone lesions in patients [96]. Chronic lymphocytic leukemia (CLL) B cells have also been shown to have increased surface expression of RANK and RANKL, which leads to the induction of IL-8 secretion in B-CLL cells [97]. Strikingly, in 8% of ABC DLBCL patients mutations in RANK have been observed. A frequent mutation is the A756G mutation that leads to an amino acid change at position 240 from lysine to glutamine (K240E), that is located in the intracellular domain [61]. Yet, the functional consequences of this mutation is largely unknown.

Given the effect of dysregulation of the NF- κ B pathway on several B cell related disorders, the occurrence of this RANK mutation in ABC DLBCL patients is intriguing. As the functional consequences of this mutation and of enforced RANK signaling in B cell physiology or lymphomas have not yet been described, a study was designed to investigate the role of the K240E mutation and abnormal RANK signaling in B cells. The following chapter describes the objectives and methods of the designed project.

Chapter 2

Research Objective

Aberrations in signaling pathways during different stages of B cell development have diverse pathological repercussions such as autoimmune disorders or lymphoid malignancies. Activating mutations in, or overexpression of, genes that induce survival, proliferation and prevent apoptosis, as well as inactivation of regulatory genes have been demonstrated to result in lymphomagenesis. RANK, a receptor important for both osteoclastogenesis and activation of the adaptive immune system, has been shown to be mutated in 8% of ABC-DLBCL cases, whose characteristic is the constitutive activation of NF- κ B. The recurrent A756G (K240E) mutation in RANK was detected in 8% of these patients. The functional effects of this mutation in B cells *in vivo* and whether it drives or promotes the progress of B cell pathology in general remain elusive. RANK signaling is shown to be upregulated in Hodgkin's lymphoma, as well as multiple myeloma and CLL. The exact signaling networks through which the upregulation of RANK/RANKL promotes B-cell malignancies is currently unknown.

Based on the frequent dysregulation of the RANK signaling pathway in different entities of B-cell malignancies, this study aims to elucidate the role of the K240E mutation and deregulated RANK signaling in B cell development and pathology. The conditional gene targeting approach in mice was employed to tackle this question. Human RANK(A756G) cDNA was introduced into the ubiquitously expressed murine ROSA26 locus. A STOP cassette flanked by loxP sites was located in front of the RANK cDNA, to ensure transcription would only occur after breeding with the

Cre-transgenic mice of interest, and achieve tissue and time specific deletion of the stop cassette. B-cell specific expression of RANK(A756G) was achieved by breeding the Rosa26 targeted mice with CD19-Cre mice, since CD19 is a B-cell specific surface molecule whose expression is initiated early in B cell development, following the pro-B cell stage.

The objective of this study is, to utilize a mouse model that sheds light onto the role of aberrations in RANK signaling in B cell biology. Identifying the mechanisms that are dysregulated upstream or downstream of RANK is also important for therapeutical efforts in treating several B cell malignancies.

Chapter 3

Materials

3.1 Chemicals and Reagents

All chemicals and reagents were purchased from Sigma-Aldrich, unless stated otherwise. For a detailed description of the reagents and their origin, see the “Methods” section.

3.2 Antibodies

3.2.1 Western Blot Antibodies

Name	Company
α -phospho-PLC γ 2 (Tyr1217; rabbit polyclonal IgG)	Cell Signaling
α -phospho-Akt (Ser473; rabbit polyclonal IgG)	Cell Signaling
α -phospho-p44/42 MAPK (Erk1/2) (Thr202/Tyr204; rabbit polyclonal IgG)	Cell Signaling
α -phospho-SAPK/JNK (Thr183/Tyr185; rabbit polyclonal IgG)	Cell Signaling
α - β -Actin (mouse monoclonal IgG)	Cell Signaling
α -mouse IgG HRP-linked (horse polyclonal IgG)	Cell Signaling
α -rabbit IgG HRP-linked (goat polyclonal IgG)	Cell Signaling

3.2.2 Cell Stimulation

Name	Company
Functional grade purified α -mouse CD3e (145-2C11)	e-Bioscience
Functional grade purified α -mouse CD28 (37.51)	e-Bioscience
AffiniPure rabbit α -Syrian Hamster IgG	Jackson Immuno Research

3.2.3 Flow Cytometry Antibodies

Flow cytometry antibodies listed below were conjugated to one of the following fluorochromes: phycoerythrin (PE), phycoerythrin cyanin 5 (PE-Cy5), phycoerythrin cyanin 7 (PE-Cy7), allophycocyanin (APC), allophycocyanin cyanin 7 (APC-Cy7) or eFluor 506. Only the purified α -mouse CD16/32 antibody used for Fc receptor blocking was unconjugated.

Name	Company
7-AAD Viability Staining Solution	e-Bioscience
Annexin V Apoptosis Detection Kit	e-Bioscience
Cell Trace Violet Cell Proliferation Kit	ThermoFisher Scientific
Fixable Viability Dye eFluor 506	e-Bioscience
α -mouse B220 (RA3.6B2)	e-Bioscience
α -mouse CD4 (GK1.5)	e-Bioscience
α -mouse CD5 (53-7.3)	e-Bioscience
α -mouse CD8 (53-6.7)	e-Bioscience
α -mouse CD16/32 (93), purified	e-Bioscience
α -mouse CD19 (1D3)	e-Bioscience
α -mouse CD25 (3C7)	e-Bioscience
α -mouse CD44 (IM7)	e-Bioscience
α -mouse CD62L (MEK-14)	e-Bioscience
α -mouse CD80 (16-10A1)	e-Bioscience

α -mouse CD86 (GL1)	e-Bioscience
α -mouse CD93 (AA4.1)	e-Bioscience
α -mouse CD117 (c-kit) (2B8)	e-Bioscience
α -mouse CD138	BD Pharmingen
α -mouse Ki67 (SolA15)	e-Bioscience
α -mouse IgM (II/41)	e-Bioscience
α -mouse MHCII (M5/114.15.2)	e-Bioscience
α -mouse RANK(CD265, 9A725)	ThermoFisher Scientific
α -mouse RANKL(CD254, IK22/5)	e-Bioscience

3.2.4 Direct Immunofluorescence Antibodies

Name	Company
α -mouse IgG (Alexa Fluor 488 goat polyclonal)	ThermoFisher Scientific
α -mouse IgM (Alexa Fluor 647 goat polyclonal)	ThermoFisher Scientific

3.3 Primers

All primers were synthesized by Sigma-Aldrich or Eurofins Scientific. All primers that were not previously published were designed using the freeware ApE.

3.3.1 RANK(K240E) cDNA Generation and Site-directed Mutagenesis

Name	5'-3' Sequence
hRANKF	ATGCGGTTTGCAGTTCTTCTC
hRANKR	ACTCCTTATCTCCACTTAGG
xhoI fwd	CTCGAGAACAACCTTTATCCTCCTGGAA
ecoRI rev	GAATTCAGGTGCGGGAGCGGTTAGTTC
xhoI fwd	CTCGAGAACAACCTTTATCCTCCTGGAA

ecoRI rev	GAATTCAGGTGCGGGAGCGGTTAGTTC
fwd ascI	GGCGCGCCCCACCATGAACAAC TTTATCCTCCTGG
rev ascI	GGCGCGCCAGGTGCGGGAGCGGTTAGTTC
kd fwd	GTGAAAACCGTGGCTGTGAGAATACTGAAAAACGAGGCC
kd rev	GGCCTCGTTTTTTCAGTATTCTCACAGCCACGGTTTTTCAC
ph fwd	CCCTCGAACTTTAAAGTCTGCTTCTTTGTGTTAACC
ph rev	GGTTAACACAAAGAAGCAGACTTTAAAGTTTCGAGGG

3.3.2 Southern blot Amplification Probe

Name	5'-3' Sequence
probe fwd	GATCAAAACACTAATGAACTT
probe rev	TTAATTAAAACGAATATTTGGAAT

3.3.3 Genotyping

Name	5'-3' Sequence
Cre7	TCAGCTACACCAGAGACGG
CD19c	AACCATTCAACACCCTTCC
CD19d	CCAGACTAGATACAGACCAG
RANK _{geno}	ACACTGGCTAGGAGAGATTCCTTC
Long _{geno}	ACTCGGGTGAGCATGTCTTTAATC
Short _{geno}	GTGATCTGCAACTCCAGTCTTTCTA
IRES _{geno}	ATACGCTTGAGGAGAGCCATTTG

3.3.4 Real-Time PCR

Name	5'-3' Sequence
ActinF	AGACCTCTATGCCAACACAG
ActinR	TCGTACTCCTGCTTGCTGAT
APCF	CTTGTGGCCCAGTTAAAATCTGA
APCR	CGCTTTTGAGGGTTGATTCCT
Bcl-2F	CTGCACCTGACGCCCTTCACC
Bcl-2R	CACATGACCCACCGAACTCAAAGA
CyclinD1F	GCGTACCCTGACACCAATCTC
CyclinD1R	CTCCTCTTCGCACTTCTGCTC
IKK- β F	AGCTGTCCTTACCCTGCTGA
IKK- β R	TGCTGCAGAACGATGTTTTTC
MALT1F	GGTGGATGTGTATGAATTGACCA
MALT1R	ACCGTGCCCTGCATAATATAAC
PTENF	CTTTTTCTTCAGCCACAGGC
PTENR	GCAGTTAAATTTGGCGGTGT

3.3.5 Ig Clonality and Somatic Hypermutation PCRs

Name	5'-3' Sequence
JH4	AAAGACCTGCAGAGGCCATTCTTACC
DSF	AGGGATCCTTGTGAAGGGATCTACTACTGTG
V _H A	GCGAAGCTTA (AG) GCCTGGG (AG) CTTCAGTGAAG
V _H B	GCGAAGCTTCTCACAGAGCCTGTCCAATCAC
V _H C	GCGAAGCTTTCTCAG (AT) CTCTGTC (CT) CTCACC
V _H D	GCGAAGCTTCTGCAGTCTGGAGGTGGCCTG
V _H E	GCGAAGCTTGTGGAGTCTGGGGGAGGCTTA
V _H F	GCGAAGCTT (AT) CTGGAGGAGGCTTGGTGCAA
V _H G	GCGAAGCTTGGAGAGACAGTCAAGATCTCC
D _{Q52}	ACGTCGACGCGGACGACCACAGTGCAACTG
D _{FS}	ACGTCGACTTTTGT (GC) AAGGGATCTACTACTGT
J _H 4E	AGGCTCGTAGATCCCTACACAG
J _H 4A	GGGTCTAGACTCTCAGCCGGCTCCCTCAGGG

Chapter 4

Methods

4.1 Polymerase Chain Reaction (PCR)

The polymerase chain reaction is used to amplify nucleotide sequences of interest. It utilizes two or more forward and reverse primers that bind to the single-stranded DNA in the desired region of the genome and a DNA polymerase to synthesize the fragment aimed to be amplified. A PCR consists of three phases; denaturation, where the double-stranded DNA input is denatured into single-stranded DNA molecules with the help of high temperatures that destabilize DNA; annealing, where the designed primers bind to the region of interest at a lower temperature; and extension where the DNA polymerase synthesizes the DNA fragment of interest, by adding templated nucleotides from the primer-binding site on. These three steps are repeated as several cycles, typically 30 to 35 times, to maximize the yield of the reaction [98].

In the work at hand, PCRs have been used for several purposes, such as genotyping mice, Real-Time PCR, determining the clonality of the B cell repertoire of RANK(A756G) mice, determining the level of somatic hypermutation in transgenic B cells and molecular cloning. Unless stated otherwise, the amplification reactions were set up with 0.2mM dNTP (Bioline), 0.2 μ M of each primer, 50ng template, 0.04U/ μ l of Phire HotStart II DNA polymerase (ThermoFisher Scientific) in reaction buffer (ThermoFisher Scientific). Reaction volumes were chosen to be 25 or 50

μl , depending on the application. All reactions were implemented in a PCR thermocycler (Bio-Rad). Further specifications of reactions for different applications are given in the respective sections. PCR products were visualized by agarose gel electrophoresis, as previously described [99].

4.2 Genotyping PCR

Presence of the RANK(A756G) and CD19-Cre alleles in mouse progeny was determined through amplification of transgene-specific sequences by genotyping PCR. For this purpose, DNA was isolated from the tails of 3-week old mice by using the Wizard SV Genomic DNA Purification System Kit (Promega). The allele containing ROSA26^{loxSTOPlox}-RANK(A756G) was detected by a 4-primer PCR (long, short, IRES, RANK genotyping primers), capable of amplifying both the sequence of the recombined locus with the IRES-RANK primer pair and the wildtype locus with the long-short primer pair. The recombinant locus yields at 570 base-pair band whereas the wildtype locus yields a 300 base-pair band. The Cre allele of CD19-Cre mice was detected utilizing a 3-primer PCR with CD19c/CD19d/Cre7 primers. The recombinant and wildtype loci yield bands of size 715 base-pair and 492 base-pair, respectively. The PCR conditions for RANK and CD19-Cre genotyping PCRs are as follows:

RANK genotyping PCR

Phire HotStart activation	30", 98°C
35 cycles	denaturation: 5", 98°C annealing: 5", 62°C extension: 15", 72°C
End elongation:	1', 72°C

CD19-Cre genotyping PCR

Phire HotStart activation	30", 98°C
35 cycles	denaturation: 5", 98°C annealing: 5", 57°C extension: 15", 72°C
End elongation:	1', 72°C

4.3 Real-Time PCR

RNA was freshly isolated from sorted RANK(A756G) expressing and wildtype B cells by using RNeasy Mini Kit (QIAGEN), according to the manufacturer's instructions. RNA concentration of the samples was determined by NanoDrop. (Thermo Fischer Scientific Inc.) RNA was reverse transcribed using SuperScript II (Invitrogen) according to the manufacturer's instructions. Briefly, with 20 μ l reaction of 100 ng- 1 μ g total RNA, 0.5mM dNTPs, 250ng random primers, 5mM DTT, and 10U/ μ l of SuperScriptTM II RT was set up. The generated cDNA was used in duplicates or triplicates for RT-PCR reactions, with primers that span exon-exon boundaries to ensure cDNA-specific amplification. The qPCR Core Kit for SYBR Green I (Roche) was used to perform RT-PCR. Gene expression patterns were normalized to the housekeeping gene, Actin. The reaction was carried out in a Light Cycler 480 II (Roche) and analyzed for quality using melting curves. The conditions for the amplification reaction are as follows:

HotGoldStar activation	10', 95 °C
45 cycles	denaturation: 15", 95 °C annealing: 20", 60 °C extension: 40", 72 °C

4.4 Ig Clonality PCR

The clonality of the B cell repertoire in mice was determined by PCR, as described previously [100]. Briefly, GFP+ B cells and CD19+ B cells were sorted

from RANK(A756G)^{CD19-Cre} and CD19-Cre mice, respectively. B cell genomic DNA was isolated using DNeasy Blood&Tissue Kit (QIAGEN), according to the manufacturer's instructions. A clonality PCR with the primer pair DFS-JH₄ was implemented using the Expand Long Template PCR System (Roche), according to the manufacturer's instructions. DFS primer hybridizes to the 5' recombination signaling sequence of all murine DH segments, whereas JH₄ hybridizes downstream of the JH₄ segment, leading to the amplification of four possible DJH recombinations with a "ladder" appearance on the agarose gel in a polyclonal B cell repertoire. The conditions of the PCR reaction are as follows:

94°C	2'
35 cycles of:	
94°C	1'
60°C	90"
68°C	2' (3" increment)
68°C	10'

4.5 Detecting Somatic Hypermutation Frequency

Somatic hypermutation frequency was detected implementing a PCR method as previously described [101]. Briefly, a set of 5' consensus primers (specified in the "Materials" section) that are homologous to murine VH or DH genes in combination with a 3' primer downstream of the JH₄ cluster are used to amplify many several fragments at once. The product of this first reaction is then used for a second PCR, utilizing a nested PCR approach, where the amplified product is analyzed in separate reactions with a single VH or DH primer in combination with a 3' nested JH primer. GFP+ B cells and CD19+ B cells of RANK(A756G)^{CD19-Cre} and CD19-Cre mice, respectively were sorted and their genomic DNA was isolated as mentioned in section 4.4, and 50 ng of it was used for the PCR, where the Expand Long Template PCR System (Roche) was used according to the manufacturer's instructions. The PCR product was run on agarose gel, and the bands were excised and cleaned up using peqGOLD gel extraction kit (Peqlab Biotechnologie). The extracted DNA

fragments were cloned into a TOPO TA vector using the TOPO TA Cloning Kit for Sequencing (ThermoFisher Scientific) according to manufacturer's instructions. The cloned DNA fragments were sequenced by Source BioScience and the sequencing results were analyzed using ApE freeware and the IMGT/V-QUEST database.

4.6 Molecular Cloning and Retroviral Transduction

In the presented work, molecular cloning technique was applied to generate retroviral expression vectors of wildtype RANK and RANK(A756G), using the vector pMIGR1 as well as the pRosa26^{loxSTOPlox-RANK(A756G)} targeting vector for the generation of a mouse knockin, as described previously [102, 103]. The generation of the pRosa26^{loxSTOPlox-RANK(A756G)} vector and the retroviral expression vector for wildtype RANK was done by Dr. Nathalie Knies. Briefly, cDNA of interest was amplified by PCR, using a DNA polymerase with proofreading capability (Phusion High Fidelity DNA Polymerase-ThermoFisher Scientific), flanked by restriction endonuclease recognition sites. This cDNA insert was ligated to a TOPO TA vector, according to the manufacturer's instructions. One Shot Top10 chemically competent E.coli (Invitrogen) were used for all TOPO TA Cloning procedures. Following the initial ligation reaction, 2 μ g of the TOPO TA vector containing the insert was digested with the restriction enzymes of interest. Depending on the application, 2 μ g of the pRosa26 targeting vector or pMIGR1 was also digested with the same restriction enzymes (overnight at 37°C), and the product was run on an agarose gel the following day. Digested fragments of the desired insert and the desired end vector were extracted from the gel using the QIAquick Gel Extraction Kit (Qiagen), according to the manufacturer's instructions. The purified vector backbone and insert were then ligated using T4 ligase (Invitrogen), according to the manufacturer's instructions. The ligation product was then used for transformation of Subcloning Efficiency™ DH5alpha™ chemically competent E.coli (Invitrogen) according to the manufacturer's protocol, and the successfully transformed bacteria were selected for by using ampicillin containing LB agar plates, as ampicillin resistance gene beta-

lactamase was the selection marker of both target vectors. For the generation of pRosa26^{loxSTOPlox-RANK(A756G)} targeting vector, only a single restriction enzyme was used to linearize the vector backbone, therefore dephosphorylation of the two ends of the backbone was performed by incubating the digested vector in 0.025U/ μ l Calf Intestinal Alkaline Phosphatase (ThermoFisher Scientific) at 37°C for 1h, to increase ligation efficiency, prior to ligation.

The pMIGR1 vector used for retroviral transduction of Bal17 cells with wildtype RANK and RANK(A756G), is an MSCV based vector, carrying an IRES (internal ribosomal entry site)-GFP sequence, which enables GFP expression and thus allows fluorescence assisted cell tracking of the cells that contain the vector. The human mutant RANK cDNA sequence was generated by a site-directed mutagenesis PCR utilizing the primer pair hRANK forward and hRANK reverse, as described in the “Materials” section. The amplification conditions for the reaction were 95°C for 1’, 18 cycles of 95°C for 50”, 60°C for 50”, 68°C for 8’, followed by an end-extension step at 68°C for 7’, utilizing the Phusion DNA polymerase. The amplified insert was cloned into the pMIGR1 vector as described above. After successful cloning of the insert and verification by sequencing data, the construct was retrovirally transduced to Bal17 cells. Retroviral transduction is the process by which nonviral gene is introduced into a mammalian cell through a virus. The introduced DNA sequence is integrated into the genome of the cellular host, therefore leading to stable expression of the gene [104]. For this purpose PhoenixE packaging cells were used to produce the retroviral particles carrying the RANK gene. PhoenixE cells that carry the viral genes gag, pol, and env needed for retroviral particle assembly were transiently transfected with the retroviral constructs containing mutant or wildtype RANK, using the TransIT-LT1 Transfection Reagent (Mirus Bio LLC), according to the manufacturer’s instructions. 6 hours after transfection, the medium on the PhoenixE cells were changed to PhoenixE culture medium and supernatant containing viral particles was collected and filtered (0.45 μ m) at 24 and 48 hours post-transfection. 1×10^6 Bal17 cells were resuspended in viral supernatant, supplemented with 10 μ M polybrene, which is a cationic polymer that enhances viral adsorption to the plasma membrane of the cell. The cells were then spin infected by centrifugation (2400rpm, 32°C, 90min) and cultured for 12 hours, followed by another round of spin infection.

Transduction efficiency was determined by flow cytometry, according to GFP expression, and the GFP+ Bal17 cells were subjected to FACS, before use in downstream applications.

4.7 Southern Blot

Electroporation of embryonic stem cells (ESC) and Southern blot for the screening of ESCs positive for Rosa26 locus recombination was performed by Dr. Nathalie Knies, as described previously [105]. Briefly, cultured ESCs were electroporated with the pRosa26^{loxSTOPlox-RANK(A756G)} vector, and incubated overnight. Genomic DNA was isolated by phenol/chloroform extraction. 20 μg of DNA was digested with 1.6U/ μl XbaI (New England Biolabs) overnight at 37°C, followed by slow agarose gel electrophoresis. The gel was then depurinated in 0.25M HCl; denatured in 1.5M NaCl with 0.5M NaOH; and neutralized in 1M Tris with 1.5M NaCl (pH 7.4). Single stranded DNA molecules obtained after this procedure were transferred overnight onto a positively charged nylon membrane (HYBOND-nylon membrane, GE Healthcare) with capillary force. The DNA was crosslinked to the membrane by shortwave ultraviolet radiation (254nm, 120J) in a CL-1000 Ultraviolet Crosslinker (UVP). Rosa26 probe was labeled radioactively, and purified on Micro SpinTM S-200 HR columns (GE Healthcare), according to the manufacturer's instructions. The membrane was incubated in 40 ng of radioactively labeled Rosa26 probe in Church buffer (1mM EDTA, 0.25M sodium phosphate buffer (pH7.2), 7% SDS (w/v), 1% BSA (w/v)), overnight at 65°C. The membrane was washed the following day with wash buffer ((2x SSC, 0.1% SDS (w/v)) and (0.2x SSC, 0.1% SDS (w/v))) and visualized with a PhosphorImagerTM (Molecular Dynamics). The image was analyzed with ImageQuant^{T M} software. ESC clones positive for Rosa26 homologous recombination with best morphology and growth characteristics were injected into C57BL6/J blastocysts and transferred to foster mice as previously described. Blastocyst microinjection and generation of knockin mice with germline transmission of the targeted allele was performed by Polygene.

4.8 Cell Culture

The mouse mature B cell lymphoma cell line Bal17, freshly isolated primary B cells and CD4+ T cells were cultured in RPMI-1640 medium supplemented with 10% fetal bovine serum (FBS) (v/v) (Capricorn), 1% pen/strep (v/v), 1% L-glutamine (v/v) and 0.1% 2-mercaptoethanol (v/v). ST2 mouse bone marrow stromal cell line and PhoenixE packaging cells were kept in DMEM, supplemented as described above. Bal17 cells were split 1:10 every 3 days and ST2 and PhoenixE cells were split 1:5 every two days by trypsinizing (1% Trypsin/EDTA (v/v)). All cells were cultured under standard cell culture conditions; at 37°C, 5% CO₂ and 95% humidity. The cells were frozen for conservation in RPMI or DMEM medium, supplemented with 10%DMSO (v/v) and 10% FBS (v/v). Freshly isolated primary lymphocytes were prepared in RPMI-1640 medium supplemented with 5% fetal bovine serum (FBS) (v/v) (Capricorn), 1% pen/strep (v/v), 1% L-glutamine (v/v) and 0.1% 2-mercaptoethanol (v/v), until cultured. All media and supplements except for the FBS were purchased from Gibco.

4.9 Cell Purification

Primary cells from spleen, lymph nodes and Peyer's patches were isolated by mashing organs through 100 and 70 μm filters in preparation medium as described above. Peritoneal cavity was washed out with the help of a needle with preparation medium for cellular content. Bone marrow cells are isolated by flushing the marrow out of the bone with the help of a needle and preparation medium, and mashing through a 100 μm filter. All isolated samples underwent a red blood cell lysis procedure, and were resuspended in 1 ml red blood cell lysis buffer (G-DEX11, Intron Biotechnology) for 5 minutes. Following this the cells were counted by Trypan Blue staining (Trypan Blue Stain 0.4%(w/v), Gibco) and CD19+ B cells or CD4+ T cells were enriched by negative magnetic labeling, as described by Miltenyi Biotec (Mouse CD4+ T Cell Isolation Kit and Mouse B Cell Isolation Kit, Miltenyi Biotec). In this system of magnetic separation (MACS), the cells of interest accumulate in

the flow-through, untouched and therefore unactivated. The flow-through containing the cells of interest was centrifuged at 400g for 5 minutes to collect the cells. Cells were washed with preparation medium and used for further analysis.

4.10 Cell Stimulation

RANK(A756G) expressing or wildtype B cells and CD4+ T cells were purified by fluorescence-activated cell sorting or magnetic labeling, respectively. After the purification step the cells were rested for 2 hours at 37°C, with a concentration of 20×10^6 cells/ml, in resting medium RPMI, containing 1% BSA, 1% pen/step, 1% L-glutamine and 0.1% 2-mercaptoethanol. Following the resting, the cells were washed with PBS and resuspended at a concentration of 2×10^6 /ml. CD4+T cells were stimulated on a 96 F-well plate pre-coated with AffiniPure rabbit α -syrian hamster IgG (H+L) crosslinking antibody overnight at 4°C (1 μ g/ml final concentration), and treated with functional grade purified α -mouse CD3e (5 μ g/ml final concentration) for one hour at 37°C. 2×10^5 CD4+T cells per well were added to the wells with α -mouse CD28 (1 μ g/ml final concentration) and incubated at 37°C for 1 to 96 hours. RANK(A756G) expressing or wildtype B cells were stimulated on 96 F-well plates or 6-well plates after sorting, and incubated with 100 ng/ml (final concentration) mouse recombinant RANKL (R&D systems), 2 μ g (final concentration) neutralizing antibody purified mouse α -RANKL (eBioscience) or 0.5 μ M (final concentration) CpG (Invivogen) for 1 to 48 hours at 37°C.

Bal17 cells were retrovirally transfected, fluorescently sorted for GFP+ cells and kept under normal cell culture conditions until stimulation. 2×10^6 Bal17 cells were stimulated with 100 ng/ml (final concentration) mouse recombinant RANKL for 5 minutes to 48 hours at 37°C. All stimulated cells were spun down at 400g for 5 minutes and washed with PBS once, before use for downstream applications.

4.11 Preparing Cell Lysates and Western Blot Analysis

Whole cell lysates for protein analysis were prepared by lysing 5×10^6 B cells in ice cold CHAPS buffer, supplemented with phosphatase inhibitors (50mM NaF, 0.1mM Na_3VO_4) and protease inhibitors (EDTA free Protease Inhibitor Cocktail Tablets, Roche Diagnostics). Concentrations of lysates were determined spectrophotometrically, by implementing the Bradford Assay (Bio-Rad), according to the manufacturer's instructions. The lysates were then denatured in SDS sample buffer at 95°C for 5 minutes before loading onto the polyacrylamide gel, as described before [106]. Polyacrylamide gel electrophoresis method separates proteins across an electrically charged field based on their molecular weight and charge. The separated proteins were transferred onto a nitrocellulose membrane (Amersham Protran, GE Healthcare) electrophoretically with a wet-blotting approach in transfer buffer. Following transfer, membranes were blocked in 5% skim milk powder in TBST and incubated overnight with specific primary antibodies diluted 1:1000 in 5% BSA in TBST. HRP-conjugated secondary antibodies (1:5000 in 5% skim milk powder in TBST) were added the next day after washing the membranes with TBST. For chemiluminescent detection, the detection systems LumigenTM TMA-6, Solution A+B (GE Healthcare) or Detection Reagent 1+2/Peroxid Solution (Thermo Scientific, Pierce) were utilized. The antibodies used for Western blotting are listed in the "Materials" chapter. The buffers used in this procedure are as follows:

CHAPS buffer	10mM Tris (pH7.5) 1mM MgCl ₂ 1mM EGTA 10% glycerol (v/v) 0.5% CHAPS (w/v)
SDS sample buffer	62.5mM Tris/HCl (pH6.8) 2% SDS (w/v) 10% glycerol (v/v) 5% 2-mercaptoethanol (v/v) 0.02% bromphenol blue (w/v)
SDS-PAGE running buffer	25mM Tris (pH 8.3) 2M glycine 1% SDS (w/v) at 120V
Transfer buffer	50mM Tris (pH 8.5) 40mM glycine 0.03% SDS (w/v) 20% methanol (v/v) added freshly (at 350 mA for 90')
TBST	0.025% Tween-20 (v/v) 20mM Tris (pH7.4) 137mM NaCl

4.12 Enzyme-Linked Immunosorbent Assay (ELISA)

The ELISA method relies on chemiluminescent detection of antigen-antibody interactions on a plate [107]. Detection of serum immunoglobulins of transgenic and wildtype mice was performed using the Mouse Immunoglobulin Panel, manufactured by Southern Biotech. Briefly, the sera obtained from mice were diluted 1:500 with blocking buffer, a 96-well flat bottom plate was incubated overnight at 4°C with 1:100 diluted capture antibody in coating buffer (goat- α mouse Ig (H+L), Southern Biotech) and washed three times the following day. Blocking buffer was added to the plate and the plate was incubated for 1 hour. After washing the plate 3 times, 1:3 serial dilutions of the pre-diluted serum were done and the plate was incubated at

room temperature for 1 hour, and washed 3 times afterwards. Detection antibody, 1:250 diluted in blocking buffer was added on the wells and the plate was incubated for 1 hour at room temperature. Following the incubation, the plate was washed 5 times and substrate buffer (with freshly added phosphatase substrate from Sigma Aldrich) was added on the wells.

Time course measurements (5, 10, 15 and 20 minutes) were performed in a microplate reader (Tecan Group), using the Magellan software to detect the serum immunoglobulin levels. Measurements utilized the transmission of light during the alkaline phosphatase reaction at 450 nm. The reference wavelength for background noise was 570 nm. The serum concentrations of immunoglobulins were determined by standard-curve calculations. The contents of the buffers used are as follows:

Coating buffer	1 pack ELISA/ELISPOT Coating buffer powder (Southern Biotech) dissolved in 1 L H ₂ O
Blocking buffer	PBS, 1% BSA
Washing buffer	PBS, 0.05% Tween
Substrate buffer	100 ml dH ₂ O, 12 ml Di-ethanol, 30 μ l MgCl ₂ pH 9.8, adjusted with 18.5% hydrochloric acid

The detection of autoantibodies in sera of transgenic and wildtype mice was performed using Autoimmune ELISA kits purchased from Alpha Diagnostic International. The sera obtained from mice were initially diluted 1:50 and the manufacturer's instructions for the kit were followed.

4.13 Flow Cytometry and Fluorescence-activated Cell Sorting (FACS)

Flow cytometry method is based on computer-processed light scatter and fluorescent signals received from a fluorescently labeled single cell suspension after laser excitation. This method can be used to determine the size and granularity of cells, as well as expression of surface markers, which can be fluorescently labeled using antibodies against certain epitopes of surface molecules conjugated to fluorescent

molecules. Flow cytometry can also be used for detection of intracellular proteins, after proper cell fixation and permeabilization methods are applied [108].

In this study, flow cytometry is used to perform immunophenotyping of lymphocytes isolated from spleen, lymph nodes, Peyer's patches, peritoneal cavity and bone marrow of mice. After cells were prepared as explained in section 4.9 and counted, they were resuspended and washed in FACS buffer (PBS, 3% FBS) (400g, 5', 4°C) and incubated with 1:200 diluted CD16/32, to block free F_c receptors, washed in FACS buffer again and incubated for 20' at 4°C with respective fluorescently conjugated antibodies against surface molecules. The antibodies were diluted either 1:200 or 1:400. All antibodies were diluted in FACS buffer. The cells were acquired using a FACSCantoII flow cytometer.

The FACS method was implemented to sort and enrich certain cell types labeled fluorescently. The transgenic B cells were sorted regularly using GFP expression for downstream applications. Cells isolated from the spleen or lymph nodes of wildtype mice were stained with a fluorescent CD19 antibody, as documented in the "Materials" section and sorted for B cells. All sorting experiments were performed on a FACS Aria III sorter. The cells were sorted directly into filtered sterile FBS and washed with FACS buffer before use in downstream applications.

4.14 Histology

Preparation of organs for histology and histological analysis were done in collaboration with Professor Wilko Weichert (DKFZ, Heidelberg). Briefly, the isolated organs were fixed in 4% paraformaldehyde overnight and paraffin embedded. Tissue sections of thickness 3–5 μ m were prepared and cell nuclei and tissue structure were visualized by haematoxylin&eosin (H&E) staining. To visualize immunoglobulin complexes in kidneys of transgenic mice, immunofluorescence with scanning electron microscopy from kidneys fixed in 4% paraformaldehyde was performed by Dr. Stephan Macher-Göppinger (DKFZ, Heidelberg).

4.15 Immunofluorescence

Immunofluorescence to detect anti-nuclear autoantibody presence in transgenic mice was performed together with Torben Gehring. Hep-2 slides were purchased from Euroimmun AG. The sera obtained from transgenic and wildtype mice were diluted 1:100 in PBS, applied on the slides and incubated at room temperature for 30 minutes. Slides were washed with PBS and detection antibodies (as listed in “Materials” section) were added on the slides. After 30 minutes of incubation at room temperature in the dark, the slides were washed and covered with coverslips. A Leica DMRBE fluorescent microscope was used to photograph the slides. The photographs were not modified with any software.

4.16 Statistical Analysis

Statistical significance for the results was analyzed with the unpaired two-tailed Student’s *t* test and ordinary one-way ANOVA, using Prism Version 6.0, Graphpad Software Inc. Differences between analyzed groups were labeled as significant if $p\text{-value} \leq 0.05$.

Chapter 5

Results

5.1 RANK(A756G) Mutation *in vitro*

To investigate the RANK(A756G) mutation and its potential role in dysregulation of signaling, retroviral transduction experiments with RANK(A756G) were performed. The Bal17 cell line, a murine cell line derived from a mature B cell lymphoma was used as the cellular system for enforced RANK(A756G) expression. The amino acid change lysine to glutamic acid at position 240 (K240E) was introduced by site-directed mutagenesis to wildtype RANK (nucleotide change A756G). Figure 5.1 depicts the wildtype and mutant RANK, with the position of the mutation. Retroviral expression vectors were generated by cloning the human RANK(A756G) and wildtype RANK cDNA into the pMIGR1 vector, which contains an internal ribosomal entry site (IRES) and the coding sequence of eGFP, enabling the tracking of infected cells by flow cytometry.

Once RANK(A756G), wildtype RANK or empty pMIGR1 vectors were retrovirally introduced in Bal17 cells, the cells were sorted for GFP+ cells to select the successfully transduced cells. The transduced cells were then incubated in culture with or without recombinant mouse RANKL (100 ng/ml) for one hour. This timepoint was chosen after initial timecourse experiments ranging from 5 minutes to 48 hours. After stimulation, surface expression of B cell activation markers were analyzed by flow cytometry. Unstimulated cells that are infected by both wildtype

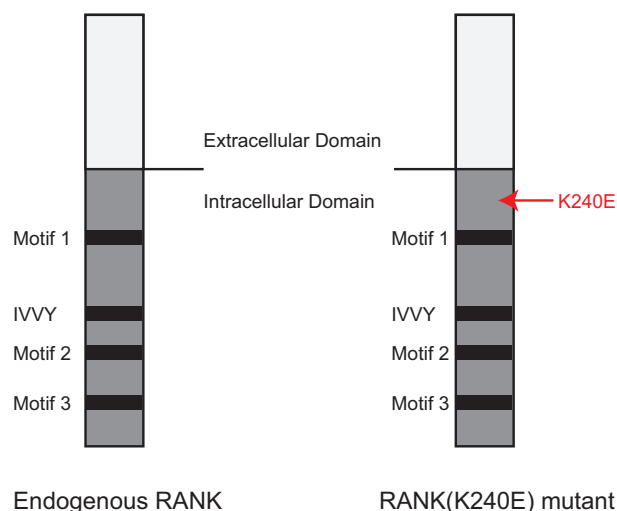


Figure 5.1: Schematic depiction of RANK(A756G) mutation. Red arrow indicates mutation. Motif 1 PFQEP(369-373), Motif 2 PVQEET(559-564) and Motif 3 PVQEQG(604-609) are TRAF binding motifs, and IVVY is a recently described TRAF independent motif, cooperating with TRAF binding motifs to promote osteoclastogenesis. These four motifs enable RANK to mediate its downstream functions.

RANK and RANK(A756G) showed a marginal increase in the expression of the surface activation marker CD80 compared to cells infected with empty pMIGR1, whereas surface MHCII levels are similar in all three conditions. In response to stimulation with RANKL for 1 hour however, RANK(A756G) expressing Bal17 cells had slightly higher surface expression of both CD80 and MHCII, compared to Bal17 cells that are expressing wildtype RANK, thus showing increased B cell activation upon RANKL stimulation in RANK(A756G) expressing Bal17 cells and indicating gain of function (Figure 5.2).

5.2 Mouse Model of Conditional RANK(A756G) Expression

5.2.1 Targeting of the ROSA26 Locus

Since RANK(A756G) mutant induces slightly stronger B-cell activation than wildtype RANK upon RANKL stimulation, this mutant form of RANK was used

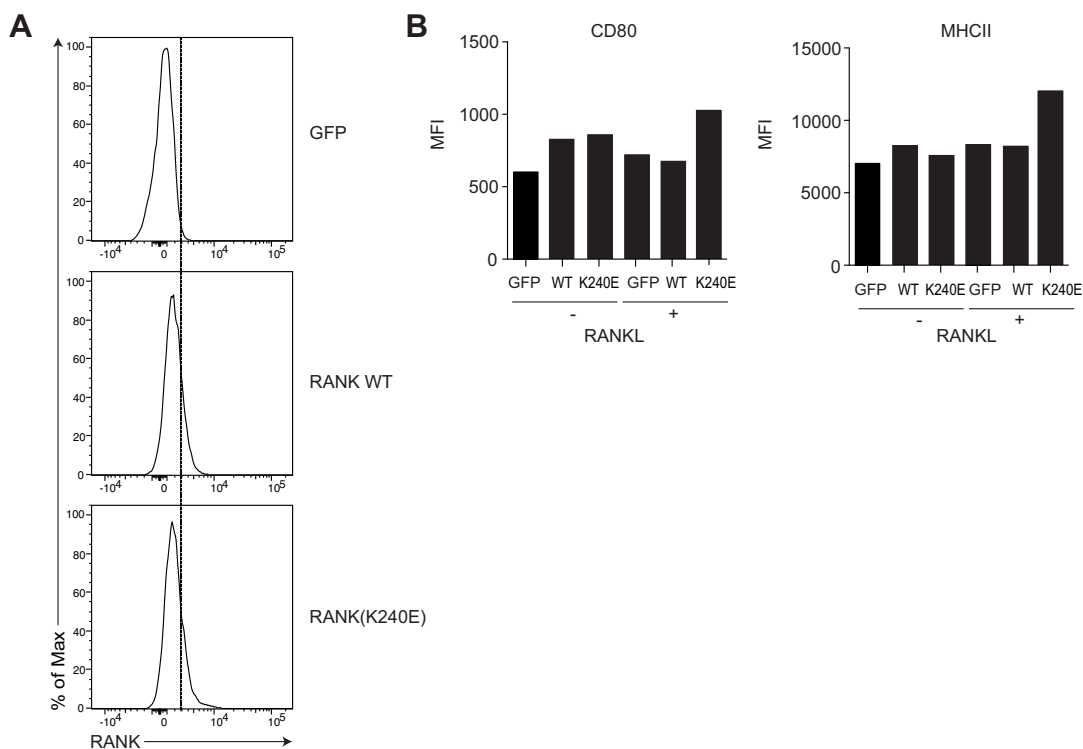


Figure 5.2: RANK(A756G) expression in Bal17 cells leads to marginally higher B cell activation. Bal17 cells transduced with RANK(A756G), wildtype RANK or empty pMIGR1 vector as control were sorted for GFP and stimulated or not stimulated with 100 ng/ml recombinant mouse RANKL for 1 hour, and analyzed for the expression of B cell surface activation markers by flow cytometry. Level of RANK surface expression is in cells transduced with wildtype and mutant RANK is the same, ruling out any differences in outcome due to different RANK expression levels. Data shown are representative of four experiments.

to study enforced RANK signaling *in vivo*. For this purpose, a genetically modified mouse model was generated by the conventional endogenous ROSA26 locus targeting.

The endogenous murine ROSA26 locus has been well characterized and is widely used for the generation of genetic knock-in mouse models. It is located on chromosome 6 and contains three exons. ROSA26 is shown to have ubiquitous promoter activity and is expressed in moderate levels. Insertion of the desired gene into this locus proceeds via homologous recombination and is considerably efficient due to high frequencies of recombination in this area. In addition, homologous recombination events in this area have been shown to have no phenotypic effect on the mouse

[109].

The targeting vector was generated by cloning the RANK(A756G) cDNA into a previously described pROSA26 targeting vector after *AscI* digestion. The consensus sequence CCACC was added directly before the start codon of RANK(A756G) to ensure optimal translation initiation. The RANK(A756G) cDNA was positioned downstream of an adenovirus splice acceptor site (SA), followed by a neomycin resistance stop cassette (NEO-STOP), flanked by loxP sites on both sides. An IRES-eGFP cassette flanked by an FRT site (IRESeGFP), and a polyadenylation sequence (pA) were inserted downstream of the RANK(A756G) cDNA. Homologous recombination of the targeting vector into the locus was achieved by the “short-arm” and “long-arm” of homology on the vector, which contained sequences identical to the ones surrounding the site of integration within intron 1.

The occurrence of correct recombination in targeted embryonic stem cells was visualized by Southern blot. *Xba*-I digested genomic DNA was separated by size through an agarose gel and then was exposed to a 5' probe, which enables the detection of a 4.6 kb DNA fragment for the WT allele and a 9.2 kb DNA fragment for the allele that contains the correctly inserted targeting vector. Figure 5.3 depicts the targeting strategy and shows a representative embryonic stem cell clone with successful targeting. Breeding of the germline transmitting chimeras with C57BL/6 mice lead to the generation of the ROSA26loxSTOPlox-RANK(A756G) mouse strain, carrying the RANK(A756G) cDNA heterozygously in the ROSA26 locus. Transcription of RANK(A756G) is only possible after breeding with Cre-transgenic mice, when the loxP-flanked NEO-STOP cassette is excised from intron 1. The SA site upstream of the RANK(A756G) cDNA sequence enables the correct splicing of the stop cassette, leading to the transcription of an RANK(A756G)-IRES-eGFP bicistronic mRNA. The IRES site enables the translation of eGFP protein from the bicistronic transcript, and the RANK(A756G) is translated starting from the start codon. The green fluorescence provided by the eGFP protein enables detection of cells that express RANK(A756G) by flow cytometry analysis, and allows cell tracking, throughout the life of a transgenic mouse.

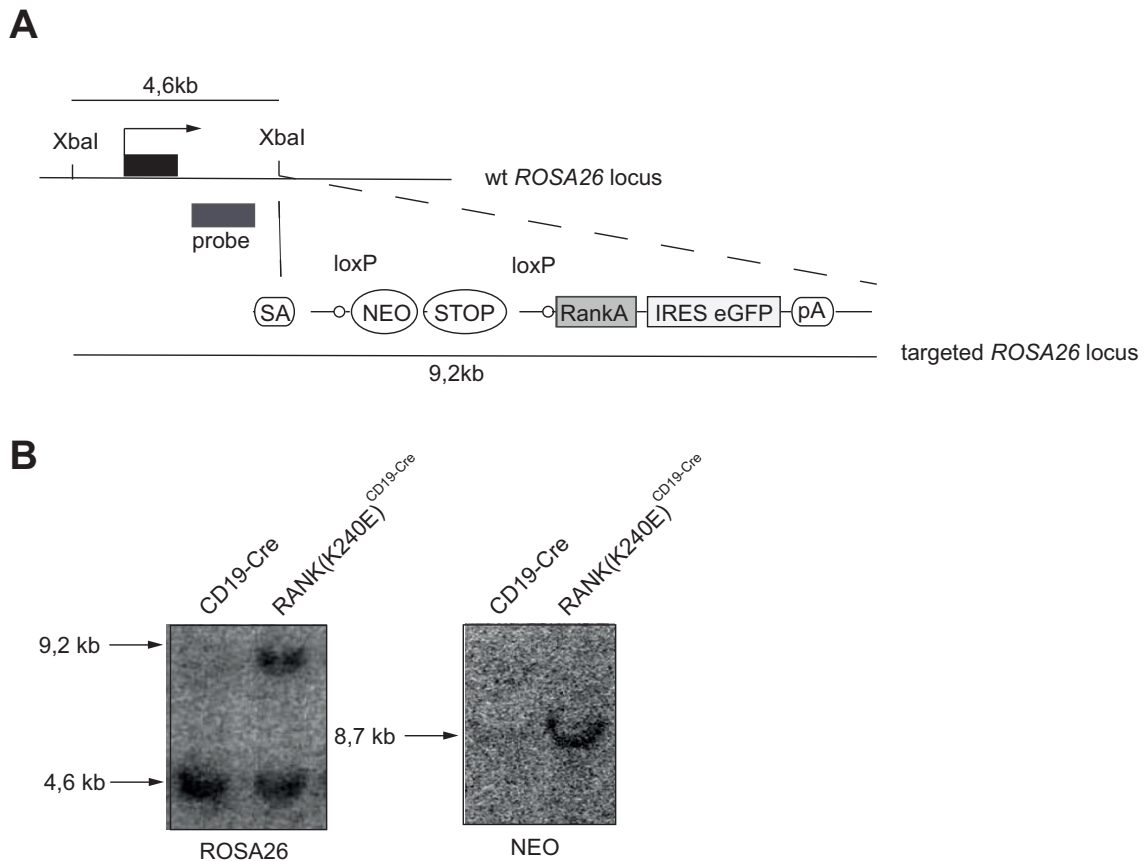


Figure 5.3: Generating the RANK(A756G) knockin strain and targeting of the ROSA26 locus (A) RANK(A756G) targeting strategy. IRES, internal ribosomal entry site; NEO, neomycin; pA, poly(A); SA, splice acceptor. The wildtype ROSA26 locus, the targeting vector, and the ROSA26 locus upon homologous recombination are depicted. (B) Southern blot analysis. Lanes 1 and 2 show genomic DNA from wildtype and transgenic mice. The size of the fragment showing the WT ROSA26 locus is 4.6 kb, the recombined locus is 9.2 kb, and Cre-mediated removal of the STOP cassette results in an 8.7-kb fragment.

5.2.2 B cell-specific expression of RANK(A756G)

In order to express RANK(A756G) in a B cell-specific manner, transgenic ROSA26^{loxSTOPlox-RANK(A756G)} mice were bred with CD19-Cre mice, which enabled the excision of the NEO-STOP cassette only in cells with an active CD19 promoter, namely, B cells in the pre-B cell stage and onwards, allowing RANK(A756G) expression early in the life of a B cell. Figure 5.4A shows a representative breeding scheme for this mouse model. Excision of the NEO-STOP cassette through Cre-mediated

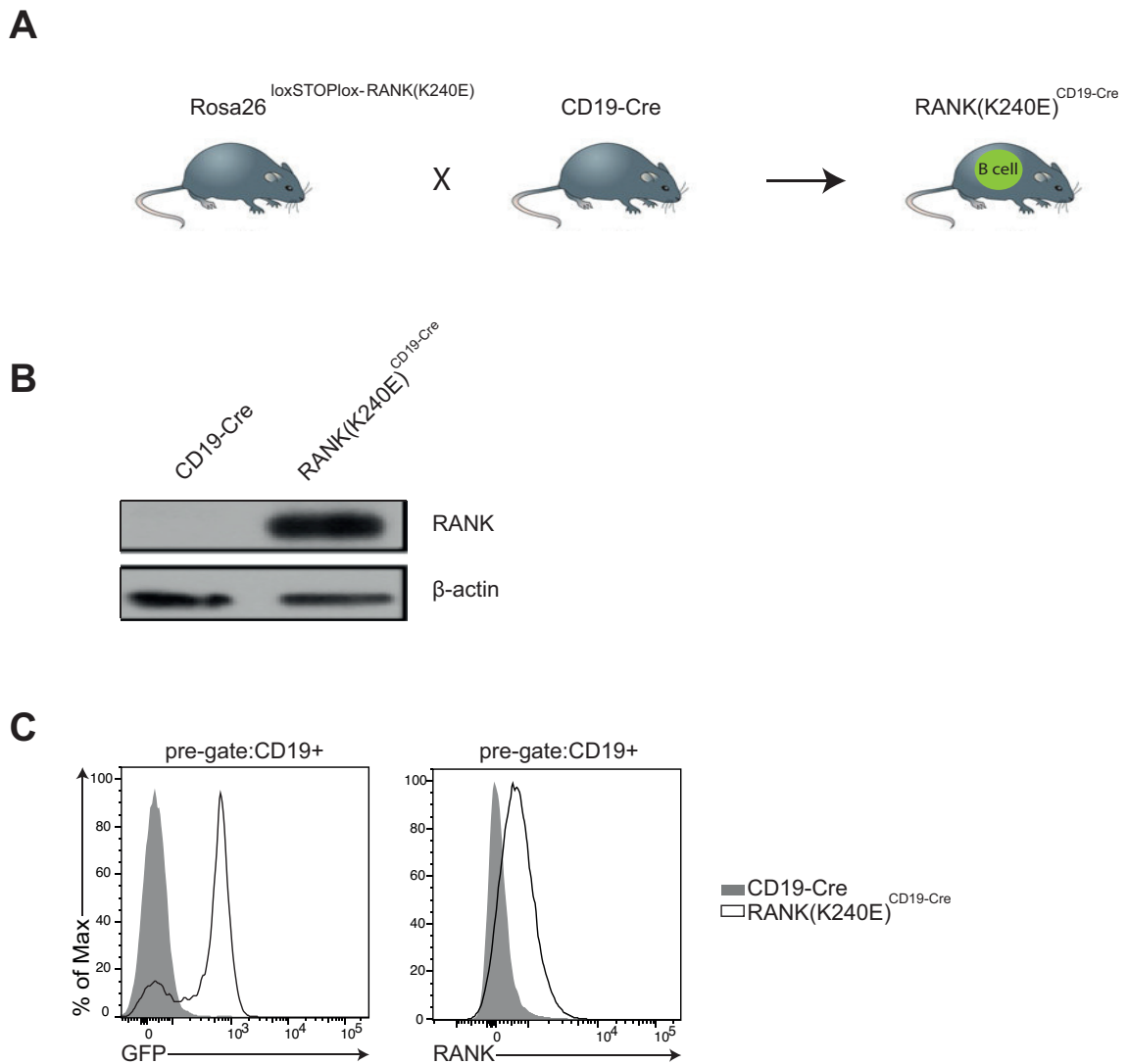


Figure 5.4: Mouse breeding and B cell specific expression of RANK(A756G). (A) Breeding scheme. For B cell specific expression of RANK(A756G), ROSA26^{loxSTOPlox-RANK(A756G)} mice were bred with CD19-Cre mice, a surface protein whose expression is restricted to B cells. Cre expression leads to the excision of the loxSTOPlox cassette, enabling transgene expression, along with GFP. RANK(A756G) expressing B cells can thus be tracked with the aid of flow cytometry. (B) MACS isolated B cells from CD19-Cre and RANK(A756G)^{CD19-Cre} mice were subjected to western blot analysis for RANK expression. (C) Cells isolated from the spleens of CD19-Cre and RANK(A756G)^{CD19-Cre} mice were analyzed by flow cytometry for surface RANK and GFP expression. Live cells were pre-gated for CD19 expression.

excision of the flanking loxP sites, allows the transcription of the RANK(A756G)-eGFP bicistronic mRNA. As a result, functionality of the generated mouse model could be tested by flow cytometry analysis for the presence of GFP in B cells, as well as western blot analysis. Flow cytometry analysis in spleens of 5-week old transgenic mice showed that around 80% of the B cells are GFP positive, indicating RANK(A756G) expression. RANK(A756G) expression was also visualized by western blot from B cells isolated from the spleen of transgenic mice and surface expression of RANK(A756G) on B cells was demonstrated by flow cytometry analysis, confirming the functionality of the generated mouse strain (Figure 5.4B). From now on, the transgenic mice will be referred to as the RANK(A756G)^{CD19-Cre} for simplicity.

5.2.3 RANK(A756G)^{CD19-Cre} mice have splenomegaly, lymphadenopathy and show reduced survival

RANK(A756G)^{CD19-Cre} mice were initially observed long-term in a defined cohort to elucidate any pathological effects that B cell-specific RANK(A756G) expression might have on mice. The mice were regularly checked for signs of disease, using parameters such as weight and wasting, ruffling symptoms, lethargy or hunched posture. A majority of the aged RANK(A756G)^{CD19-Cre} mice showed no signs of disease, or a significant weight change, however they died abruptly around 6 months of age, while the CD19-Cre mice remained healthy and have survived. A detailed necropsy of these mice showed that RANK(A756G)^{CD19-Cre} mice had splenomegaly and lymphadenopathy, with a 1.5 fold increase in spleen weight and significantly elevated cell numbers in the spleen and lymph nodes (Figure 5.5A). Survival analysis of an extended cohort of RANK(A756G)^{CD19-Cre} mice (n=18) mice has shown that these mice have a mean survival rate of 6.6 months (Figure 5.5B).

In order to fully understand the cause of the observed reduction in survival, post-mortem histological analyses were performed. Organ histologies have shown substantial cell infiltration and disrupted architecture in lymph nodes, cellular infiltration in the bronchioli in lungs, and the cause of death was identified as kidney failure due to extensive glomerulonephritis (Figure 5.5C).

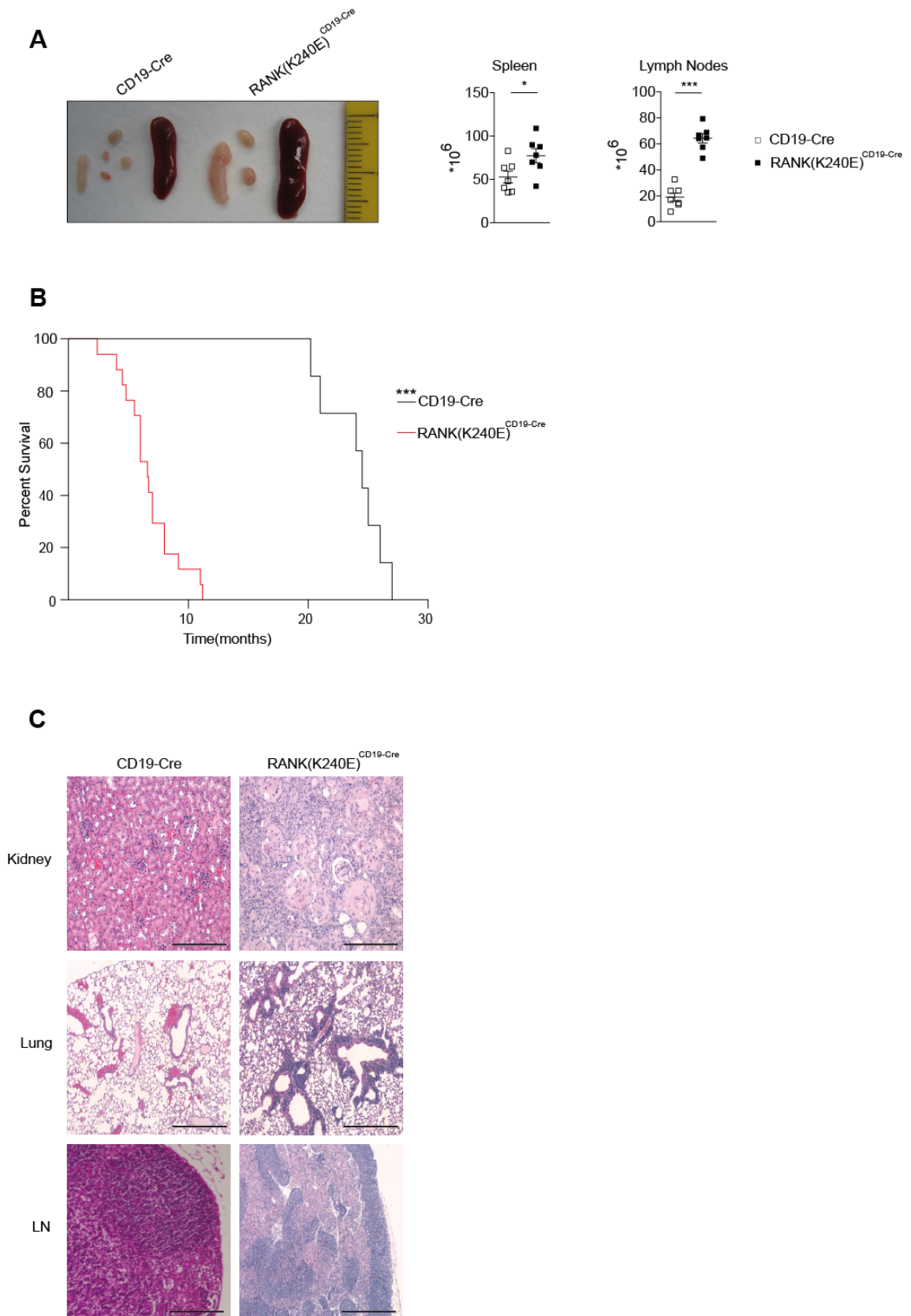


Figure 5.5: RANK (K240E) expression drives disease in vivo. (A) Macroscopic appearance of representative spleens and mesenteric lymph nodes (in cm) and total cell counts in spleen and lymph nodes of analyzed mice, bars indicate mean. (B) Kaplan–Meier curve of CD19-Cre and RANK(A756G)^{CD19-Cre} mice (n = 18, respectively)(***p ≤ 0.0001). (C) Glomerulonephritis-related kidney failure and cellular infiltration of lungs and lymph nodes in RANK(A756G)^{CD19-Cre} mice were revealed by H&E staining(Scale bars: 1 mm). The data shown in A-C are obtained from 6 month old, terminally ill animals.

5.2.4 RANK(A756G)^{CD19-Cre} mice have immune deposits in kidneys and accompanying proteinuria

Since the cause of death was defined as glomerulonephritis-related kidney failure, the reason for kidney failure was investigated further in histological samples from kidneys by immunofluorescence and scanning electron microscopy (SEM). This analysis revealed massive mesangial and subendothelial immune deposits in the kidneys of RANK(A756G)^{CD19-Cre} mice. The deposits were organized with regular spacing, as is often observed in cases of lupus nephritis. This led to the conclusion that the extensive glomerular damage and resulting kidney failure occurred due to immune complex accumulation in the kidneys (Figure 5.6A). In line with these findings, all of the terminally ill RANK(A756G)^{CD19-Cre} mice (n=15) suffered from proteinuria, as determined by Bradford assay, also indicating glomerular damage (Figure 5.6B).

5.2.5 RANK(A756G) expression in B cells leads to B cell activation, proliferation and B1 B cell expansion

After observing the systemic phenotypic effects of B cell-specific RANK(A756G) expression in mice, and identifying the cause of reduced survival as kidney failure due to immune complex deposition, the cellular responses that might lead to this phenotype were investigated in depth. A flow cytometry analysis of the spleens of terminally ill RANK(A756G)^{CD19-Cre} and wildtype mice for B cell activation mark-

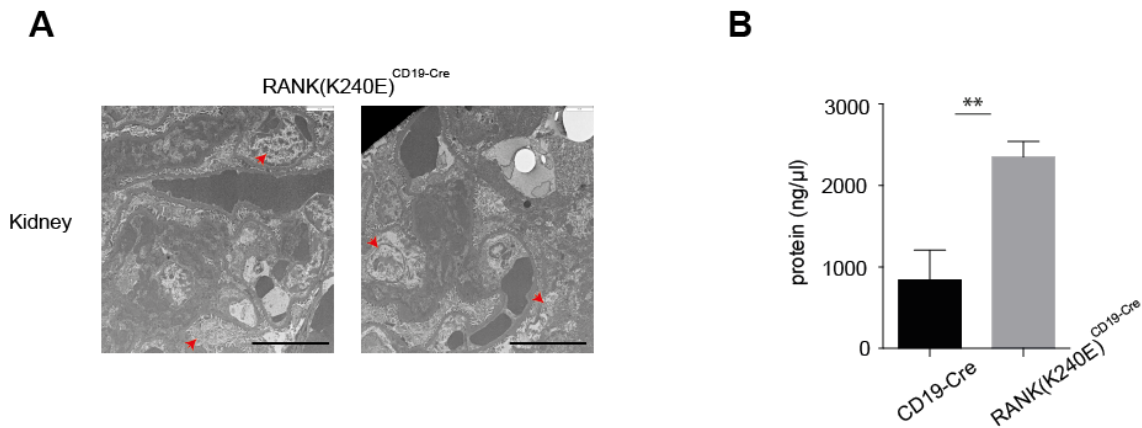


Figure 5.6: RANK^{CD19-Cre} mice succumb to deteriorating renal function. (A) SEM of kidneys in RANK(A756G)^{CD19-Cre} mice showed massive subendothelial immune deposit accumulation (representative of three mice of each genotype) (Scale bars: 1mm). Arrows indicate areas of interest. (B) Kidney failure in RANK(A756G)^{CD19-Cre} mice is also evident in significantly increased proteinuria (n=15, respectively). The data shown in A and B are obtained from terminally ill 6 month old animals. (**p ≤ 0.01)

ers CD80 and CD86 showed that B cells in RANK(A756G)^{CD19-Cre} mice were highly activated. B cell size was also increased in RANK(A756G)^{CD19-Cre} mice, indicating activation-induced cell blasting (Figure 5.7A). CD4+ and CD8+ T cell compartments, however remained unaffected and showed no significant difference in effector or memory T cell compartments (Figure 5.7B). Analysis of RANK(A756G)^{CD19-Cre} mice at various weeks of age, ranging from 5 to 24, showed persistent expansion in the B1 B cell compartment, which was defined as the CD19⁺B220^{low} population, in the spleen, lymph nodes and peritoneal cavity (Figure 5.7C). Further analysis showed a selective expansion of CD5+ B1a cells over the CD5- B1b cell population (Figure 5.7D).

Terminally ill RANK(A756G)^{CD19-Cre} mice showed elevated CD19+ B cell numbers in the lymph nodes and peritoneal cavity, whereas the B cell numbers in the spleen remained normal, compared to the CD19-Cre mice (Figure 5.8A). An intracellular Ki67 staining and flow cytometric analysis of cells from lymph nodes, spleen and peritoneal cavity of terminally ill showed that both B1 and B2 B cells were more proliferative in RANK(A756G)^{CD19-Cre} mice compared to their CD19-Cre

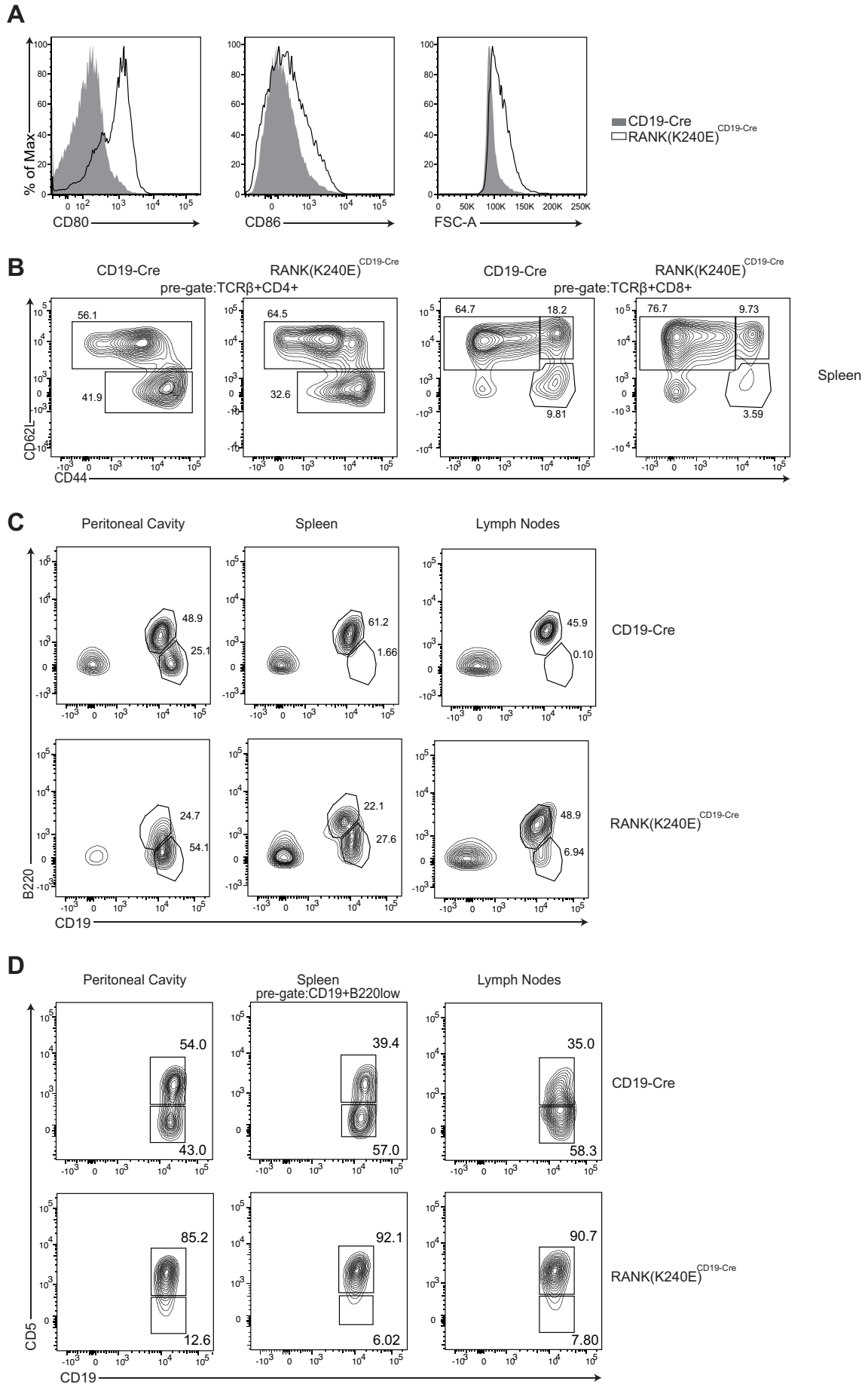


Figure 5.7: RANK(A756G) expression leads to B cell activation, proliferation and B1a cell expansion. (A) RANK (K240E) expressing B cells show an activated phenotype in vivo: surface CD80, CD86 expression and forward-scatter area (FSC-A) were measured using flow cytometry. (B) Representative analysis of T-cell populations in the spleen of terminally ill RANK (K240E)CD19-Cre mice and 6 month old CD19-Cre control animals by flow cytometry. (C) Analysis of B1 and B2 cell populations in peritoneal cavity, spleen and lymph nodes of 6 month old animals by flow cytometry revealed B1 cell expansion. (D) B1a cell expansion in 6 month old RANK(A756G)^{CD19-Cre} mice revealed by flow cytometry. The cells were pre-gated for CD19⁺B220^{low} B1 population. The numbers refer to the mean percentages. The data shown in A-D are representative of five independent experiments, with a total number of at least 12 mice analyzed per genotype.

littermates. (Figure 5.8B). Terminally ill RANK(A756G)^{CD19-Cre} mice also had elevated numbers of plasma cells (CD138⁺B220^{low}) in the spleen and bone marrow (Figure 5.8C).

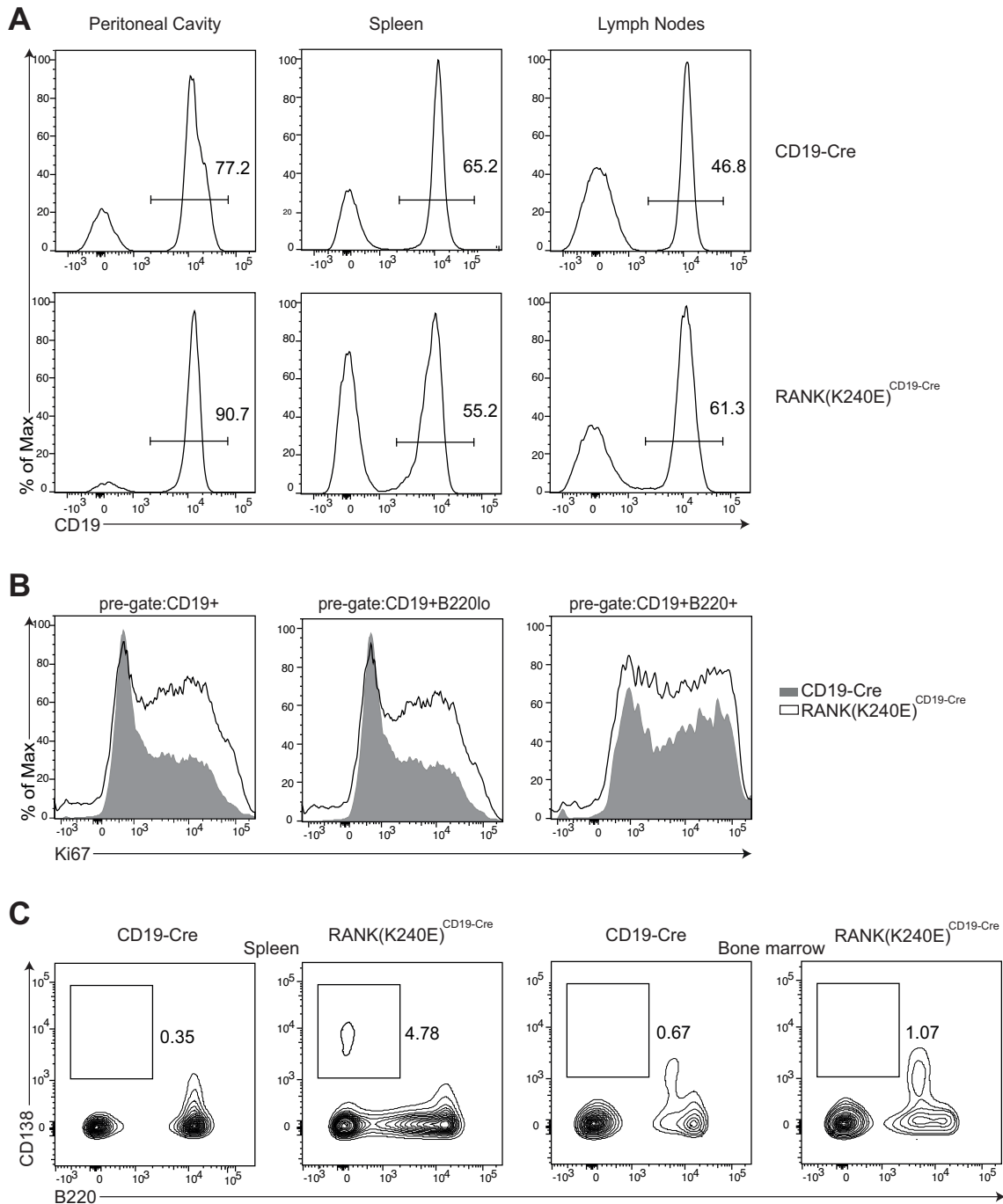


Figure 5.8: Terminally ill RANK(A756G)^{CD19-Cre} mice have elevated plasma cells and a highly proliferative B cell phenotype (A) Percentage of B cells in peritoneal cavity, spleen and lymph nodes of 6 month old terminally ill mice. (B) Ex-vivo intracellular Ki-67 staining and flow cytometry analysis of total, B1 and B2 B cells from 6 month old mice. (C) Increased percentage of plasma cells in the spleen and bone marrow of RANK(A756G)^{CD19-Cre} mice. The numbers refer to the mean percentages. The data shown in A-G are representative of five independent experiments, with a total number of at least 12 mice analyzed per genotype.

5.2.6 RANK(A756G) expressing B cells upregulate MHCII and CD86 in the bone marrow

To further dissect how enforced RANK(A756G) expression affects B cell physiology and development, developing B cells in the bone marrow were investigated more closely. Incidentally, bone marrow is also a site for RANKL expression. Osteoblasts and bone marrow stromal cells, which are in close contact with the developing B cells express RANKL. For this purpose, B cells were isolated from the bone marrows of RANK(A756G)^{CD19-Cre} mice and their littermate controls and were analyzed in detail by flow cytometry. The numbers and percentages of pro- and pre- B cells along with immature and recirculating B cells were normal in RANK(A756G)^{CD19-Cre} mice. To examine whether the presence of RANKL in the vicinity of developing RANK(A756G) expressing B cells leads to aberrant signaling, the activation state of immature B cells in the bone marrow has been analyzed by flow cytometry, utilizing the surface activation markers CD80, CD86 and MHCII. Analysis of AA4.1+GFP+ immature B cells, where GFP is used as a marker for RANK(A756G) expression, and AA4.1+GFP- immature B cells, which have not yet expressed CD19 or RANK(A756G), revealed that GFP+ RANK(A756G) expressing immature B cells have much higher levels of surface MHCII and CD86 compared to GFP- immature B cells (Figure 5.9). This analysis lead to the conclusion that RANK(A756G) expressing B cells were prematurely activated in the bone marrow.

5.2.7 RANK(A756G)^{CD19-Cre} mice have significantly increased anti-nuclear antibodies an immunoglobulins in serum

In light of the findings that showed premature activation of RANK(A756G) expressing immature B cells in the bone marrow, increased systemic presence of plasma cells in terminally ill RANK(A756G)^{CD19-Cre} mice, and immune complex deposition in kidneys, the presence of systemic autoantibodies in RANK(A756G)^{CD19-Cre} mice was investigated. Sera from RANK(A756G)^{CD19-Cre} mice and CD19-Cre mice were collected, both at early timepoints (between weeks 9-11) and when they were terminally ill. ELISA analysis was performed on the collected serum samples for several

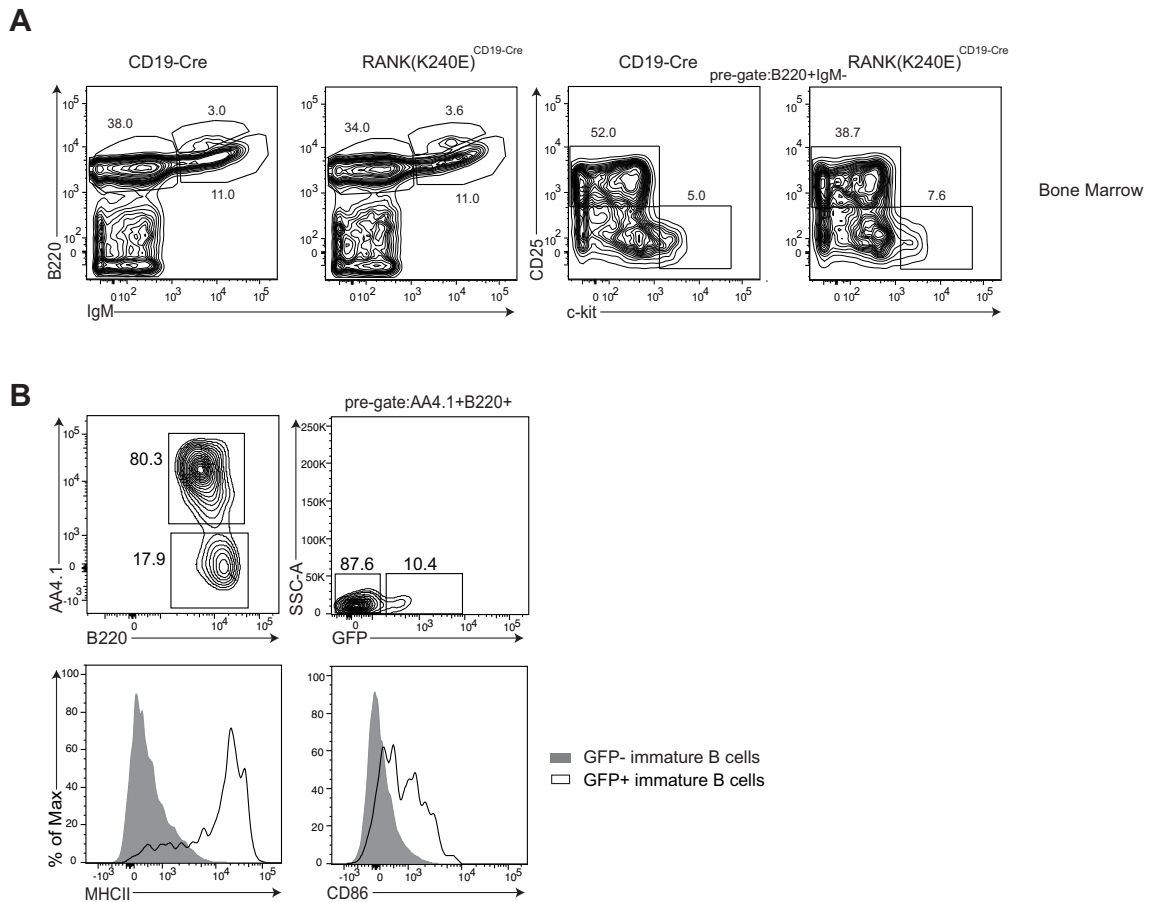
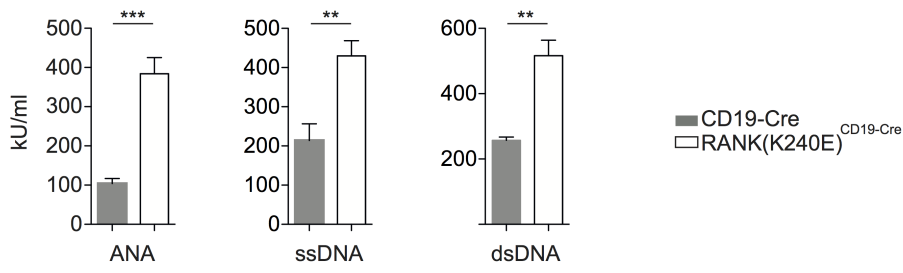


Figure 5.9: RANK(A756G) expressing B cells are prematurely activated in the bone marrow. (A) Representative analysis of B cell populations within bone marrow show normal B cell development in both CD19-Cre and RANK(A756G)^{CD19-Cre} mice. (B) Upregulation of B cell surface activation markers CD86 and MHCII on B cells upon expression of RANK(A756G), as determined by flow cytometry. Expression of transgene in immature B cells was traced by GFP expression. The numbers refer to the mean percentages. The data shown are representative of three independent experiments.

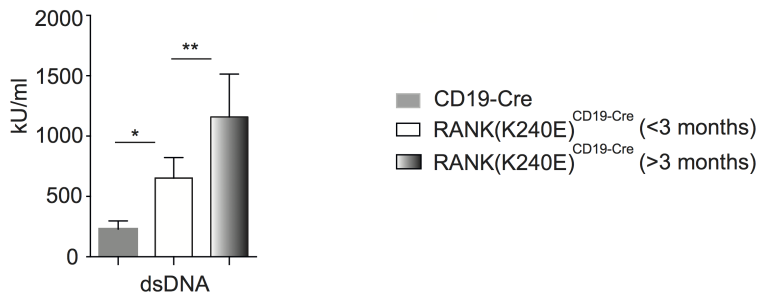
autoantibodies, such as antibodies against ssDNA, dsDNA, total ANAs and cardiolipin. The results demonstrated significantly elevated levels of ANAs, in particular anti-ssDNA and anti-dsDNA in RANK(A756G)^{CD19-Cre} mice. Anti-dsDNA antibodies were detected in the serum starting early in life, and their levels gradually increased until the mice became terminally ill (Figure 5.10A and B). Additionally, presence of anti-nuclear IgG and IgM class autoantibodies against cytosolic proteins in the serum of RANK(A756G)^{CD19-Cre} mice was visualized by HEp-2 assay, where

the binding of serum ANAs to self antigens of a human epithelial cell line can be visualized through indirect immunofluorescence (Figure 5.10C).

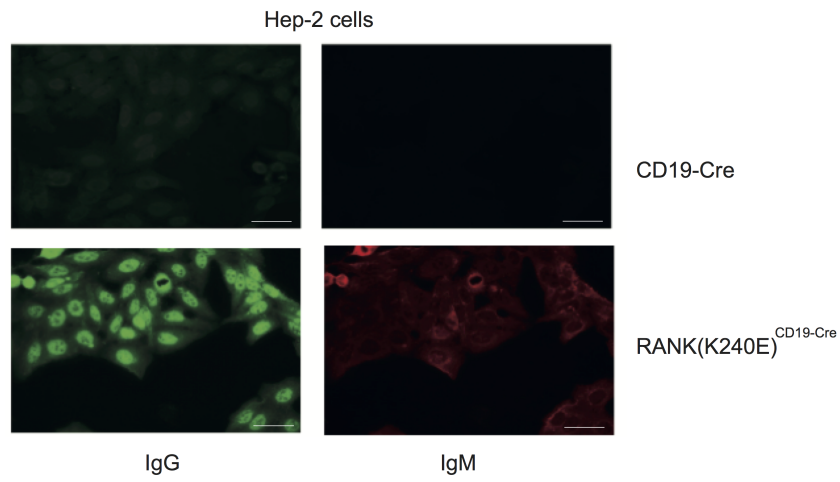
A



B



C



D

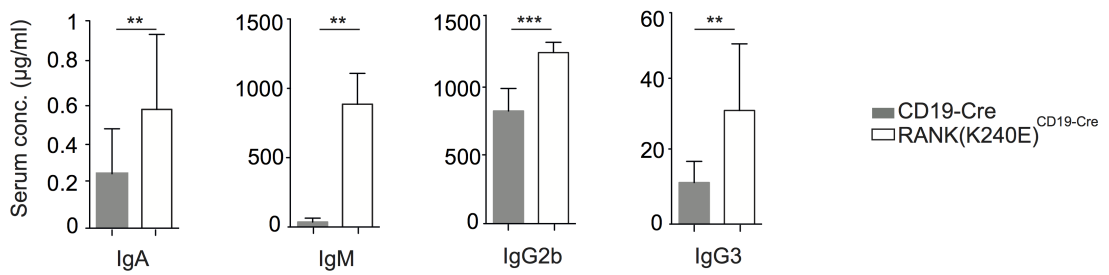


Figure 5.10: RANK(A756G)^{CD19-Cre} mice have antinuclear antibodies in serum. (A) Basal serum levels of total ANAs, anti-ssDNA and anti-dsDNA in 6 month old mice. (B) Serum levels of anti-dsDNA antibodies in RANK(A756G)^{CD19-Cre} mice increase with age. (C) Detection of serum anti-nuclear IgG and autoreactive IgM by immunofluorescence in RANK(A756G)^{CD19-Cre} mice by Hep-2 assay. (D) Basal serum levels of IgA, IgM, IgG2b and IgG3 in 3 month old mice. ($n \leq 7$ per genotype). The data are shown as the mean \pm SEM.

Analysis of sera collected from RANK(A756G)^{CD19-Cre} mice and their CD19-Cre littermate controls by ELISA also revealed significantly elevated levels of serum IgM, IgA, IgG2b and IgG3. (Figure 5.10D)

5.2.8 RANK(A756G)^{CD19-Cre} mice have a polyclonal B cell repertoire and show increased somatic hypermutation

In order to further characterize the antibody repertoire of RANK(A756G)^{CD19-Cre} mice, the clonality of B cells was investigated. By using a pair of primers, one of which hybridizes to the 5'RSS sequence of all murine D segments of the IgH locus (DFS), and the other to a region 50 bp downstream of the 4th and final J segment in the IgH locus (JH4) in a polymerase chain reaction with genomic DNA isolated from GFP+ sorted B cells of terminally ill mice, along with CD19+ sorted B cells of littermate controls, the clonality of the antibody repertoire was determined. As shown in Figure 5.11A, RANK(A756G)^{CD19-Cre} mice have a polyclonal BCR repertoire, as do the CD19-Cre mice, in line with a lymphoproliferative systemic autoimmune disease.

The rate of somatic hypermutation was determined in the RANK(A756G)^{CD19-Cre} mice, utilizing a set of consensus primers that hybridize to V, D or J segments of the IgH locus in a polymerase chain reaction with genomic DNA, isolated from B cells in the aforementioned manner. Subcloning and sequencing of the obtained genomic fragments have revealed that the B cells from RANK(A756G)^{CD19-Cre} carry a significantly higher number of mutations in their V region compared to CD19-Cre littermate controls, indicating an increased rate of somatic hypermutation (Figure

5.11B).

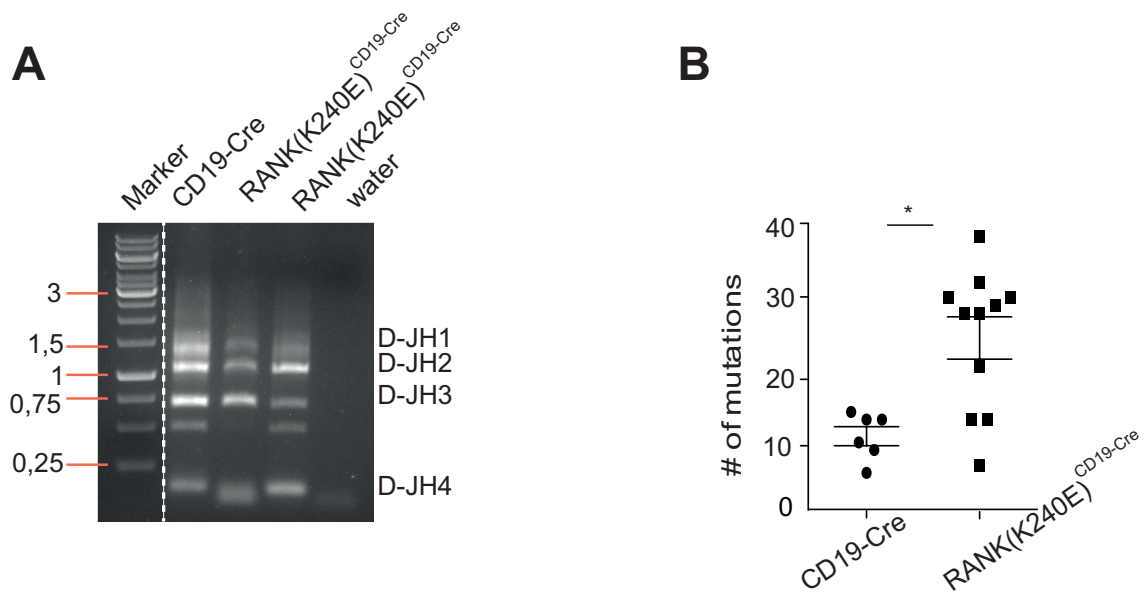


Figure 5.11: B cell repertoire of $\text{RANK(A756G)}^{\text{CD19-Cre}}$ mice is polyclonal and heavily mutated. (A) Ig clonality analysis of 6 month old mice by PCR from genomic DNA isolated from GFP+ and CD19+ sorted B cells from $\text{RANK(A756G)}^{\text{CD19-Cre}}$ and CD19-Cre mice respectively, representative of 7 mice per genotype. Polyclonal B cells show all four possible D-JH recombinations. (B) SHM analysis of 6 month old mice by PCR from genomic DNA isolated from GFP+ and CD19+ sorted B cells from $\text{RANK(A756G)}^{\text{CD19-Cre}}$ and CD19-Cre mice respectively, representative of 7 mice per genotype, revealed significantly increased rate of SHM in $\text{RANK(A756G)}^{\text{CD19-Cre}}$ mice. (* $p \leq 0.05$)

5.3 Cellular implications of RANK(A756G) expression in B cells

5.3.1 RANK(A756G) expressing B cells are dependent on RANKL for survival and proliferation *in vitro*

To determine whether the observed lymphoproliferative effect of RANK(A756G) expression on B cells is ligand dependent, total B cells were isolated from RANK

(K240E)^{CD19-Cre} mice and CD19-Cre mice by FACS sorting of GFP+ cells and CD19+ cells, respectively, and stained with CellTrace Violet. CellTrace Violet is a non-fluorescent dye that diffuses into the cell membrane and gets cleaved by cellular esterases, which converts it to a fluorescent dye. During cell division, daughter cells receive half of the dye of the mother cell, leading to a signal reduction measured at the flow cytometer through each generation. The stained B cells were kept in culture for 5 days in three different conditions: unstimulated; stimulated with 100 ng/ μ l soluble RANKL; or first stimulated with 100 ng/ μ l soluble RANKL, and then treated with a neutralizing antibody α -RANKL 24 hours after RANKL stimulation. Survival of cells over 5 days was measured by staining with Annexin-V, which binds to the phosphatidylserine on the surface of apoptotic cells and 7-AAD, which binds to dsDNA and is generally excluded from cells with an intact plasma membrane, and flow cytometry analysis. Cell proliferation was measured by flow cytometry analysis of the CellTrace Violet stain. An analysis of survival and proliferation showed that RANK(A756G) expressing B cells do not survive *in vitro* in the absence of RANKL. RANKL stimulated RANK(A756G) expressing B cells however, survive and proliferate *in vitro*, an effect that is abolished upon treatment with the neutralizing antibody α -RANKL. CD19-Cre B cells on the other hand did not survive in culture in response to RANKL stimulation. These results indicate that although RANK(A756G) expression itself does not increase survival in B cells, it provides survival and proliferative advantage upon RANKL binding (Figure 5.12).

5.3.2 Murine RANKL activates RANK(A756G) expressing B cells *in vitro*

Along with the survival advantage and proliferative effects of RANKL on RANK (K240E) expressing B cells, RANK(A756G) B cells stimulated with murine RANKL also show an activated phenotype. GFP+ sorted B cells from RANK(A756G)^{CD19-Cre} mice and CD19+ sorted B cells from CD19-Cre mice have been stimulated with 100 ng/ μ l soluble RANKL for 48 hours in culture and then analyzed for activation by flow cytometry for the surface markers CD80, CD86 and MHCII. As shown in Figure 5.13, stimulation with RANKL leads to an activated phenotype in RANK(A756G)

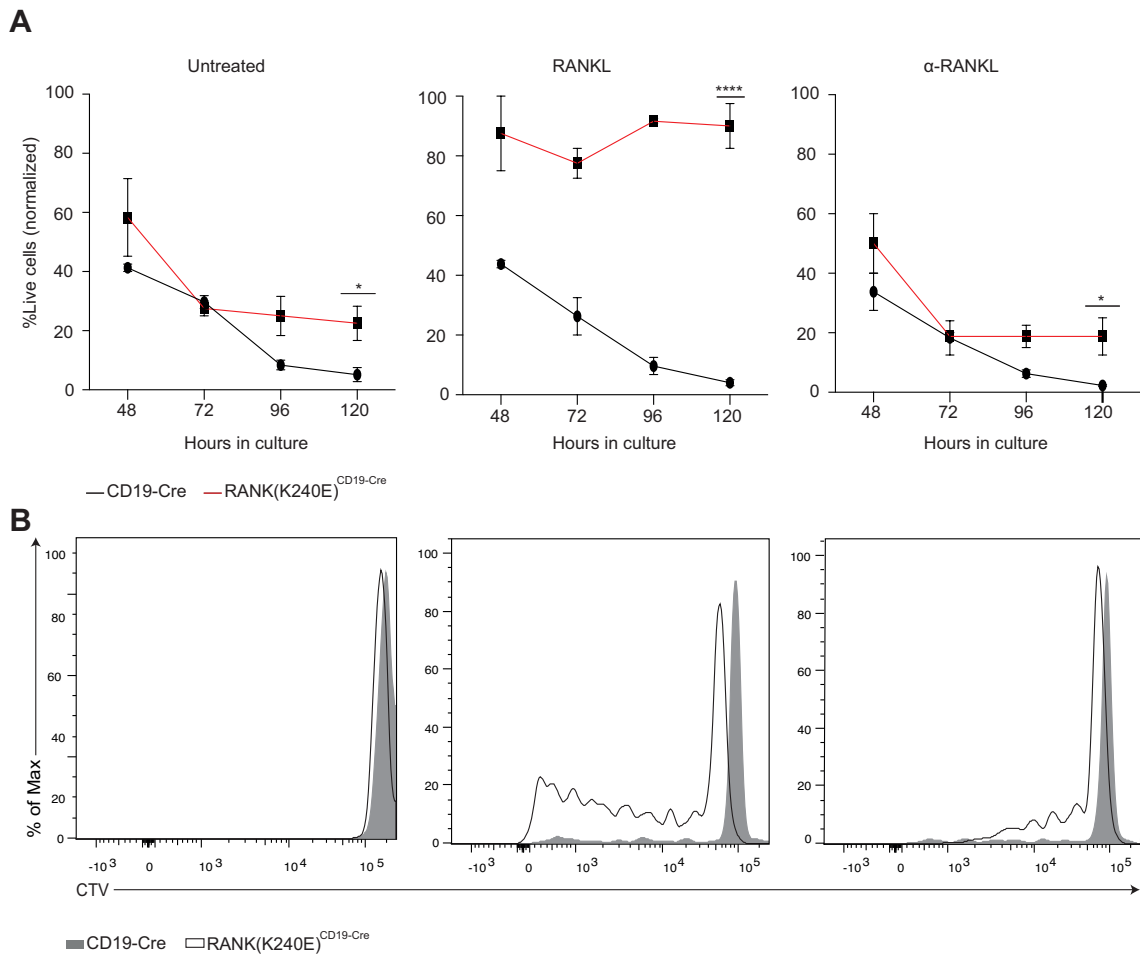


Figure 5.12: RANK(A756G) expressing B cells are dependent on RANKL for survival and proliferation in vitro. GFP⁺ and CD19⁺ sorted B cells from 2-4 month old RANK(A756G)^{CD19-Cre} and CD19-Cre control mice, respectively, were stained with CellTrace Violet proliferation dye and kept in culture in the presence or absence of 100 ng/ml recombinant mouse RANKL or 2 μ g purified α -RANKL for 5 days. Flow cytometry analysis with Annexin-V and 7AAD stained B cells (A) revealed enhanced survival and proliferation (B) in the presence of RANKL. The data shown are representative of 4 independent experiments with a total of 8 mice per genotype.

expressing B cells, whereas it does not affect the activation of CD19-Cre B cells. Treatment with α -RANKL 24 hours after RANKL stimulation reduced the upregulation of the surface activation markers. Taken together, these data point to an activated B cell phenotype with increased survival and proliferative advantage that is dependent on the RANK-RANKL binding. Murine RANKL, which shares 85% homology with human RANKL, was used in all the *in vitro* experiments, to mimic the *in vivo* situation where only murine RANKL is available for the RANK(A756G) expressing B cells. This was able to bind and activate human RANK expressed on the murine B cells.

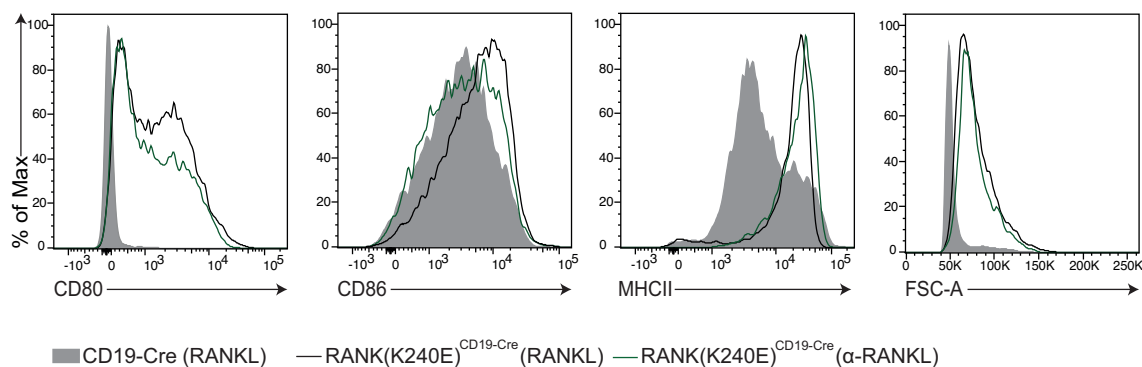


Figure 5.13: murine RANKL activates RANK(A756G) expressing B cells in vitro. GFP+ and CD19+ sorted B cells from 2-4 month old RANK(A756G)^{CD19-Cre} and CD19-Cre control mice respectively, were kept in culture in the presence or absence of recombinant mouse RANKL or 2 μ g purified neutralizing antibody α -RANKL for 48 hours and analyzed for activation markers CD80, CD86, MHCII and FSC-A by flow cytometry (n=6)

5.3.3 *In vitro* and *in vivo* activated T cells express RANKL

Since RANK(A756G) expressing B cells are dependent on RANKL for survival and proliferation, the possible cell-cell interactions which would enable the RANK(A756G) expressing B cells in RANK(A756G)^{CD19-Cre} mice to bind RANKL were investigated next. Previous studies have shown that bone marrow stromal cells, which are in close contact with the B cells during their development in the bone marrow express RANKL, as well as activated T cells which contact B cells in the periphery.

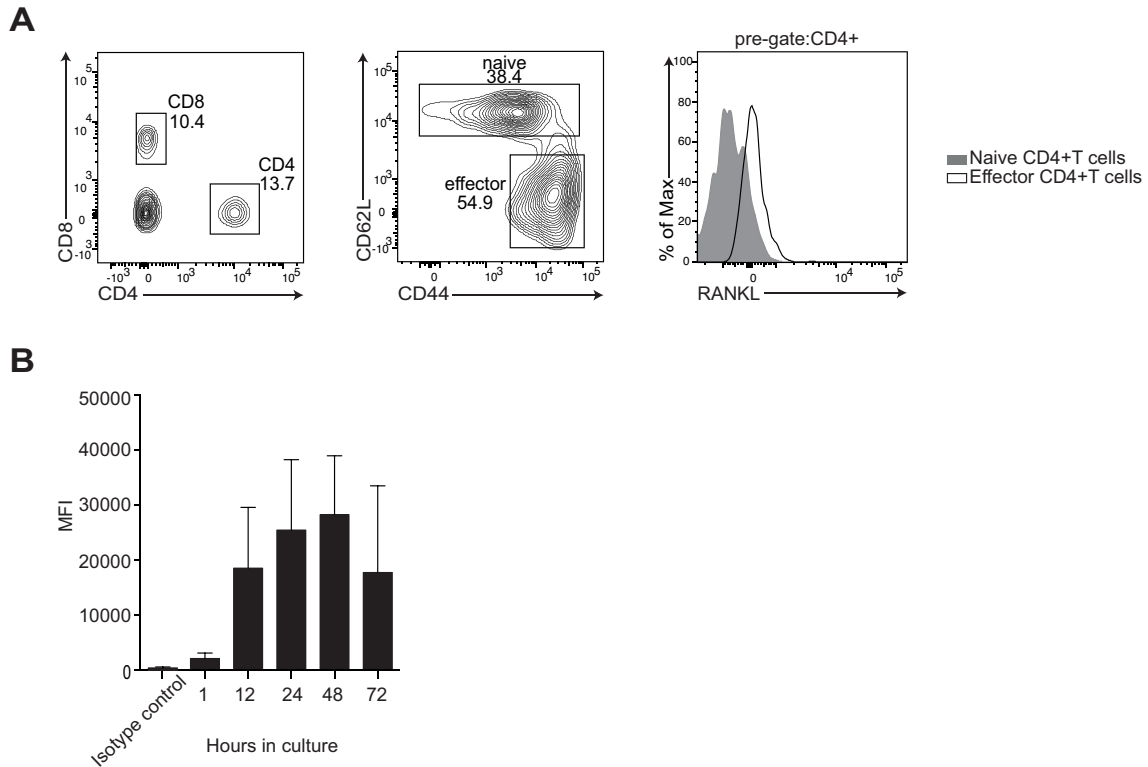


Figure 5.14: Activated CD4⁺T cells express RANKL *in vivo*. (A) MACS purified CD4⁺ T cells from the spleens of RANK(A756G)^{CD19-Cre} mice were analyzed by flow cytometry for surface RANKL expression. (B) Kinetics of RANKL surface expression on MACS purified and CD3/CD28 activated CD4⁺T cells, as determined by flow cytometry analysis and represented as mean fluorescence intensity. Surface RANKL expression peaks 48 hours after stimulation. The data are representative of at least two independent experiments.

As Figure 5.14A shows, effector CD4⁺ T cells from the spleen and lymph nodes of RANK(A756G)^{CD19-Cre} and CD19-Cre mice, which are gated as the CD44^{high}, CD62L^{low} cells in flow cytometry analysis, have upregulated surface RANKL expression, compared to the naive CD4⁺ T cell compartment which is CD62L^{high}CD44^{low}. In order to determine the kinetics of the upregulation of surface RANKL expression upon activation on T cells, CD4⁺ T cells were magnetically isolated (MACS) from spleens and lymph nodes of RANK(A756G)^{CD19-Cre} and CD19-Cre mice, activated *in vitro* by CD3/CD28 ligation and checked for upregulation of surface RANKL by flow cytometry. Figure 5.14B shows surface RANKL expression starts to increase as early as 1 hour after activation, and reaches its peak at 48 hours, before declining at 72 hours. Similar results were observed for both RANK(A756G)^{CD19-Cre}

and CD19-Cre control mice (data not shown). Taken together these data show that activated CD4⁺ T cells express surface RANKL in a time-dependent manner and are a potential source of RANKL for RANK(A756G) expressing B cells during their interaction in the secondary lymphoid tissues such as the spleen or lymph nodes.

5.3.4 *In vitro* activated T cells induce a more activated phenotype in RANK(A756G) expressing B cells than in wildtype B cells

After confirming and establishing the kinetics of surface RANKL expression in *in vivo* and *in vitro* activated T cells, respectively, the effect of the interaction between RANK(A756G) expressing B cells and RANKL expressing T cells were investigated next. CD4⁺ T cells isolated via negative magnetic labelling (MACS), from the spleens and lymph nodes of RANK(A756G)^{CD19-Cre} mice were activated *in vitro* with CD3/CD28 for 48 hours, the time point when the surface expression of RANKL peaks. RANK(A756G) expressing B cells isolated by sorting for GFP, and CD19-Cre B cells isolated by sorting for CD19⁺ cells were added on the activated CD4⁺ T cells at this time point. Activation status of the B cells was measured 24 hours later using flow cytometry analysis for the surface activation markers CD80, CD86 and MHCII. This analysis has revealed that RANK(A756G) expressing B cells have a more activated phenotype after interacting with activated T cells compared to the CD19-Cre B cells, indicated by a higher CD80 and CD86 surface expression, as well as an increased forward-scatter due to larger cell size. Therefore, the RANK-RANKL interaction among B and T cells is non-redundant and provides a marked increase in B cell activation. The data therefore demonstrated that RANKL binding with RANK provides the RANK(A756G) expressing B cells with an additional activating signal, and leads to a highly activated B cell population that would have survival and proliferative advantage in the periphery upon contact with CD4⁺ T cells (Figure 5.15A).

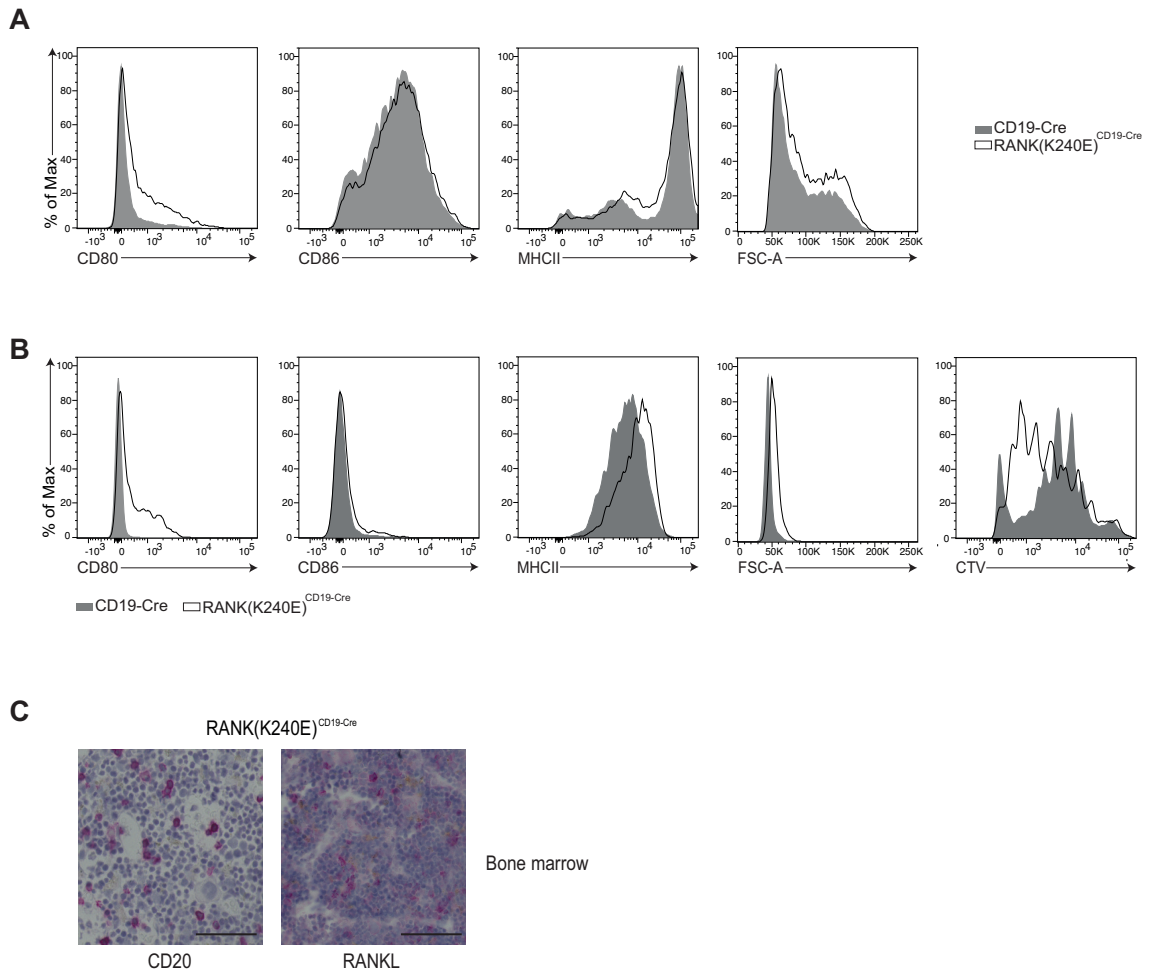


Figure 5.15: RANK(A756G) expressing B cells are highly activated by CD4+ T cells. GFP+ and CD19+ sorted B cells from 2-4 month old RANK(A756G)^{CD19-Cre} and CD19-Cre control mice, respectively, were incubated with MACS isolated, CD3/CD28 activated CD4+ T cells for 48 hours and analyzed for B cell surface activation markers by flow cytometry. The data shown are representative of 3 independent experiments with at least 6 mice per genotype. (C) IHC staining of bone marrows from 2-4 month old RANK (K240E)CD19-Cre mice show CD20+ B cells in the vicinity of RANKL+ bone marrow stromal cells (Scale bars: 1mm).

5.3.5 ST2, a bone marrow stromal cell line, induces a more activated phenotype and an increased proliferative capacity in RANK(A756G) expressing B cells

As another potential resource of RANKL for RANK(A756G) expressing B cells, bone marrow stroma has an essential role in the development and differentiation of

B cells. As was explained in Section 5.2.6, immature RANK(A756G) expressing B cells upregulate MHCII and CD86 on their surface, indicating a prematurely activated phenotype. To further elucidate the effect of RANKL expression by stromal cells on RANK(A756G) expressing B cells, a RANKL expressing stromal cell line, ST2 was used in co-culture experiments. GFP⁺ sorted RANK(A756G) expressing B cells from spleens of RANK(A756G)^{CD19-Cre} mice and CD19⁺ sorted B cells from CD19-Cre mice were stained with CellTrace Violet and cocultured with pre-plated ST2 cells for 96 hours, and checked for surface activation markers as well as proliferation by flow cytometry. Figure 5.15B shows that RANK(A756G) expressing B cells proliferate more than CD19-Cre B cells in the presence of ST2 cells. ST2 cells also induce a more activated phenotype in RANK(A756G) expressing B cells, indicated by a higher expression of surface CD80, CD86, MHCII and also an increase in cellular size. Taken together, these data indicate that RANK(A756G) expressing B cells are highly activated and proliferate more *in vitro* in the presence of RANKL expressing ST2 cells, supporting the observation of the presence of prematurely activated immature B cells in the bone marrow of RANK(A756G)^{CD19-Cre} mice. In addition, immunohistochemistry (IHC) staining for RANKL and CD20 in serial sections from the bone marrows of RANK(A756G)^{CD19-Cre} mice showed CD20⁺ B cells in the vicinity of RANKL expressing cells, as expected, where they interact with the bone marrow stroma during their development (Figure 5.15C).

5.3.6 RANK(A756G) expressing B cells show activation of PI3K and MAPK pathways upon RANKL stimulation

To elucidate which signaling pathways are involved in RANK(A756G) mediated B cell leads to enhanced survival, proliferation and activation, RANK(A756G) expressing B cells from the spleens of RANK(A756G)^{CD19-Cre} mice have been sorted for GFP⁺ and stimulated with 100 ng/ul RANKL or 0.5 μ CpG for 48 hours in culture, along with CD19⁺ sorted CD19-Cre B cells. Total cell lysates were obtained following stimulation and immunoblotted for phosphorylation in proteins that are known to be downstream of RANK. While components of both the canonical and the non-canonical NF- κ B pathway showed no difference in phosphorylation upon

RANKL stimulation (data not shown), Akt and ERK and JNK family MAP kinases have shown remarkably increased phosphorylation in response to RANKL stimulation, and in lower levels in response to CpG stimulation. CD19-Cre B cells on the other hand, did not respond to RANKL stimulation, as no difference in phosphorylation levels of Akt or MAPKs was observed and these cells were only responsive to CpG stimulation, showing that RANK(A756G) expressing B cells achieve survival and proliferative advantages due to an upregulation in PI3K and MAPK signaling upon RANKL binding, and not in steady state (Figure 5.16A). In addition, the pharmacological inhibition of the JNK and PI3K pathways lead to reduced survival of transgenic B cells, when administered 24 hours after stimulation with RANKL, further indicating that RANK(A756G) expression leads to the survival of transgenic B cells through the activation of MAPK and PI3K pathways upon RANKL stimulation (Figure 5.16B).

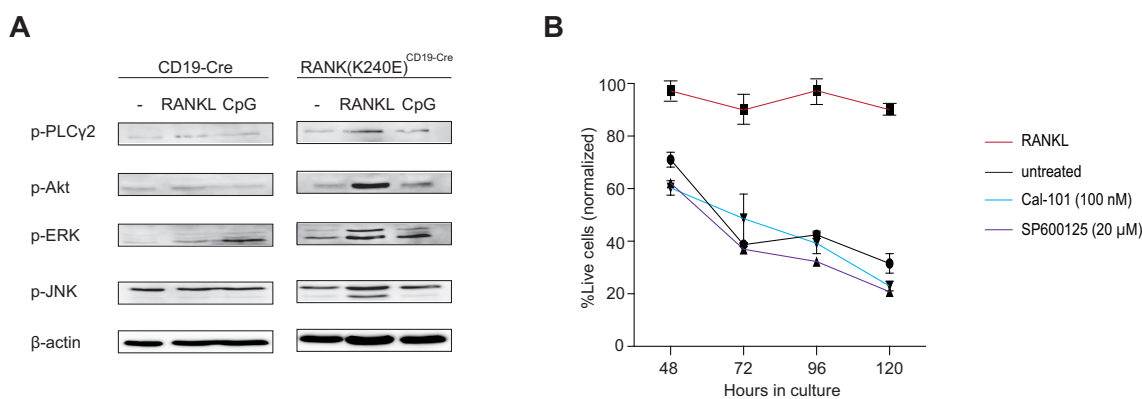


Figure 5.16: RANK(A756G) expressing B cells upregulate MAPK and PI3K signaling upon RANKL stimulation. (A) GFP⁺ and CD19⁺ sorted B cells from 4 month old RANK(A756G)^{CD19-Cre} and CD19-Cre control mice, respectively, were stimulated with 100 ng/ml recombinant mouse RANKL or 0.5 μM CpG for 48 hours, and subsequently subjected to western blotting. (B) Pharmacological inhibition of JNK pathway with SP600125 and PI3K pathway with Cal-101 24 hours after stimulation with RANKL abolishes the survival benefit of RANK(A756G) expressing B cells. The data shown are representative of at least two independent experiments.

5.3.7 RANK(A756G) expressing B cells differentially express genes related to survival, proliferation and signaling

As previously explained, RANK(A756G) expression in B cells drives survival, proliferation and activation. After establishing that RANK signaling leads to such effects through the activation of MAPK and PI3K pathways, the differential expression of genes important in cell survival and proliferation in RANK(A756G) B cells was investigated. For this purpose, RT-PCR analysis was performed on cDNA isolated from GFP+ and CD19+ sorted and pooled B cells from the spleen, lymph nodes and peritoneal cavity of 20-week-old RANK(A756G)^{CD19-Cre} sorted B cells from CD19-Cre mice, respectively. The target genes were chosen based on microarray analysis and their relevance in cell survival and proliferation (data not shown). Differences in gene expression patterns demonstrated by the microarray data were reproduced for several genes by RT-PCR. Among them were the apoptosis related genes such as Bcl-2, APC and PTEN; from which Bcl2 is an anti-apoptotic and APC and PTEN are pro-apoptotic genes. As expected, Bcl-2 was upregulated, whereas APC and PTEN were downregulated in RANK(A756G) expressing B cells. CyclinD1, which is a positive regulator of cellular proliferation has been upregulated in RANK(A756G) expressing B cells; as are Malt1 and IKK β , which are positive regulators of the NF- κ B pathway (Figure 5.17). Taken together these data indicate that RANK(A756G)

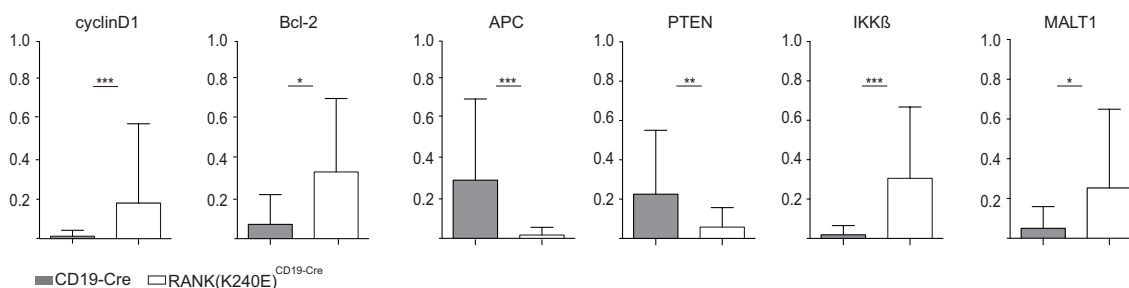


Figure 5.17: RANK(A756G) expressing B cells upregulate prosurvival and antiapoptotic genes in vivo. Transcript levels of cyclinD1, Bcl-2, APC, PTEN, IKKB and MALT-1 in GFP+ and CD19+ sorted B cells from 20 week old RANK(A756G)^{CD19-Cre} and CD19-Cre control mice, respectively. Normalized to Actin; $n \geq 7$ per genotype.

expression in B cells leads to the upregulation of genes that are positive regulators of survival and proliferation and downregulation of genes that promote apoptosis, an effect that is mediated through the upregulation of MAPK and PI3K signaling upon ligand binding.

Chapter 6

Discussion

Receptor activator of NF- κ B is an important receptor standing in the cross-roads of several pathways which regulate cellular growth and replication. Given its influence on both bone homeostasis and development of several components of the immune system and its essential role in “osteimmunology”, the aim of the present study was to elucidate the effects of deregulated RANK signaling in B cells *in vivo*.

To tackle this question, B cell restricted enforced expression of the RANK(A756G) mutation, which was described for 8% of ABC-DLBCL patients, was the selected approach. Analysis of this genetic mouse model revealed that deregulated RANK signaling in the pre-B cell stage is sufficient to drive lymphoproliferation and autoimmunity *in vivo*, with SLE-like manifestations such as glomerulonephritis and the presence of ANAs in the serum. Initial experiments *in vitro* in Bal17 cells were performed to gain a fundamental understanding of the consequences of enforced RANK expression in B cells. These showed that the RANK(A756G) mutant expression leads to a marginal increase in B cell activation in response to RANKL stimulation, compared to the wildtype RANK expressed at equal amounts. *Ex vivo* experiments with transgenic RANK(A756G) expressing B cells also showed that in the absence of the ligand stimulation, RANK(A756G) expression in transgenic B cells provides marginal survival advantage over wild type B cells. On the other hand, *ex vivo* experiments also showed that lymphoproliferative effects of RANK(A756G) were mainly ligand dependent. Therefore, the overexpression of this receptor on the surface of B cells is largely responsible for the survival benefit of the transgenic B

cells. Hence, it can be concluded that the enforced RANK(A756G) expression leads to enhanced survival and proliferation of transgenic B cells due to a synergistic effect between RANK overexpression and the K240E mutation.

Based on the literature and the observations in Bal-17 cells in this study, the postulated hypothesis was that enforced RANK(K240) expression in B cells would drive pathology. The disease induced by B cell specific enforced RANK(A756G) expression manifested itself through a shortened lifespan, enlarged secondary lymphoid organs and glomerulonephritis-related kidney failure. Deterioration of renal function was also clearly reflected in the development of proteinuria in RANK (K240E)^{CD19-Cre} mice. A closer look at the kidneys revealed massive accumulation of immune complexes, reminiscent of lupus nephritis [110]. Kidney disease is a very common complication in systemic autoimmune diseases and 90% of systemic lupus erythematosus (SLE) patients suffer from some form of kidney disease [111]. The B cell phenotype in RANK(A756G)^{CD19-Cre} mice was highly activated and proliferative, and showed an expansion of the B1 B cell compartment, with an emphasis on the B1a B cells, a trait which was described for several mouse models of lupus [112]. The most solid indication of an autoimmune disease in these mice was provided by the presence of ANAs in the serum. ANAs, and especially anti-dsDNA presence is a very strong indicative of SLE in humans and mouse models [113]. An increase in serum immunoglobulins, mostly in IgM, IgG2b, IgA and IgG3 was also observed. It was demonstrated in several mouse models of lupus that B2 B cells preferentially class switch to IgA and IgG2b during disease [114]; whereas IgM is the immunoglobulin spontaneously secreted by B1 B cells [115]. An increase in plasma cells in the spleen and bone marrow in transgenic mice was also observed. In line with this finding, an elevation of plasma cells in the circulating blood and tonsils during disease flares in SLE patients, along with increased numbers of plasma cells in the bone marrow in SLE mouse models were previously reported [116, 117]. The B cell repertoire of the transgenic mice was polyclonal and showed increased rates of somatic hypermutation, which was also described in SLE mouse models [118]. Taken together, the data obtained showed that enforced RANK(A756G) expression on B cells during early stages of development in the bone marrow drives an autoimmune disease characterized by B cell activation and proliferation, renal failure and presence of ANAs.

We observed that enforced RANK(A756G) expression leads to the activation and enhanced survival and proliferation of transgenic B cells upon RANKL binding through the MAPK and PI3K signaling pathways, and that inhibiting the JNK and PI3K pathways leads to a drastic drop in transgenic cell survival. Transgenic B cells that start expressing RANK(A756G) during the pre-B cell stage in the bone marrow. These already have access to the RANKL secreted by the bone marrow stromal cells, which might provide them with an initial activating “hit” and a survival advantage through the immune checkpoints in the bone marrow aimed to eliminate autoreactive cells by activating these signaling pathways. Indeed, a closer look into the bone marrow of RANK(A756G)^{CD19-Cre} mice revealed that upon RANK(A756G) expression, immature transgenic B cells had a marked increase in the surface expression of MHCII and CD86. Immature B cells developing in the bone marrow of B16 mice are unable to upregulate MHCII and CD86 upon antigen binding, a phenomenon that is thought to prevent premature activation of a B cell, and thus autoimmunity [119]. A prematurely activated B cell phenotype in the bone marrow, as is observed in RANK(A756G)^{CD19-Cre}, might lead to the escape of many autoreactive B cells from the central tolerance checkpoint to the periphery, resulting in the autoimmune phenotype that is observed in mice.

Considering the many similarities between autoimmunity and lymphoma, it is not surprising that the expression of a somatic mutation that is observed in DLBCL patients leads to autoimmunity in mice, although it might initially seem unanticipated. SLE is associated with a 2.7 fold increase in NHL risk overall [120]. Both diseases require the breakdown of checkpoints that control lymphocyte proliferation, both contain somatic and inherited mutations in several important components of pathways that regulate apoptosis and cell proliferation, such as the Fas mutation that is common to both lymphomas and autoimmune diseases [121]. In addition, both diseases can be triggered by Epstein-Bar virus infections, show dysregulation of the cytokines IL-4, IL-6, IL-8 and IL-10 and overexpression of the B-cell activating factor (BAFF) is found in SLE and rheumatoid arthritis, as well as NHL [122, 123, 124, 125, 126].

Importantly, we have observed that the phenotype in RANK(A756G)^{CD19-Cre} mice was ligand dependent and that the RANKL provided the transgenic B cells with

a survival and proliferative advantage. *Ex vivo* experiments with RANK(A756G) expressing B cells showed that murine RANKL stimulation was required to activate transgenic B cells and enhanced the survival and proliferative abilities of the transgenic B cells. This effect was partially abrogated by administration of neutralizing α -RANKL antibody on the stimulated cells. Neutralizing antibody had no effect in the absence of RANKL.

After establishing that transgenic B cells require RANKL for survival and proliferation, an important question to answer was to identify the source of RANKL, and how the interaction of transgenic B cells with the RANKL expressing cells would affect the physiology of the B cell. Several cell types express either membrane-bound or soluble RANKL, of which two are most important for B cell development and a response against pathogens. One is the osteoblasts, which are part of the bone marrow stroma where B cells develop, and the other is the CD4+ T cells, which interact with B cells in the periphery during antigen response, and express RANKL upon activation. To test whether B cell interaction with these two cell types would lead to any changes in B cell activation or proliferation, co-culture experiments were performed. Indeed, upon co-culturing with *in vitro* activated CD4+ T cells, the transgenic B cells showed higher activation compared to wild type B cells. Similarly, transgenic B cells co-cultured with a bone marrow stromal cell line ST2, were more activated and proliferated more compared to wild type B cells. These findings led to the conclusion that RANKL expression by bone marrow stromal cells and activated CD4+T cells provided the transgenic B cells with an additional activating signal, leading to a proliferative advantage for RANK(A756G) expressing B cells.

TNF family receptors and ligands have long been implicated in inflammatory and autoimmune diseases. Elevated TNF levels have been observed in autoimmune diseases such as rheumatoid arthritis and inflammatory bowel disease [127]. Deregulation of and mutations in Fas/FasL signaling axis, also members of the TNF superfamily, have been implicated in mice models of SLE, as well as in SLE patients [128]. High levels of BAFF, also a TNF superfamily member, in the serum of SLE patients is also associated with increased autoantibody presence and belimumab, a monoclonal antibody that inhibits BAFF is approved by the FDA for SLE treatment [129, 130]. TNF blockade alleviates antigen-induced arthritis in rats.

Inhibition of TL1A/DR3, another TNF/TNFR superfamily member is indicated as a potential therapeutic approach for several autoimmune diseases such as inflammatory bowel disease and rheumatoid arthritis [131]. Mice lacking RANKL in T cells were protected from experimental autoimmune encephalomyelitis (EAE), and pharmacological RANKL inhibition also prevented the development of EAE [132].

Similarly to autoimmune diseases, deregulation of RANK-RANKL signaling axis is also implicated in several types of lymphoid malignancies. RANK and RANKL expression is detected on Hodgkin's lymphoma cell lines, enabling an autocrine positive feedback loop that enhances cell survival and proliferation. B-CLL cells also overexpress RANK, which leads to an evasion of apoptosis through IL-8. RANKL expressed by multiple myeloma cells also induce a proliferation of the cells of myeloid lineage in the bone marrow through IL-6, enhancing the access of malignant cells to the proliferation inducing ligand (APRIL) produced by the myeloid cells (63). The RANK(A756G) mutation is observed in 8% of a cohort of ABC-DLBCL patients.

Taking all this data into consideration, the following model of disease development for RANK(A756G)^{CD19-Cre} mice is proposed. B cells start expressing the transgene RANK(A756G) during the pre-B cell stage bind RANKL that is expressed on the bone marrow stroma. This leads to a prematurely activated cell phenotype with survival advantages through upregulation of MAPK and PI3K pathways. Thereby central checkpoints are circumvented, even if they are autoreactive. These proliferative autoreactive cells in turn, move to the periphery where they encounter their nuclear antigens (as a result of cell death, for instance). CD4+T cells that have upregulated surface RANKL which might enhance their proliferative and survival abilities, leading to excessive production of autoantibodies and immunoglobulins, which in turn accumulate in the kidneys, resulting in defects in renal function and lead to death through severe kidney failure. The novel mouse model described here reveals that RANK(A756G) overexpression drives disease *in vivo* by enhancing B cell survival and proliferation; provides insight into the role of RANK signaling in B cells, outside the context of bone-related disorders and sheds new light on a possible target receptor in B-cell related malignancies, where RANK signaling is known to be deregulated. These include several lymphoid malignancies, such as Hodgkin's lymphoma, CLL and multiple myeloma, as well as autoimmune disorders. Based on the find-

ing of ligand-dependent signaling of RANK(A756G), RANKL inhibitors might be functional in RANK(A756G)-mutated ABC-DLBCL. Furthermore, it was observed that the JNK and PI3K pathways are crucial for mediating RANK(A756G) induced proliferation. Based on the success of the PI3K inhibitor CAL-101 in clinical trials, this might also be useful for RANK-mutated ABC-DLBCL [133]. RANK-RANKL signaling axis is already being targeted for treatment of skeleton-related diseases and the RANKL inhibitor Denosumab was approved by the FDA for osteoporosis and skeleton-related events following malignancies such as bone metastases and giant cell tumor of bone. The study at hand indicates that RANKL inhibitors could also be used for the treatment of B cell malignancies, possibly in combination with other therapies.

Nomenclature

ABC activated B-cell-like, page 14

AID Activation-Induced Deaminase, page 5

ANA Anti-Nuclear Antibodies, page 11

APC Antigen Presenting Cell, page 2

BAFF B-cell Activating Factor, page 13

BCR B cell Receptor, page 3

Blimp-1 B-lymphocyte induced maturation protein 1, page 5

BTK Bruton's tyrosine kinase, page 8

C Constant, page 3

CD Cluster of Differentiation, page 2

CLL chronic lymphocytic leukemia, page 19

CLP Common Lymphoid Progenitor, page 3

CSR Class-Switch Recombination, page 5

D Diversity, page 3

DC Dendritic cells, page 18

DLBCL Diffuse large B-cell lymphoma, page 14

EBF Early B-cell Factor, page 3

- ELISA Enzyme-Linked Immunosorbent Assay, page XI
- ELISA Enzyme-Linked Immunosorbent Assay, page 37
- ERK extracellular signal regulated kinase, page 17
- FACS Fluorescence-activated Cell Sorting, page XI
- FACS Fluorescence-activated Cell Sorting, page 38
- FO Follicular, page 4
- GC Germinal Center, page 4
- HRS Hodgkin and Reed-Sternberg, page 14
- HSC Hematopoietic Stem Cell, page 3
- I κ B inhibitor of κ B, page 16
- Ig Immunoglobulin, page 4
- IKK I κ B kinase complex, page 17
- IL Interleukin, page 3
- ITAM Immunoreceptor Tyrosine-Based Activation Motif, page 8
- ITIM Immunoreceptor Tyrosine-Based Inhibitory Motif, page 8
- J Joining, page 3
- JNK Jun amino-terminal kinase, page 17
- MAPK mitogen-activated protein kinase, page 8
- MHC Major Histocompatibility Complex, page 2
- MPP Multipotent Progenitor Cell, page 3
- MZ Marginal Zone, page 4
- NF- κ B nuclear factor-kappa B, page 6
- OPG Osteoprotegerin, page 15

PAMP Pathogen Associated Molecular Pattern, page 1

PCR Polymerase Chain Reaction, page X

PCR Polymerase Chain Reaction, page 27

PD-1 Programmed Death 1, page 8

PLC- γ Phospholipase C- γ , page 8

PRR Pattern Recognition Receptor, page 1

RAG Recombination-Activating Gene, page 3

RANK receptor activator of NF- κ B, page 14

RANKL RANK Ligand, page 15

SAPK stress-activated protein kinase, page 17

SHM Somatic Hypermutation, page 5

SLE Systemic Lupus Erythematosus, page 11

Syk Spleen Tyrosine Kinase, page 8

TACE TNF- α convertase, page 15

TdT deoxyribonucleotidyltransferase, page 4

TLR Toll-like Receptor, page 12

TNF tumor necrosis factor, page 15

V Variable, page 3

List of Figures

- 1.1 **B cell receptor signaling cascade.** Crosslinking of the BCR following receptor-specific antigen binding activates a signaling cascade through which receptor associated Src-family protein kinases phosphorylate the ITAMs of $Ig\alpha$ and $Ig\beta$, which phosphorylate and activate Syk and BTK, leading to the activation of PLC- γ 2. PLC- γ 2 then cleaves the membrane bound PIP_2 into IP_3 and DAG. IP_3 and DAG conduct the Ca^{2+} influx regulated activation of PKC β , which leads to the activation of the NF- κ B pathway through the assembly of the CBM complex. DAG also mediates the activation of MAPKs and the transcription factor AP-1 through small G proteins Ras and Raf. IP_3 regulated Ca^{2+} influx also leads to the activation of the transcription factor NFAT. NFAT, AP-1 and NF- κ B transcription factors in turn, induce expression of genes related to cell survival, proliferation and differentiation. 9
- 1.2 **Receptor Activator of NF- κ B signaling cascade.** Upon binding its ligand, RANKL, RANK recruits TRAFs which relay the signal downstream, and induce the activation of JNK, ERK and p38 MAPKs, the PI3K pathway and the alternative and canonical NF- κ B pathways, leading to cell survival, proliferation and osteoclastogenesis. RANKL can be found in membrane-bound or soluble form, cleaved by metalloproteases. OPG, a soluble decoy receptor for RANKL distinct from RANK is essential in balancing the RANK-RANKL signaling axis and abrogating signaling by binding excess RANKL. . . . 16

- 5.1 **Schematic depiction of RANK(A756G) mutation.** Red arrow indicates mutation. Motif 1 PFQEP(369-373), Motif 2 PVQEET(559-564) and Motif 3 PVQEQG(604-609) are TRAF binding motifs, and IVVY is a recently described TRAF independent motif, cooperating with TRAF binding motifs to promote osteoclastogenesis. These four motifs enable RANK to mediate its downstream functions. 42
- 5.2 **RANK(A756G) expression in Bal17 cells leads to marginally higher B cell activation.** Bal17 cells transduced with RANK(A756G), wildtype RANK or empty pMIGR1 vector as control were sorted for GFP and stimulated or not stimulated with 100 ng/ml recombinant mouse RANKL for 1 hour, and analyzed for the expression of B cell surface activation markers by flow cytometry. Level of RANK surface expression is in cells transduced with wildtype and mutant RANK is the same, ruling out any differences in outcome due to different RANK expression levels. Data shown are representative of four experiments. 43
- 5.3 **Generating the RANK(A756G) knockin strain and targeting of the ROSA26 locus** (A) RANK(A756G) targeting strategy. IRES, internal ribosomal entry site; NEO, neomycin; pA, poly(A); SA, splice acceptor. The wildtype ROSA26 locus, the targeting vector, and the ROSA26 locus upon homologous recombination are depicted. (B) Southern blot analysis. Lanes 1 and 2 show genomic DNA from wildtype and transgenic mice. The size of the fragment showing the WT ROSA26 locus is 4.6 kb, the recombined locus is 9.2 kb, and Cre-mediated removal of the STOP cassette results in an 8.7-kb fragment. 45

- 5.4 Mouse breeding and B cell specific expression of RANK(A756G).**
 (A) Breeding scheme. For B cell specific expression of RANK(A756G), ROSA26^{loxSTOPlox-RANK(A756G)} mice were bred with CD19-Cre mice, a surface protein whose expression is restricted to B cells. Cre expression leads to the excision of the loxSTOPlox cassette, enabling transgene expression, along with GFP. RANK(A756G) expressing B cells can thus be tracked with the aid of flow cytometry. (B) MACS isolated B cells from CD19-Cre and RANK(A756G)^{CD19-Cre} mice were subjected to western blot analysis for RANK expression. (C) Cells isolated from the spleens of CD19-Cre and RANK(A756G)^{CD19-Cre} mice were analyzed by flow cytometry for surface RANK and GFP expression. Live cells were pre-gated for CD19 expression. 46
- 5.5 RANK (K240E) expression drives disease in vivo.** (A) Macroscopic appearance of representative spleens and mesenteric lymph nodes (in cm) and total cell counts in spleen and lymph nodes of analyzed mice, bars indicate mean. (B) Kaplan–Meier curve of CD19-Cre and RANK(A756G)^{CD19-Cre} mice (n = 18, respectively)(***p ≤ 0.0001). (C) Glomerulonephritis-related kidney failure and cellular infiltration of lungs and lymph nodes in RANK(A756G)^{CD19-Cre} mice were revealed by H&E staining(Scale bars: 1 mm). The data shown in A-C are obtained from 6 month old, terminally ill animals. 49
- 5.6 RANK^{CD19-Cre} mice succumb to deteriorating renal function.**
 (A) SEM of kidneys in RANK(A756G)^{CD19-Cre} mice showed massive subendothelial immune deposit accumulation (representative of three mice of each genotype) (Scale bars: 1mm). Arrows indicate areas of interest. (B) Kidney failure in RANK(A756G)^{CD19-Cre} mice is also evident in significantly increased proteinuria (n=15, respectively). The data shown in A and B are obtained from terminally ill 6 month old animals. (**p ≤ 0.01) 50

- 5.7 **RANK(A756G) expression leads to B cell activation, proliferation and B1a cell expansion.** (A) RANK (K240E) expressing B cells show an activated phenotype in vivo: surface CD80, CD86 expression and forward-scatter area (FSC-A) were measured using flow cytometry. (B) Representative analysis of T-cell populations in the spleen of terminally ill RANK (K240E)CD19-Cre mice and 6 month old CD19-Cre control animals by flow cytometry. (C) Analysis of B1 and B2 cell populations in peritoneal cavity, spleen and lymph nodes of 6 month old animals by flow cytometry revealed B1 cell expansion. (D) B1a cell expansion in 6 month old RANK(A756G)^{CD19-Cre} mice revealed by flow cytometry. The cells were pre-gated for CD19⁺B220^{low} B1 population. The numbers refer to the mean percentages. The data shown in A-D are representative of five independent experiments, with a total number of at least 12 mice analyzed per genotype. 52
- 5.8 **Terminally ill RANK(A756G)^{CD19-Cre} mice have elevated plasma cells and a highly proliferative B cell phenotype** (A) Percentage of B cells in peritoneal cavity, spleen and lymph nodes of 6 month old terminally ill mice. (B) Ex-vivo intracellular Ki-67 staining and flow cytometry analysis of total, B1 and B2 B cells from 6 month old mice. (C) Increased percentage of plasma cells in the spleen and bone marrow of RANK(A756G)^{CD19-Cre} mice. The numbers refer to the mean percentages. The data shown in A-G are representative of five independent experiments, with a total number of at least 12 mice analyzed per genotype. 53

- 5.9 **RANK(A756G) expressing B cells are prematurely activated in the bone marrow.** (A) Representative analysis of B cell populations within bone marrow show normal B cell development in both CD19-Cre and RANK(A756G)^{CD19-Cre} mice. (B) Upregulation of B cell surface activation markers CD86 and MHCII on B cells upon expression of RANK(A756G), as determined by flow cytometry. Expression of transgene in immature B cells was traced by GFP expression. The numbers refer to the mean percentages. The data shown are representative of three independent experiments. 55
- 5.10 **RANK(A756G)^{CD19-Cre} mice have antinuclear antibodies in serum.** (A) Basal serum levels of total ANAs, anti-ssDNA and anti-dsDNA in 6 month old mice. (B) Serum levels of anti-dsDNA antibodies in RANK(A756G)^{CD19-Cre} mice increase with age. (C) Detection of serum anti-nuclear IgG and autoreactive IgM by immunofluorescence in RANK(A756G)^{CD19-Cre} mice by Hep-2 assay. (D) Basal serum levels of IgA, IgM, IgG2b and IgG3 in 3 month old mice. (n ≤ 7 per genotype). The data are shown as the mean ± SEM. 58
- 5.11 **B cell repertoire of RANK(A756G)^{CD19-Cre} mice is polyclonal and heavily mutated.** (A) Ig clonality analysis of 6 month old mice by PCR from genomic DNA isolated from GFP+ and CD19+ sorted B cells from RANK(A756G)^{CD19-Cre} and CD19-Cre mice respectively, representative of 7 mice per genotype. Polyclonal B cells show all four possible D-JH recombinations. (B) SHM analysis of 6 month old mice by PCR from genomic DNA isolated from GFP+ and CD19+ sorted B cells from RANK(A756G)^{CD19-Cre} and CD19-Cre mice respectively, representative of 7 mice per genotype, revealed significantly increased rate of SHM in RANK(A756G)^{CD19-Cre} mice. (*p ≤ 0.05) 59

- 5.12 **RANK(A756G) expressing B cells are dependent on RANKL for survival and proliferation in vitro.** GFP⁺ and CD19⁺ sorted B cells from 2-4 month old RANK(A756G)^{CD19-Cre} and CD19-Cre control mice, respectively, were stained with CellTrace Violet proliferation dye and kept in culture in the presence or absence of 100 ng/ml recombinant mouse RANKL or 2 μ g purified α -RANKL for 5 days. Flow cytometry analysis with Annexin-V and 7AAD stained B cells (A) revealed enhanced survival and proliferation (B) in the presence of RANKL. The data shown are representative of 4 independent experiments with a total of 8 mice per genotype. 61
- 5.13 **murine RANKL activates RANK(A756G) expressing B cells in vitro.** GFP⁺ and CD19⁺ sorted B cells from 2-4 month old RANK(A756G)^{CD19-Cre} and CD19-Cre control mice respectively, were kept in culture in the presence or absence of recombinant mouse RANKL or 2 μ g purified neutralizing antibody α -RANKL for 48 hours and analyzed for activation markers CD80, CD86, MHCII and FSC-A by flow cytometry (n=6) 62
- 5.14 **Activated CD4⁺T cells express RANKL in vivo.** (A) MACS purified CD4⁺ T cells from the spleens of RANK(A756G)^{CD19-Cre} mice were analyzed by flow cytometry for surface RANKL expression. (B) Kinetics of RANKL surface expression on MACS purified and CD3/CD28 activated CD4⁺T cells, as determined by flow cytometry analysis and represented as mean fluorescence intensity. Surface RANKL expression peaks 48 hours after stimulation. The data are representative of at least two independent experiments. 63

- 5.15 **RANK(A756G) expressing B cells are highly activated by CD4+ T cells.** GFP+ and CD19+ sorted B cells from 2-4 month old RANK(A756G)^{CD19-Cre} and CD19-Cre control mice, respectively, were incubated with MACS isolated, CD3/CD28 activated CD4+ T cells for 48 hours and analyzed for B cell surface activation markers by flow cytometry. The data shown are representative of 3 independent experiments with at least 6 mice per genotype. (C) IHC staining of bone marrows from 2-4 month old RANK (K240E)CD19-Cre mice show CD20+ B cells in the vicinity of RANKL+ bone marrow stromal cells (Scale bars: 1mm). 65
- 5.16 **RANK(A756G) expressing B cells upregulate MAPK and PI3K signaling upon RANKL stimulation.** (A) GFP+ and CD19+ sorted B cells from 4 month old RANK(A756G)^{CD19-Cre} and CD19-Cre control mice, respectively, were stimulated with 100 ng/ml recombinant mouse RANKL or 0.5 μ M CpG for 48 hours, and subsequently subjected to western blotting. (B) Pharmacological inhibition of JNK pathway with SP600125 and PI3K pathway with Cal-101 24 hours after stimulation with RANKL abolishes the survival benefit of RANK(A756G) expressing B cells. The data shown are representative of at least two independent experiments. 67
- 5.17 **RANK(A756G) expressing B cells upregulate prosurvival and antiapoptotic genes in vivo.** Transcript levels of cyclinD1, Bcl-2, APC, PTEN, IKKB and MALT-1 in GFP+ and CD19+ sorted B cells from 20 week old RANK(A756G)^{CD19-Cre} and CD19-Cre control mice, respectively. Normalized to Actin; n \geq 7 per genotype. . . . 68

Bibliography

- [1] Charles Janeway. *Immunobiology : the immune system in health and disease*. Garland Science, New York, 6th edition, 2005.
- [2] Daolin Tang, Rui Kang, Carolyn B. Coyne, Herbert J. Zeh, and Michael T. Lotze. PAMPs and DAMPs: Signal 0s that spur autophagy and immunity. *Immunological reviews*, 249(1):158–175, 2012.
- [3] F. A. Bonilla and H. C. Oettgen. Adaptive immunity. *J Allergy Clin Immunol*, 125(2 Suppl 2):S33–40, 2010.
- [4] M. D. Cooper and M. N. Alder. The evolution of adaptive immune systems. *Cell*, 124(4):815–22, 2006.
- [5] J. Parkin and B. Cohen. An overview of the immune system. *Lancet*, 357(9270):1777–89, 2001.
- [6] P. J. Delves and I. M. Roitt. The immune system. First of two parts. *N Engl J Med*, 343(1):37–49, 2000.
- [7] P. J. Delves and I. M. Roitt. The immune system. Second of two parts. *N Engl J Med*, 343(2):108–17, 2000.
- [8] U. H. von Andrian and C. R. Mackay. T-cell function and migration. Two sides of the same coin. *N Engl J Med*, 343(14):1020–34, 2000.
- [9] R. R. Hardy, K. Hayakawa, D. R. Parks, L. A. Herzenberg, and L. A. Herzenberg. Murine B cell differentiation lineages. *J Exp Med*, 159(4):1169–88, 1984.
- [10] K. Pieper, B. Grimbacher, and H. Eibel. B-cell biology and development. *J Allergy Clin Immunol*, 131(4):959–71, 2013.

- [11] Martin S. Naradikian, Jean L. Scholz, Michael A. Oropallo, and Michael P. Cancro. *Understanding B Cell Biology*. Springer Basel, Basel, 2014.
- [12] R. R. Hardy and K. Hayakawa. B cell development pathways. *Annu Rev Immunol*, 19:595–621, 2001.
- [13] F. W. Alt, G. D. Yancopoulos, T. K. Blackwell, C. Wood, E. Thomas, M. Boss, R. Coffman, N. Rosenberg, S. Tonegawa, and D. Baltimore. Ordered rearrangement of immunoglobulin heavy chain variable region segments. *EMBO J*, 3(6):1209–19, 1984.
- [14] A. Durandy, N. Taubenheim, S. Peron, and A. Fischer. Pathophysiology of B-cell intrinsic immunoglobulin class switch recombination deficiencies. *Adv Immunol*, 94:275–306, 2007.
- [15] G. Cinamon, M. Matloubian, M. J. Lesneski, Y. Xu, C. Low, T. Lu, R. L. Proia, and J. G. Cyster. Sphingosine 1-phosphate receptor 1 promotes B cell localization in the splenic marginal zone. *Nat Immunol*, 5(7):713–20, 2004.
- [16] M. Balazs, F. Martin, T. Zhou, and J. Kearney. Blood dendritic cells interact with splenic marginal zone B cells to initiate T-independent immune responses. *Immunity*, 17(3):341–52, 2002.
- [17] I. C. MacLennan. Germinal centers. *Annu Rev Immunol*, 12:117–39, 1994.
- [18] Y. J. Liu and C. Arpin. Germinal center development. *Immunol Rev*, 156:111–26, 1997.
- [19] G. Teng and F. N. Papavasiliou. Immunoglobulin somatic hypermutation. *Annu Rev Genet*, 41:107–20, 2007.
- [20] B. Kavli, S. Andersen, M. Otterlei, N. B. Liabakk, K. Imai, A. Fischer, A. Durandy, H. E. Krokan, and G. Slupphaug. B cells from hyper-igm patients carrying UNG mutations lack ability to remove uracil from ssDNA and have elevated genomic uracil. *J Exp Med*, 201(12):2011–21, 2005.
- [21] R. M. Zinkernagel, M. F. Bachmann, T. M. Kundig, S. Oehen, H. Pirchet, and H. Hengartner. On immunological memory. *Annu Rev Immunol*, 14:333–67, 1996.

- [22] A. Radbruch, G. Muehlinghaus, E. O. Luger, A. Inamine, K. G. Smith, T. Dorner, and F. Hiepe. Competence and competition: the challenge of becoming a long-lived plasma cell. *Nat Rev Immunol*, 6(10):741–50, 2006.
- [23] E. Montecino-Rodriguez and K. Dorshkind. B-1 B cell development in the fetus and adult. *Immunity*, 36(1):13–21, 2012.
- [24] R. R. Hardy. B-1 B cell development. *J Immunol*, 177(5):2749–54, 2006.
- [25] J. W. Tung, M. D. Mrazek, Y. Yang, L. A. Herzenberg, and L. A. Herzenberg. Phenotypically distinct B cell development pathways map to the three B cell lineages in the mouse. *Proc Natl Acad Sci U S A*, 103(16):6293–8, 2006.
- [26] I. E. Godin, J. A. Garcia-Porrero, A. Coutinho, F. Dieterlen-Lievre, and M. A. Marcos. Para-aortic splanchnopleura from early mouse embryos contains B1a cell progenitors. *Nature*, 364(6432):67–70, 1993.
- [27] B. Rowley, L. Tang, S. Shinton, K. Hayakawa, and R. R. Hardy. Autoreactive B-1 B cells: constraints on natural autoantibody B cell antigen receptors. *J Autoimmun*, 29(4):236–45, 2007.
- [28] F. Martin, A. M. Oliver, and J. F. Kearney. Marginal zone and B1 B cells unite in the early response against t-independent blood-borne particulate antigens. *Immunity*, 14(5):617–29, 2001.
- [29] K. A. Hogquist, T. K. Starr, and S. C. Jameson. Receptor sensitivity: when T cells lose their sense of self. *Curr Biol*, 13(6):R239–41, 2003.
- [30] Caroline Grönwall, Jaya Vas, and Gregg J. Silverman. Protective roles of natural IgM antibodies. *Frontiers in Immunology*, 3:66, 2012.
- [31] N. Baumgarth. The double life of a B-1 cell: self-reactivity selects for protective effector functions. *Nat Rev Immunol*, 11(1):34–46, 2011.
- [32] A. F. Cunningham, A. Flores-Langarica, S. Bobat, C. C. Dominguez Medina, C. N. Cook, E. A. Ross, C. Lopez-Macias, and I. R. Henderson. B1b cells recognize protective antigens after natural infection and vaccination. *Front Immunol*, 5:535, 2014.

- [33] K. Hayakawa, R. R. Hardy, D. R. Parks, and L. A. Herzenberg. The “Ly-1 B” cell subpopulation in normal immunodefective, and autoimmune mice. *J Exp Med*, 157(1):202–18, 1983.
- [34] H. T. Maecker, J. P. McCoy, and R. Nussenblatt. Standardizing immunophenotyping for the human immunology project. *Nat Rev Immunol*, 12(3):191–200, 2012.
- [35] Jennifer A. Woyach, Amy J. Johnson, and John C. Byrd. The B-cell receptor signaling pathway as a therapeutic target in CLL. *Blood*, 120(6):1175–1184, 2012.
- [36] T. Brummer, W. Elis, M. Reth, and M. Huber. B-cell signal transduction: tyrosine phosphorylation, kinase activity, and calcium mobilization. *Methods Mol Biol*, 271:189–212, 2004.
- [37] S. Sato, D. A. Steeber, P. J. Jansen, and T. F. Tedder. CD19 expression levels regulate b lymphocyte development: human CD19 restores normal function in mice lacking endogenous CD19. *J Immunol*, 158(10):4662–9, 1997.
- [38] D. C. Parker. T cell-dependent B cell activation. *Annu Rev Immunol*, 11:331–60, 1993.
- [39] J. Stavnezer, J. E. Guikema, and C. E. Schrader. Mechanism and regulation of class switch recombination. *Annu Rev Immunol*, 26:261–92, 2008.
- [40] J. Stavnezer. Antibody class switching. *Adv Immunol*, 61:79–146, 1996.
- [41] S. Yurasov, H. Wardemann, J. Hammersen, M. Tsuiji, E. Meffre, V. Pascual, and M. C. Nussenzweig. Defective B cell tolerance checkpoints in systemic lupus erythematosus. *J Exp Med*, 201(5):703–11, 2005.
- [42] E. T. Luning Prak, M. Monestier, and R. A. Eisenberg. B cell receptor editing in tolerance and autoimmunity. *Ann N Y Acad Sci*, 1217:96–121, 2011.
- [43] R. C. Lindsley, M. Thomas, B. Srivastava, and D. Allman. Generation of peripheral B cells occurs via two spatially and temporally distinct pathways. *Blood*, 109(6):2521–8, 2007.

- [44] M. Inaoki, S. Sato, B. C. Weintraub, C. C. Goodnow, and T. F. Tedder. CD19-regulated signaling thresholds control peripheral tolerance and autoantibody production in B lymphocytes. *J Exp Med*, 186(11):1923–31, 1997.
- [45] K. Schroeder, M. Herrmann, and T. H. Winkler. The role of somatic hypermutation in the generation of pathogenic antibodies in SLE. *Autoimmunity*, 46(2):121–7, 2013.
- [46] D. P. D’Cruz, M. A. Khamashta, and G. R. Hughes. Systemic lupus erythematosus. *Lancet*, 369(9561):587–96, 2007.
- [47] Anne Davidson and Betty Diamond. Autoimmune diseases. *New England Journal of Medicine*, 345(5):340–350, 2001.
- [48] G. A. Rook. Hygiene hypothesis and autoimmune diseases. *Clin Rev Allergy Immunol*, 42(1):5–15, 2012.
- [49] P. K. Gregersen and L. M. Olsson. Recent advances in the genetics of autoimmune disease. *Annu Rev Immunol*, 27:363–91, 2009.
- [50] William E. Paul. *Fundamental immunology*. Wolters Kluwer Health/Lippincott Williams & Wilkins, Philadelphia, 7th edition, 2013.
- [51] C. S. Via, A. Shustov, V. Rus, T. Lang, P. Nguyen, and F. D. Finkelman. In vivo neutralization of TNF-alpha promotes humoral autoimmunity by preventing the induction of CTL. *J Immunol*, 167(12):6821–6, 2001.
- [52] S. L. Kalled, A. H. Cutler, S. K. Datta, and D. W. Thomas. Anti-CD40 ligand antibody treatment of SNF1 mice with established nephritis: preservation of kidney function. *J Immunol*, 160(5):2158–65, 1998.
- [53] D. T. Boumpas, R. Furie, S. Manzi, G. G. Illei, D. J. Wallace, J. E. Balow, A. Vaishnav, and B. G. Lupus Nephritis Trial Group. A short course of BG9588 (anti-CD40 ligand antibody) improves serologic activity and decreases hematuria in patients with proliferative lupus glomerulonephritis. *Arthritis Rheum*, 48(3):719–27, 2003.

- [54] E. G. Boyce and B. E. Fusco. Belimumab: review of use in systemic lupus erythematosus. *Clin Ther*, 34(5):1006–22, 2012.
- [55] A. L. Shaffer, A. Rosenwald, and L. M. Staudt. Lymphoid malignancies: the dark side of B-cell differentiation. *Nat Rev Immunol*, 2(12):920–32, 2002.
- [56] T. Boehm, L. Mengle-Gaw, U. R. Kees, N. Spurr, I. Lavenir, A. Forster, and T. H. Rabbitts. Alternating purine-pyrimidine tracts may promote chromosomal translocations seen in a variety of human lymphoid tumours. *Embo j*, 8(9):2621–31, 1989.
- [57] Rodrig Marculescu, Trang Le, Paul Simon, Ulrich Jaeger, and Bertrand Nadel. V(D)J-mediated translocations in lymphoid neoplasms: A functional assessment of genomic instability by cryptic sites. *The Journal of Experimental Medicine*, 195(1):85–98, 2002.
- [58] Frank Gärtner, Frederick W. Alt, Robert J. Monroe, and Katherine J. Seidl. Antigen-independent appearance of recombination activating gene (rag)-positive bone marrow B Cells in the spleens of immunized mice. *The Journal of Experimental Medicine*, 192(12):1745–1754, 2000.
- [59] Ines Schwering, Andreas Bräuninger, Verena Distler, Julia Jesdinsky, Volker Diehl, Martin-Leo Hansmann, Klaus Rajewsky, and Ralf Küppers. Profiling of Hodgkin’s Lymphoma cell line L1236 and germinal center B Cells: Identification of hodgkin’s lymphoma-specific genes. *Molecular Medicine*, 9(3-4):85–95, 2003.
- [60] J. W. Friedberg and R. I. Fisher. Diffuse large B-cell lymphoma. *Hematol Oncol Clin North Am*, 22(5):941–52, ix, 2008.
- [61] Mara Compagno, Wei Keat Lim, Adina Grunn, Subhadra V. Nandula, Manisha Brahmachary, Qiong Shen, Francesco Bertoni, Maurilio Ponzoni, Marta Scandurra, Andrea Califano, Govind Bhagat, Amy Chadburn, Riccardo Dalla-Favera, and Laura Pasqualucci. Mutations of multiple genes cause deregulation of NF- κ B in diffuse large B-cell lymphoma. *Nature*, 459(7247):717–721, 2009.

- [62] G. S. Nowakowski and M. S. Czuczman. ABC, GCB, and double-hit diffuse large B-cell lymphoma: Does subtype make a difference in therapy selection? *Am Soc Clin Oncol Educ Book*, pages e449–57, 2015.
- [63] E. Bachy and G. Salles. Treatment approach to newly diagnosed diffuse large B-cell lymphoma. *Semin Hematol*, 52(2):107–18, 2015.
- [64] K. Dunleavy, S. Pittaluga, M. S. Czuczman, S. S. Dave, G. Wright, N. Grant, M. Shovlin, E. S. Jaffe, J. E. Janik, L. M. Staudt, and W. H. Wilson. Differential efficacy of bortezomib plus chemotherapy within molecular subtypes of diffuse large B-cell lymphoma. *Blood*, 113(24):6069–76, 2009.
- [65] T. Wada, T. Nakashima, N. Hiroshi, and J. M. Penninger. RANKL-RANK signaling in osteoclastogenesis and bone disease. *Trends Mol Med*, 12(1):17–25, 2006.
- [66] X. Feng. RANKing intracellular signaling in osteoclasts. *IUBMB Life*, 57(6):389–95, 2005.
- [67] M. C. Walsh and Y. Choi. Biology of the RANKL-RANK-OPG system in immunity, bone, and beyond. *Front Immunol*, 5:511, 2014.
- [68] J. Bollrath and F. R. Greten. IKK/NF-kappaB and STAT3 pathways: central signalling hubs in inflammation-mediated tumour promotion and metastasis. *EMBO Rep*, 10(12):1314–9, 2009.
- [69] Y. Fan, R. Mao, and J. Yang. NF-kappaB and STAT3 signaling pathways collaboratively link inflammation to cancer. *Protein Cell*, 4(3):176–85, 2013.
- [70] H. J. Kim, N. Hawke, and A. S. Baldwin. NF-kappaB and IKK as therapeutic targets in cancer. *Cell Death Differ*, 13(5):738–47, 2006.
- [71] G. Pearson, F. Robinson, T. Beers Gibson, B. E. Xu, M. Karandikar, K. Berman, and M. H. Cobb. Mitogen-activated protein (MAP) kinase pathways: regulation and physiological functions. *Endocr Rev*, 22(2):153–83, 2001.
- [72] R. Seger and E. G. Krebs. The MAPK signaling cascade. *FASEB J*, 9(9):726–35, 1995.

- [73] R. Houben, B. Michel, C. S. Vetter-Kauczok, C. Pfohler, B. Laetsch, M. D. Wolter, J. H. Leonard, U. Trefzer, S. Ugurel, D. Schrama, and J. C. Becker. Absence of classical MAP kinase pathway signalling in merkel cell carcinoma. *J Invest Dermatol*, 126(5):1135–42, 2006.
- [74] J. A. Fresno Vara, E. Casado, J. de Castro, P. Cejas, C. Belda-Iniesta, and M. Gonzalez-Baron. PI3K/Akt signalling pathway and cancer. *Cancer Treat Rev*, 30(2):193–204, 2004.
- [75] M. A. Knowles, F. M. Platt, R. L. Ross, and C. D. Hurst. Phosphatidylinositol 3-kinase (PI3K) pathway activation in bladder cancer. *Cancer Metastasis Rev*, 28(3-4):305–16, 2009.
- [76] H. Hsu, D. L. Lacey, C. R. Dunstan, I. Solovyev, A. Colombero, E. Timms, H. L. Tan, G. Elliott, M. J. Kelley, I. Sarosi, L. Wang, X. Z. Xia, R. Elliott, L. Chiu, T. Black, S. Scully, C. Capparelli, S. Morony, G. Shimamoto, M. B. Bass, and W. J. Boyle. Tumor necrosis factor receptor family member RANK mediates osteoclast differentiation and activation induced by osteoprotegerin ligand. *Proc Natl Acad Sci U S A*, 96(7):3540–5, 1999.
- [77] M. Nollet, S. Santucci-Darmanin, V. Breuil, R. Al-Sahlanee, C. Cros, M. Topi, D. Momier, M. Samson, S. Pagnotta, L. Cailleteau, S. Battaglia, D. Farlay, R. Dacquin, N. Barois, P. Jurdic, G. Boivin, D. Heymann, F. Lafont, S. S. Lu, D. W. Dempster, G. F. Carle, and V. Pierrefite-Carle. Autophagy in osteoblasts is involved in mineralization and bone homeostasis. *Autophagy*, 10(11):1965–77, 2014.
- [78] A. E. Hughes, S. H. Ralston, J. Marken, C. Bell, H. MacPherson, R. G. Wallace, W. van Hul, M. P. Whyte, K. Nakatsuka, L. Hovy, and D. M. Anderson. Mutations in TNFRSF11A, affecting the signal peptide of RANK, cause familial expansile osteolysis. *Nat Genet*, 24(1):45–8, 2000.
- [79] Allison R. Pettit, Hong Ji, Dietrich von Stechow, Ralph Müller, Steven R. Goldring, Yongwon Choi, Christophe Benoist, and Ellen M. Gravallese. TRANCE/RANKL knockout mice are protected from bone erosion in a serum

- transfer model of arthritis. *The American Journal of Pathology*, 159(5):1689–1699, 2001.
- [80] D. W. Dempster, C. L. Lambing, P. J. Kostenuik, and A. Grauer. Role of RANK ligand and denosumab, a targeted RANK ligand inhibitor, in bone health and osteoporosis: a review of preclinical and clinical data. *Clin Ther*, 34(3):521–36, 2012.
- [81] Andrea Brendolan and Jorge H. Caamaño. Mesenchymal cell differentiation during lymph node organogenesis. *Frontiers in Immunology*, 3:381, 2012.
- [82] William C. Dougall, Moira Glaccum, Keith Charrier, Kathy Rohrbach, Kenneth Brasel, Thibaut De Smedt, Elizabeth Daro, Jeffery Smith, Mark E. Tometsko, Charles R. Maliszewski, Allison Armstrong, Victor Shen, Steven Bain, David Cosman, Dirk Anderson, Philip J. Morrissey, Jacques J. Peschon, and JoAnn Schuh. RANK is essential for osteoclast and lymph node development. *Genes & Development*, 13(18):2412–2424, 1999.
- [83] S. W. Rossi, M. Y. Kim, A. Leibbrandt, S. M. Parnell, W. E. Jenkinson, S. H. Glanville, F. M. McConnell, H. S. Scott, J. M. Penninger, E. J. Jenkinson, P. J. Lane, and G. Anderson. RANK signals from CD4(+)3(-) inducer cells regulate development of aire-expressing epithelial cells in the thymic medulla. *J Exp Med*, 204(6):1267–72, 2007.
- [84] E. Gonzalez-Suarez, A. P. Jacob, J. Jones, R. Miller, M. P. Roudier-Meyer, R. Erwert, J. Pinkas, D. Branstetter, and W. C. Dougall. RANK ligand mediates progestin-induced mammary epithelial proliferation and carcinogenesis. *Nature*, 468(7320):103–7, 2010.
- [85] T. Chino, K. E. Draves, and E. A. Clark. Regulation of dendritic cell survival and cytokine production by osteoprotegerin. *J Leukoc Biol*, 86(4):933–40, 2009.
- [86] T. Akiyama, M. Shinzawa, and N. Akiyama. RANKL-RANK interaction in immune regulatory systems. *World J Orthop*, 3(9):142–50, 2012.

- [87] T. Perlot and J. M. Penninger. Development and function of murine B cells lacking RANK. *J Immunol*, 188(3):1201–5, 2012.
- [88] M. P. Whyte. Paget’s disease of bone and genetic disorders of RANKL/OPG/RANK/NF-kappaB signaling. *Ann N Y Acad Sci*, 1068:143–64, 2006.
- [89] A. Pangrazio, B. Cassani, M. M. Guerrini, J. C. Crockett, V. Marrella, L. Zammataro, D. Strina, A. Schulz, C. Schlack, U. Kornak, D. J. Mellis, A. Duthie, M. H. Helfrich, A. Durandy, D. Moshous, A. Vellodi, R. Chiesa, P. Veys, N. Lo Iacono, P. Vezzoni, A. Fischer, A. Villa, and C. Sobacchi. RANK-dependent autosomal recessive osteopetrosis: characterization of five new cases with novel mutations. *J Bone Miner Res*, 27(2):342–51, 2012.
- [90] S. Jabbar, J. Drury, J. N. Fordham, H. K. Datta, R. M. Francis, and S. P. Tuck. Osteoprotegerin, RANKL and bone turnover in postmenopausal osteoporosis. *J Clin Pathol*, 64(4):354–7, 2011.
- [91] Sakae Tanaka. Regulation of bone destruction in rheumatoid arthritis through RANKL-RANK pathways. *World Journal of Orthopedics*, 4(1):1–6, 2013.
- [92] L. Zhang, Y. Teng, Y. Zhang, J. Liu, L. Xu, J. Qu, K. Hou, X. Yang, Y. Liu, and X. Qu. Receptor activator for nuclear factor kappa B expression predicts poor prognosis in breast cancer patients with bone metastasis but not in patients with visceral metastasis. *J Clin Pathol*, 65(1):36–40, 2012.
- [93] M. R. Smith, F. Saad, S. Oudard, N. Shore, K. Fizazi, P. Sieber, B. Tombal, R. Damiao, G. Marx, K. Miller, P. Van Veldhuizen, J. Morote, Z. Ye, R. Dansey, and C. Goessl. Denosumab and bone metastasis-free survival in men with nonmetastatic castration-resistant prostate cancer: exploratory analyses by baseline prostate-specific antigen doubling time. *J Clin Oncol*, 31(30):3800–6, 2013.
- [94] K. Y. Won, R. K. Kalil, Y. W. Kim, and Y. K. Park. RANK signalling in bone lesions with osteoclast-like giant cells. *Pathology*, 43(4):318–21, 2011.

- [95] P. Fiumara, V. Snell, Y. Li, A. Mukhopadhyay, M. Younes, A. M. Gillenwater, F. Cabanillas, B. B. Aggarwal, and A. Younes. Functional expression of receptor activator of nuclear factor kappaB in Hodgkin disease cell lines. *Blood*, 98(9):2784–90, 2001.
- [96] B. J. Schmiedel, C. A. Scheible, T. Nuebling, H. G. Kopp, S. Wirths, M. Azuma, P. Schneider, G. Jung, L. Grosse-Hovest, and H. R. Salih. RANKL expression, function, and therapeutic targeting in multiple myeloma and chronic lymphocytic leukemia. *Cancer Res*, 73(2):683–94, 2013.
- [97] P. Secchiero, F. Corallini, E. Barbarotto, E. Melloni, M. G. di Iasio, M. Tiribelli, and G. Zauli. Role of the RANKL/RANK system in the induction of interleukin-8 (il-8) in B chronic lymphocytic leukemia (B-CLL) cells. *J Cell Physiol*, 207(1):158–64, 2006.
- [98] Bureau of Microbiology Laboratory Centre for Disease Control National Laboratory of Enteric Pathogens. The polymerase chain reaction: An overview and development of diagnostic PCR protocols at the LCDC. *The Canadian Journal of Infectious Diseases*, 2(2):89–91, 1991.
- [99] P. Y. Lee, J. Costumbrado, C. Y. Hsu, and Y. H. Kim. Agarose gel electrophoresis for the separation of DNA fragments. *J Vis Exp*, (62), 2012.
- [100] High frequency of normal DJH joints in B cell progenitors in severe combined immunodeficiency mice. *The Journal of Experimental Medicine*, 178(3):1007–1016, 1993.
- [101] A. Ehlich, V. Martin, W. Muller, and K. Rajewsky. Analysis of the B-cell progenitor compartment at the level of single cells. *Curr Biol*, 4(7):573–83, 1994.
- [102] F. Costantini and E. Lacy. Introduction of a rabbit beta-globin gene into the mouse germ line. *Nature*, 294(5836):92–4, 1981.
- [103] P. Mombaerts, A. R. Clarke, M. A. Rudnicki, J. Iacomini, S. Itohara, J. J. Lafaille, L. Wang, Y. Ichikawa, R. Jaenisch, M. L. Hooper, and et al. Mutations

- in T-cell antigen receptor genes alpha and beta block thymocyte development at different stages. *Nature*, 360(6401):225–31, 1992.
- [104] C. Cepko and W. Pear. Overview of the retrovirus transduction system. *Curr Protoc Mol Biol*, Chapter 9:Unit9 9, 2001.
- [105] Konstanze Pechloff. Conditional in vivo expression of the fusion kinase itk-syk. June 2013.
- [106] B. J. Smith. SDS polyacrylamide gel electrophoresis of proteins. *Methods Mol Biol*, 1:41–55, 1984.
- [107] R. H. Yolken. Enzyme-linked immunosorbent assay (ELISA): a practical tool for rapid diagnosis of viruses and other infectious agents. *Yale J Biol Med*, 53(1):85–92, 1980.
- [108] S. F. Ibrahim and G. van den Engh. Flow cytometry and cell sorting. *Adv Biochem Eng Biotechnol*, 106:19–39, 2007.
- [109] P. Soriano. Generalized lacZ expression with the ROSA26 cre reporter strain. *Nat Genet*, 21(1):70–1, 1999.
- [110] H. Bagavant and S. M. Fu. Pathogenesis of kidney disease in systemic lupus erythematosus. *Curr Opin Rheumatol*, 21(5):489–94, 2009.
- [111] Catherine Toong, Stephen Adelstein, and Tri Giang Phan. Clearing the complexity: immune complexes and their treatment in lupus nephritis. *International Journal of Nephrology and Renovascular Disease*, 4:17–28, 2011.
- [112] S. R. Morshed, K. Mannoor, R. C. Halder, H. Kawamura, M. Bannai, H. Sekikawa, H. Watanabe, and T. Abo. Tissue-specific expansion of NKT and CD5+B cells at the onset of autoimmune disease in (NZBxNZW)F1 mice. *Eur J Immunol*, 32(9):2551–61, 2002.
- [113] B. M. Giles and S. A. Boackle. Linking complement and anti-dsDNA antibodies in the pathogenesis of systemic lupus erythematosus. *Immunol Res*, 55(1-3):10–21, 2013.

- [114] W. Guo, D. Smith, K. Aviszus, T. Detanico, R. A. Heiser, and L. J. Wysocki. Somatic hypermutation as a generator of antinuclear antibodies in a murine model of systemic autoimmunity. *J Exp Med*, 207(10):2225–37, 2010.
- [115] X. Zhang. Regulatory functions of innate-like B cells. *Cell Mol Immunol*, 10(2):113–21, 2013.
- [116] P. L. Lugar, C. Love, A. C. Grammer, S. S. Dave, and P. E. Lipsky. Molecular characterization of circulating plasma cells in patients with active systemic lupus erythematosus. *PLoS One*, 7(9):e44362, 2012.
- [117] I. M. Mumtaz, B. F. Hoyer, D. Panne, K. Moser, O. Winter, Q. Y. Cheng, T. Yoshida, G. R. Burmester, A. Radbruch, R. A. Manz, and F. Hiepe. Bone marrow of NZB/W mice is the major site for plasma cells resistant to dexamethasone and cyclophosphamide: implications for the treatment of autoimmunity. *J Autoimmun*, 39(3):180–8, 2012.
- [118] H. Zan, J. Zhang, S. Ardeshtna, Z. Xu, S. R. Park, and P. Casali. Lupus-prone MRL/faslpr/lpr mice display increased AID expression and extensive DNA lesions, comprising deletions and insertions, in the immunoglobulin locus: concurrent upregulation of somatic hypermutation and class switch dna recombination. *Autoimmunity*, 42(2):89–103, 2009.
- [119] S. Marshall-Clarke, L. Tasker, and R. M. Parkhouse. Immature b lymphocytes from adult bone marrow exhibit a selective defect in induced hyperexpression of major histocompatibility complex class ii and fail to show b7.2 induction. *Immunology*, 100(2):141–51, 2000.
- [120] K. Ekstrom Smedby, C. M. Vajdic, M. Falster, E. A. Engels, O. Martinez-Maza, J. Turner, H. Hjalgrim, P. Vineis, A. Seniori Costantini, P. M. Bracci, E. A. Holly, E. Willett, J. J. Spinelli, C. La Vecchia, T. Zheng, N. Becker, S. De Sanjose, B. C. Chiu, L. Dal Maso, P. Cocco, M. Maynadie, L. Foretova, A. Staines, P. Brennan, S. Davis, R. Severson, J. R. Cerhan, E. C. Breen, B. Birmann, A. E. Grulich, and W. Cozen. Autoimmune disorders and risk of non-Hodgkin lymphoma subtypes: a pooled analysis within the InterLymph Consortium. *Blood*, 111(8):4029–38, 2008.

- [121] L. R. Goldin and O. Landgren. Autoimmunity and lymphomagenesis. *Int J Cancer*, 124(7):1497–502, 2009.
- [122] A. Hansen, P. E. Lipsky, and T. Dorner. B-cell lymphoproliferation in chronic inflammatory rheumatic diseases. *Nat Clin Pract Rheumatol*, 3(10):561–9, 2007.
- [123] F. Mackay, P. A. Silveira, and R. Brink. B cells and the BAFF/APRIL axis: fast-forward on autoimmunity and signaling. *Curr Opin Immunol*, 19(3):327–36, 2007.
- [124] A. J. Novak, D. M. Grote, M. Stenson, S. C. Ziesmer, T. E. Witzig, T. M. Habermann, B. Harder, K. M. Ristow, R. J. Bram, D. F. Jelinek, J. A. Gross, and S. M. Ansell. Expression of BLyS and its receptors in B-cell non-hodgkin lymphoma: correlation with disease activity and patient outcome. *Blood*, 104(8):2247–53, 2004.
- [125] D. N. Martin, I. S. Mikhail, and O. Landgren. Autoimmunity and hematologic malignancies: associations and mechanisms. *Leuk Lymphoma*, 50(4):541–50, 2009.
- [126] L. Varoczy, E. Payer, Z. Kadar, L. Gergely, Z. Miltenyi, F. Magyari, P. Szodoray, and A. Illes. Malignant lymphomas and autoimmunity—a single center experience from Hungary. *Clin Rheumatol*, 31(2):219–24, 2012.
- [127] Roman Fischer, Roland Kontermann, and Olaf Maier. Targeting sTNF/TNFR1 signaling as a new therapeutic strategy. *Antibodies*, 4(1):48, 2015.
- [128] J. McNally, D. H. Yoo, J. Drappa, J. L. Chu, H. Yagita, S. M. Friedman, and K. B. Elkon. Fas ligand expression and function in systemic lupus erythematosus. *J Immunol*, 159(9):4628–36, 1997.
- [129] J. O. Pers, C. Daridon, V. Devauchelle, S. Jousse, A. Saraux, C. Jamin, and P. Youinou. BAFF overexpression is associated with autoantibody production in autoimmune diseases. *Ann N Y Acad Sci*, 1050:34–9, 2005.

-
- [130] I. Parodis, M. Axelsson, and I. Gunnarsson. Belimumab for systemic lupus erythematosus: a practice-based view. *Lupus*, 22(4):372–80, 2013.
- [131] Y. Aiba and M. Nakamura. The role of TL1A and DR3 in autoimmune and inflammatory diseases. *Mediators Inflamm*, 2013:258164, 2013.
- [132] M. M. Guerrini, K. Okamoto, N. Komatsu, S. Sawa, L. Danks, J. M. Penninger, T. Nakashima, and H. Takayanagi. Inhibition of the TNF family cytokine RANKL prevents autoimmune inflammation in the central nervous system. *Immunity*, 43(6):1174–85, 2015.
- [133] A. K. Stark, S. Sriskantharajah, E. M. Hessel, and K. Okkenhaug. PI3K inhibitors in inflammation, autoimmunity and cancer. *Curr Opin Pharmacol*, 23:82–91, 2015.

Yasemin Begüm Alankus

Klinikum rechts der Isar
Technische Universität München
Trogerstraße 4a
81675, Munich, Germany

Education

- 2016 Doctoral Student in Immunology, Ludwig Maximilian University of Munich, Faculty of Biomedicine (IMPRS Fast Track PhD Program)/Klinikum rechts der Isar, Munich, Germany
- 2012 Bachelor of Science, Molecular Biology and Genetics, Bogazici University, Istanbul, Turkey. High Honors, GPA: 3.78/4.0
- 2008 High School Diploma, American Robert College, Istanbul, Turkey

Grants, honors & awards

- 2008 Technological Research Council of Turkey, Undergraduate Student Grant

Publications

- 2015 Knies N, Alankus B, Weilemann A, et al. "Lymphomagenic CARD11/BCL10/MALT1 signaling drives malignant B-cell proliferation via cooperative NF- κ B and JNK activation" *Proc Natl Acad Sci USA*. 2015
- 2015 Canli Ö, Alankuş YB, Grootjans S, et al. Glutathione peroxidase 4 prevents necroptosis in mouse erythroid precursors. *Blood*. 2015

Languages

Turkish (Native), English (Fluent), German (Working Proficiency)